

Durham E-Theses

Synthesis of biologically active isoindolones via N-acyliminium ion cyclisations

FREEBAIRN, MAXIMILIAN, TOBIAS

How to cite:

FREEBAIRN, MAXIMILIAN, TOBIAS (2023) *Synthesis of biologically active isoindolones via N-acyliminium ion cyclisations*, Durham theses, Durham University. Available at Durham E-Theses Online: <http://etheses.dur.ac.uk/15136/>

Use policy

The full-text may be used and/or reproduced, and given to third parties in any format or medium, without prior permission or charge, for personal research or study, educational, or not-for-profit purposes provided that:

- a full bibliographic reference is made to the original source
- a [link](#) is made to the metadata record in Durham E-Theses
- the full-text is not changed in any way

The full-text must not be sold in any format or medium without the formal permission of the copyright holders.

Please consult the [full Durham E-Theses policy](#) for further details.



Durham
University

**Synthesis of biologically active isoindolones via *N*-acyliminium ion
cyclisations**

A thesis submitted for the degree of

MASTER OF SCIENCE

By

Maximilian Freebairn

09/09/2023

Declaration

This thesis is based on work conducted by the author, in the Department of Chemistry at Durham University, during the period October 2021 to September 2022. All the work described in this thesis is original, unless otherwise acknowledged in the text or by reference. None of this work has been submitted for any another degree at this or any other University.

The period of work through which this thesis was completed was adversely affected by the Covid-19 pandemic. As a consequence, access to laboratory facilities was initially limited to a rotation-based working plan.

Acknowledgments

I would firstly like to thank my supervisor Ian, for his invaluable guidance and unwavering enthusiasm throughout my time in his lab; it has been a pleasure working in such a welcoming and supportive environment. To this end, I would also like to thank Haijing, Linda and Eilish, as well as the wider research group for their friendliness and many invaluable discussions. Lastly, to my family and Sarah; completing this project would have been impossible without your support and encouragement.

Abbreviations

δ	chemical shift (NMR spectroscopy)
ν	wavenumber (IR spectroscopy)
ADME	Absorption, distribution, metabolism and excretion
BINOL	1,1'-bi-2-naphthol
br	broad (NMR spectroscopy)
cm^{-1}	inverse centimetre
CS-Cl	camphorsulfonyl chloride
d	doublet (NMR spectroscopy)
DCE	dichloroethane
DEPT	distortionless enhancement through polarisation transfer
DMSO	dimethylsulfoxide
d.r.	diastereomeric ratio
e.e	enantiomeric excess
equiv.	equivalents
<i>et al.</i>	<i>et alia</i>
FT-IR	Fourier-transform infrared
g	grams
h	hours
HOMO	highest occupied molecular orbital
HRMS	high resolution mass spectrometry
Hz	Hertz
J	coupling constant (NMR spectroscopy) in hertz
LC-MS	liquid chromatography mass spectrometry
m	medium intensity (IR spectroscopy)
m	multiplet (NMR spectroscopy)
M	moles per litre
min	minutes
mL	millilitres
mol	moles

MOM-Cl	chloromethyl methyl ether
nm	nanometres
NMR	nuclear magnetic resonance
PPA	polyphosphoric acid
ppm	parts per million
PSA	polar surface area
PTSA	<i>p</i> -toluenesulfonic acid
q	quartet (NMR spectroscopy)
R _t	retention time
r.t.	room temperature
s	strong intensity (IR spectroscopy) or singlet (NMR spectroscopy)
t	triplet (NMR spectroscopy)
TBAS	tetra- <i>N</i> -butylammonium hydrogensulfate
TBME	tert-butyl methyl ether
TFA	trifluoroacetic acid
TFAA	trifluoroacetic anhydride
TMSCl	trimethylsilyl chloride
TMSCN	trimethylsilyl cyanide
THF	tetrahydrofuran
tlc	thin layer chromatography
w	weak intensity (IR spectroscopy)

Abstract

The preparation of diverse, architecturally complex molecules for pharmaceutical libraries represents a growing area of focus under the notion of diversity-oriented synthesis. Herein, we evaluate the use of *N*-acyliminium cyclisation reactions as a means for accessing privileged, natural product-like isoindolone structures. An excellent tolerance for various reagents and cyclisation conditions was observed, with the formation of various heterocyclic scaffolds achieved under straightforward reaction conditions and in good yields. This class of reaction was correspondingly used to synthesise a series of exploratory isoindolone derived compounds, for structure-activity testing as prospective treatments for colon cancer and leishmania (Biological hypothesis and data not supplied in this thesis due to confidentiality constraints with collaborators).

Table of Contents

Declaration	ii
Acknowledgments.....	iii
Abbreviations.....	iv
Abstract.....	vi
1. Introduction	1
This work.....	2
2: Synthesis of the target molecule and derivatives	7
2:1 Background.....	7
2.1.1 <i>N</i> -acyliminium cyclisations	7
2.1.2 Establishing a synthetic route	10
2.2 Results and discussion	14
2.2.1 Synthesis of benzalpthalide and its derivatives.....	14
2.3.2 Synthesis of amine components.....	16
2.3.3 Synthesis of isoindolone product	17
2.3.4 Preparation of substituted derivatives.....	22
2.3 Summary	24
3: Use of alternative nucleophilic components	26
3.1 Background.....	26
3.1.1 Reactivity of heterocyclic aromatic systems- pyrrole, thiophene and furan.....	26
3.1.2 Reactivity of aryl-based nucleophiles.....	30
3.1.3 Impact of the forming ring size.....	31
3.2 Results and discussion overview.....	35
3.2.1 Reaction of heterocyclic aromatics	36
3.2.2 Reactions of aryl nucleophiles.....	38
3.2.3 Formation of 7-membered heterocycles.....	40
3.2.4 Reaction of other nucleophiles.....	42
3.3 Tabulated summary of results.....	43
4: Mechanistic considerations & asymmetric synthesis	46
4.1 Background.....	46
4.1.1 Precedent for Stereoselective cyclisations	47
4.1.2 Asymmetric synthesis.....	49
4.2 Results and discussion	56
4.2.1 Determining the reaction pathway.....	56
4.2.2 Diastereomeric reactions.....	58
4.2.3 Asymmetric synthesis via chiral catalysis	61

5: Conclusion and future work.....	64
6: Experimental procedures	67
6.1: General Information	67
6.2: Synthesis of benzaldehyde derivatives 35-35k	68
6.3: Synthesis of amine components	73
6.4: Synthesis of isoindolone product and substituted derivatives 1-1k	74
6.5: Synthesis of 80-96 through implementation of alternative amine components	80
6.6: Synthesis of β -nitrostyrenes 88c-88k via the Henry reaction	83
6.7: Miscellaneous	86
7: References	89

1. Introduction

Drug development is a notoriously laborious and time-consuming process. It is estimated that only 1 in 5000¹ designed compounds screened makes it to market, and with the average cost per drug now estimated at \$1.3 billion², it is unsurprising that numerous attempts have been made to expediate the synthesis of new screening collections to feed the research and development phase. A key contributor to the cost of drug development is the late-stage attrition rate of drug candidates due to unexpected toxicology. Off-target interactions of a prospective drug can lead to unexpected side effects most commonly presenting as toxicity issues, which tend to only be identified in the later stages of development. As a result, there has been much focus on identifying key characteristics of a compound that correlate to an increased chance of success.

The rule-based conventionalisation of such a strategy was formalised by Lipinski *et al.*, who established a set of guidelines (The rule of 5) based on molecular weight, hydrogen bond donors and acceptors, and the octanol/water partition coefficient that were used to predict the success of a compound as a prospective drug.³ Compounds that obey the rule of 5 typically have lower attrition rates during clinical trials, increasing their chance of reaching the market. Since the publication of Lipinski's work, further properties have been identified that also correlate to reduced attrition rates. Properties such as topological polar surface area (PSA) and rotatable bonds have been demonstrated to strongly indicate the potential success of compounds transitioning from pre-exploratory to drug status.⁴ These properties are routinely used in ADME prediction models and are consistently scrutinized as compounds progress from hits (new molecular entity, NME) through lead structure to final drug candidate status.

These indicators (predictors), while helpful, allude to a less quantitative factor that is nonetheless instrumental to drug success – molecular complexity. In recent years, increasing emphasis has been placed on diversity-oriented synthesis, with the intent of producing more architecturally complex structures.⁵ The rationale is that these molecules will possess a greater specificity for a biological target, reducing the probability of off-target interactions. Additionally, the greater molecular complexity is thought to correlate to more “natural product-like” structures. As many drugs are derived from natural products, it is hoped that creating more complex drug-like libraries offers an increased chance of discovering unique bioactive compounds. In recent years, various efforts have been made to adopt empirical approaches toward describing molecular complexity. Some of the most prominent work in this regard has been that of Lovering *et al.*, who identified a significant correlation between increasing saturation of carbon centres and increasing number of chiral centres as compounds progress through clinical testing.⁶ This finding was of particular importance due to the

nature of molecular assembly within the pharmaceutical industry. Advances in coupling reactions of sp^2 centres in recent years have made the preparation of unsaturated compounds particularly amenable to combinatorial synthesis. This has had the unintended effect of skewing pharmaceutical libraries with a greater proportion of more unsaturated compounds. As a result, there has been a growing impetus regarding the synthesis of more saturated compounds, with greater 3-dimensionality.

While increasing molecular complexity is of great importance, higher specificity also requires the optimisation of key binding interactions between the prospective drug and its intended biomolecular target. Approaches to enhance lead identification such as high throughput screening (HTS) facilitate the rapid pharmacological testing of chemical compounds, but provide little information as to the actual mechanism of interaction. Additionally, the expense of such techniques contributes to their inaccessibility for almost all except big pharma. Consequently, there has been increased focus in recent years toward *in silico* studies; using computational modelling to assist experimental studies and increasingly make predictions for drug discovery campaigns.

Computational-based studies are broadly categorised into two distinct approaches. Ligand-based methods require a structurally diverse set of binding compounds (ligands) for a given receptor. By examining the collective information and properties of the existing ligands, a model of the receptor can be constructed, and new compounds can be predicted as binders of the target biomolecule. However, this approach suffers from the intrinsic drawback that novel binding compounds are derived from existing ligands, and so tend to be structurally similar. Thus, this approach essentially rules out discovering radically different frameworks that nonetheless might bind effectively to the target receptor. By contrast, structure-based methods employ various computational techniques to “map” the domain of the receptor to which a potential molecule could bind. Molecular docking tends to be the most common technique, in which a scoring function is used to estimate the fitness of any given ligand against the binding site of the receptor. In this fashion, ligands with the highest predicted affinity can be selected, and their efficacy can be verified with *in vitro* studies. This approach requires accurate 3-dimensional structures of both the receptor and binding molecules, as well as highly intensive computational processes to model the receptor ligand binding interaction.

This work

In 2021, Doğan *et al.* published a new computational method, “DRUIDom” (DRUG interacting domain prediction) to identify interactions between drug candidate compounds and protein targets.⁷ The technique is based upon the fact that proteins consist of modular structures known as domains. These domains fold and function in a specific fashion that tends to be independent from the rest of the

protein. As such, if a domain is identified on a characterised protein, it can be detected on uncharacterised proteins by cross examining the amino acid sequences.

In this approach potential bioactive structures are statistically mapped onto structural domains of their target proteins, with the aim of identifying their interactions. Other proteins containing the same mapped domain or domain pairs subsequently become new candidate targets for the corresponding compounds. Next, a large-scale dataset of small molecule compounds, including those mapped to domains in the previous step, are clustered based on their molecular similarities, and their domain associations are propagated to other compounds within the same clusters. Bioactivity data points, obtained from public databases are subsequently filtered to construct datasets of active/interacting and inactive/non-interacting drug/compound–target pairs, and thus used as training data for calculating parameters of compound–domain mappings.

This approach has been used to predict compounds that would target LIM-kinase proteins, that are known to play a key role in the propagation of hepatocellular carcinoma. In total, 4 compounds were predicted by DRUIDom to be inhibitors of both LIMK1 and LIMK2 proteins; subsequent derivatives of one of these compounds were prepared and determined to possess cytotoxic activities on Huh7 and Mahlavu liver cancer cells, establishing a new lead structure.

Following on from this success, the same methodology has been used to generate a common molecular scaffold predicted to have activity against colon cancer (Figure 1; specific biological target not disclosed due to IP considerations). Working with our biological collaborators, we intended to synthesise the identified compound and prepare a set of substituted derivatives to explore this interesting predicted relationship. Based upon the IP status of the compounds and specific molecular targets, we have been requested to restrict our discussion to the chemical identity and preparation of the compounds only.

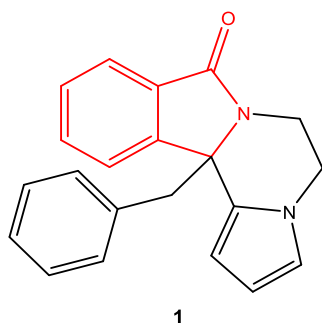


Figure 1: Structure of molecular target.

To the best of our knowledge, this structure represents a novel chemical architecture, and thus there was no precedent for its synthesis. However, the molecule contained an isoindolone backbone (shown

in red), which has gained considerable attention with regards to its presence in natural products, pharmaceuticals, and biologically active molecules. For example, the alkaloids chilenine **2**⁸, palmanine **3**⁹ and fumadensine **4**¹⁰, as well as the drugs Lenalidomide **5**¹¹ and Chlortalidone **6**¹², all contain the isoindolone moiety (Figure 2).

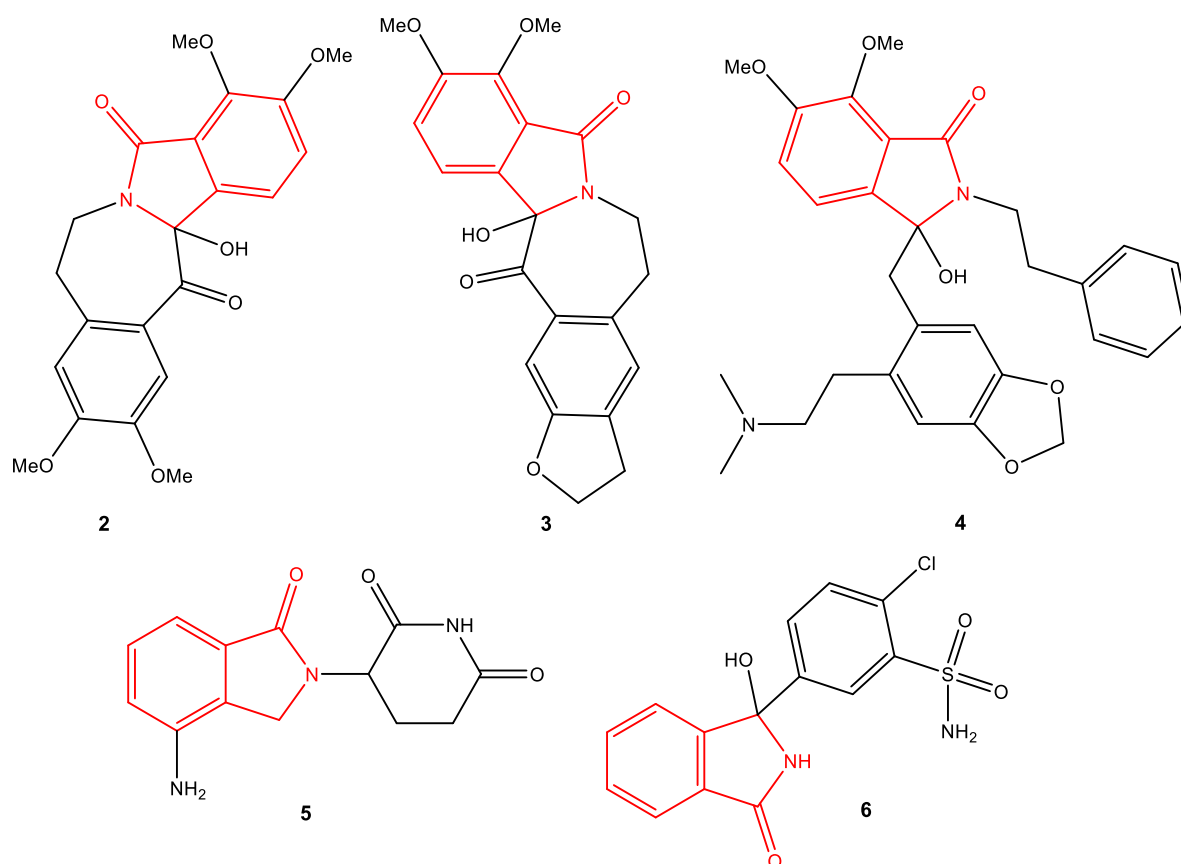
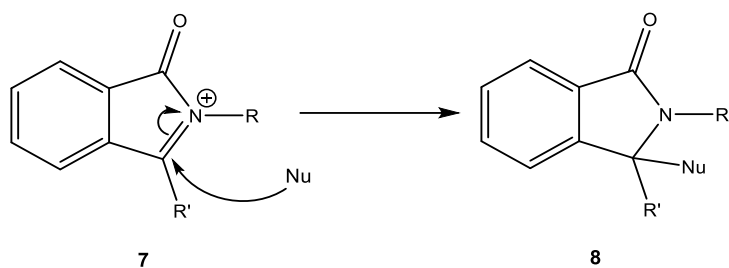


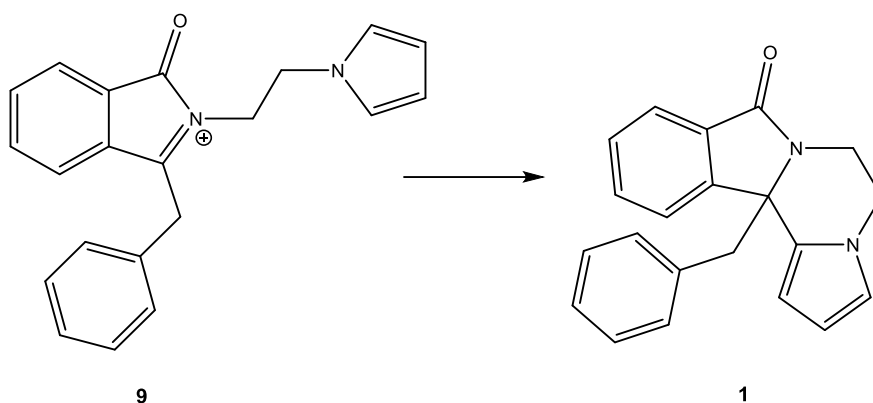
Figure 2: Structures of chilenine (2) palmanine (3) fumadensine (4), Lenalidomide (5) and Chlortalidone (6).⁸⁻¹²

Many published reactions exploit reactive nitrogen species generated from the isoindolone structure to furnish further transformations. It is well known that iminium ions are important reactive intermediates in organic synthesis; both the Mannich¹³ and Pictet-Spengler¹⁴ reactions employ such species, and have served as powerful amino-alkylation processes for over 100 years. The isoindolone structure can be used to access a subtype of the iminium ion, known as an *N*-acyliminium ion (**7**, Scheme 1). This powerful electrophile is capable of reacting with a wide variety of nucleophilic components, under relatively mild conditions.



Scheme 1: N-acyliminium ion and subsequent reaction with a nucleophile.

Utilising this chemistry, we believed that an intramolecular *N*-acyliminium ion cyclisation would be able to furnish our target molecule (Scheme 2). Our preliminary objective was therefore to establish a feasible and effective synthetic route to producing **1**, as well as various substituted derivatives such that a structure-activity relationship could be established.



Scheme 2: N-acyliminium cyclisation to furnish target molecule 1.

Beyond this first objective, however, we also wished to explore this reaction in the wider context of synthesising complex, biologically active scaffolds. As mentioned previously, there is growing impetus for increasing molecular complexity in pharmaceutical candidates. We believed that *N*-acyliminium ion cyclisations could prove valuable in this regard as a facile and versatile means to access privileged heterocyclic structures. Consequently, we sought to explore the scope and versatility of this reaction by employing alternative nucleophilic components of differing reactivities, as well as attempting the formation of different ring sizes. Exploring these aspects would have the added benefit of increasing the library of compounds available for biological testing, to gain a better understanding of any structure-activity relationship.

A final aim of this work was to explore the possibility of conducting an asymmetric synthesis of the target molecule **1**. This would allow specific access to the two potential enantiomers and thus allow any differences in biological activities to be identified. As enantioselective synthesis involving *N*-

acyliminium ions is a relatively new field of study, this would also prove interesting synthetically for advancing the area.

These three objectives reflect our overarching aim of exploring *N*-acyliminium cyclisations in the context of synthesising molecule **1**, and are separately addressed in the subsequent three chapters.

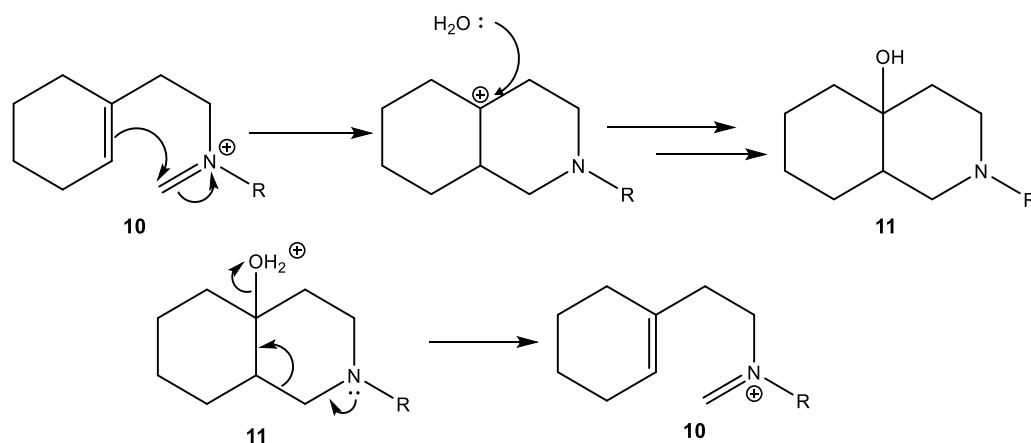
2: Synthesis of the target molecule and derivatives

2:1 Background

Our first objective was to establish a feasible and effective synthetic route of producing our target molecule **1**, using an *N*-acyliminium cyclisation as the key transformation. This required the development of a complete synthetic route to form the necessary precursor compounds (Scheme 2). Additionally, we sought to determine the reagents and conditions most suited to this reaction, which could then be employed in the synthesis of substituted compounds as well as the different heterocyclic systems covered in chapter 3.

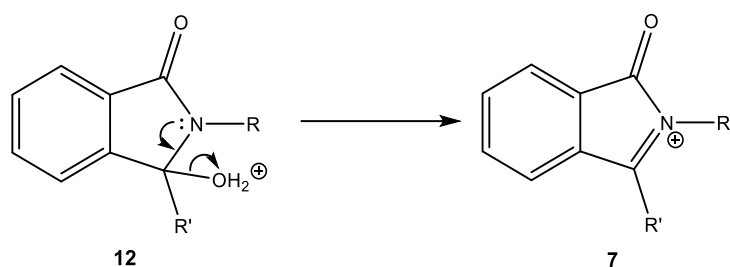
2.1.1 *N*-acyliminium cyclisations

The earliest reported reactions involving *N*-acyliminium ions stem from work performed by Belleau and Mondon during the 1950's, on the synthesis of erythrina alkaloids.¹⁵⁻¹⁷ Since then, a substantial amount of work has been performed to exploit the unique properties of *N*-acyliminium ions in organic synthesis. This species has notably been employed within intramolecular reactions, providing access to a broad range of heterocyclic structures using relatively mild reaction conditions. The electron withdrawing nature of the attached carbonyl group further increases the reactivity of the iminium, rendering it a more powerful electrophile than its *N*-alkyliminium counterpart. Nucleophiles that would be considered too unreactive for a regular Pictet-Spengler reaction, such as unactivated phenyl groups, can participate effectively in reactions with *N*-acyliminium ions.¹⁸ Additionally, reactions at an *N*-acyliminium centre tend to be more irreversible in nature than their *N*-alkyliminium counterparts. For example, the product of the olefinic *N*-alkyliminium cyclisation shown below yields an amine **11** (Scheme 3)¹⁹; however, the reverse process is also possible, with the reaction proceeding via a Grob fragmentation.²⁰ The same reaction with an *N*-acyliminium ion instead yields an amide, which is far less susceptible to the same fragmentation process.²¹



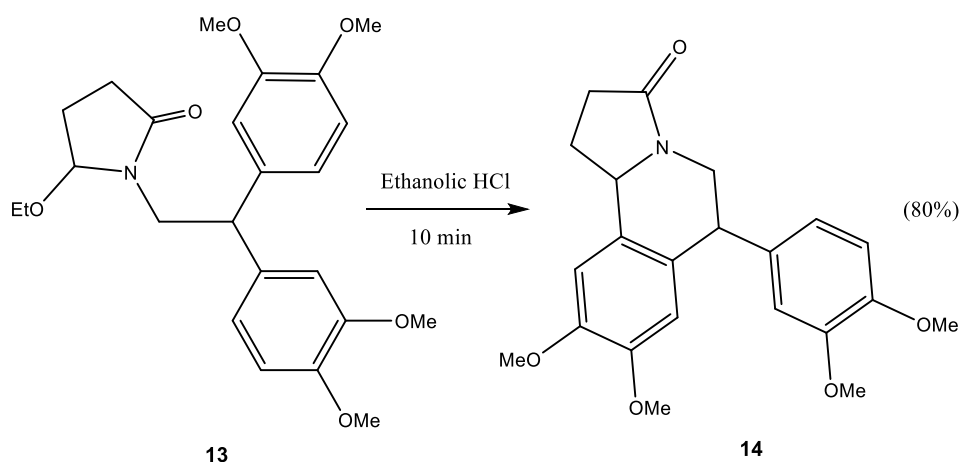
Scheme 3: N-alkyliminium (R = alkyl) cyclisation (top) and mechanism for Grob fragmentation (bottom).

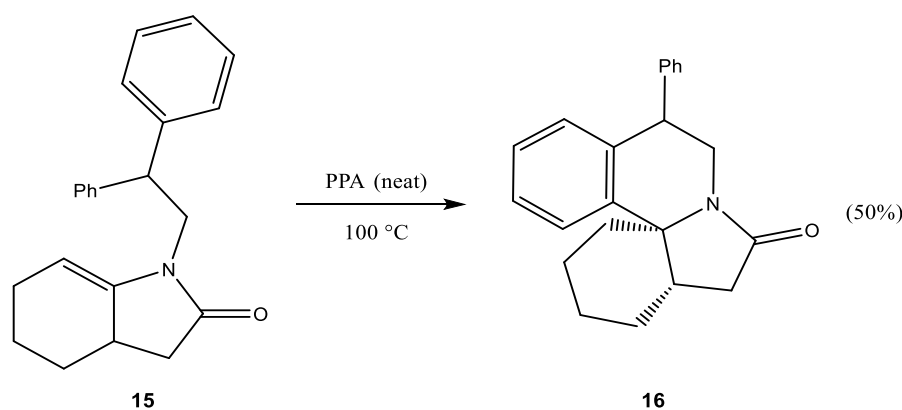
The generation of an *N*-acyliminium ion can be achieved through various means, including direct condensation of an acyl chloride and an imine²², and electrochemical oxidation of an amide.²³ Perhaps the most common method, however, involves the loss of a leaving group from the α -position of the nitrogen atom (Scheme 4). Hydroxy groups are a common choice, with the elimination facilitated by either a Brønsted or Lewis acid. Regardless of the preparation route, they are almost exclusively generated and trapped *in situ* due to their high reactivity.



Scheme 4: N-acyliminium ion generation.

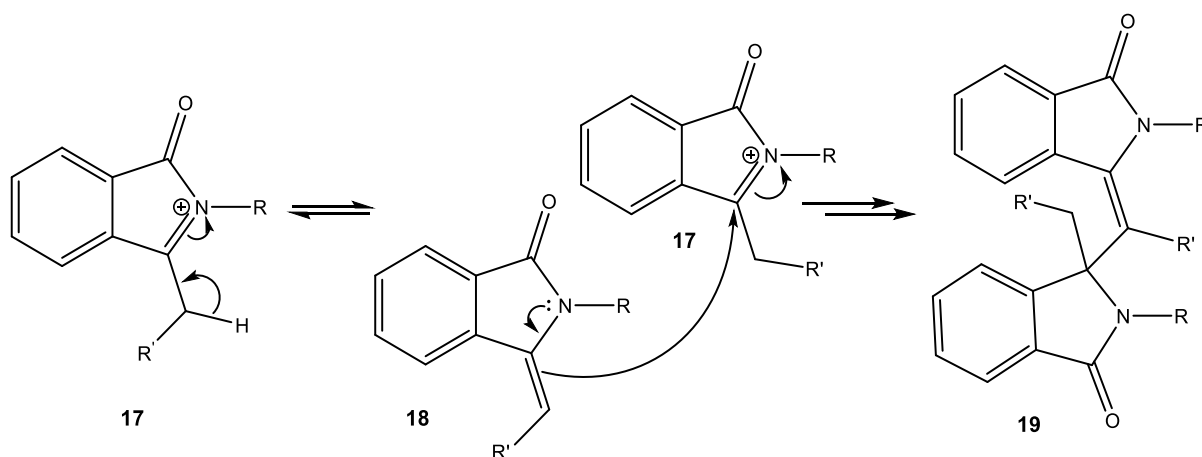
As mentioned previously, a broad range of nucleophiles can be employed with *N*-acyliminium ions, ranging from aryl to heterocyclic systems such as pyrrole, thiophene and furan, as well as alkene and enolate-derived species. More electron-rich nucleophiles such as aromatic heterocycles or activated phenyl groups generally react in a facile manner, while species such as unactivated phenyl groups or alkenes tend to require harsher conditions. In the example shown below (Scheme 5), treatment of compound **13** with ethanolic HCl at reflux yields **14** in just 10 min (80% yield), whilst the corresponding cyclisation of **15** to **16** requires dissolution in polyphosphoric acid at 100 °C for 24 hours (50% yield).¹⁸





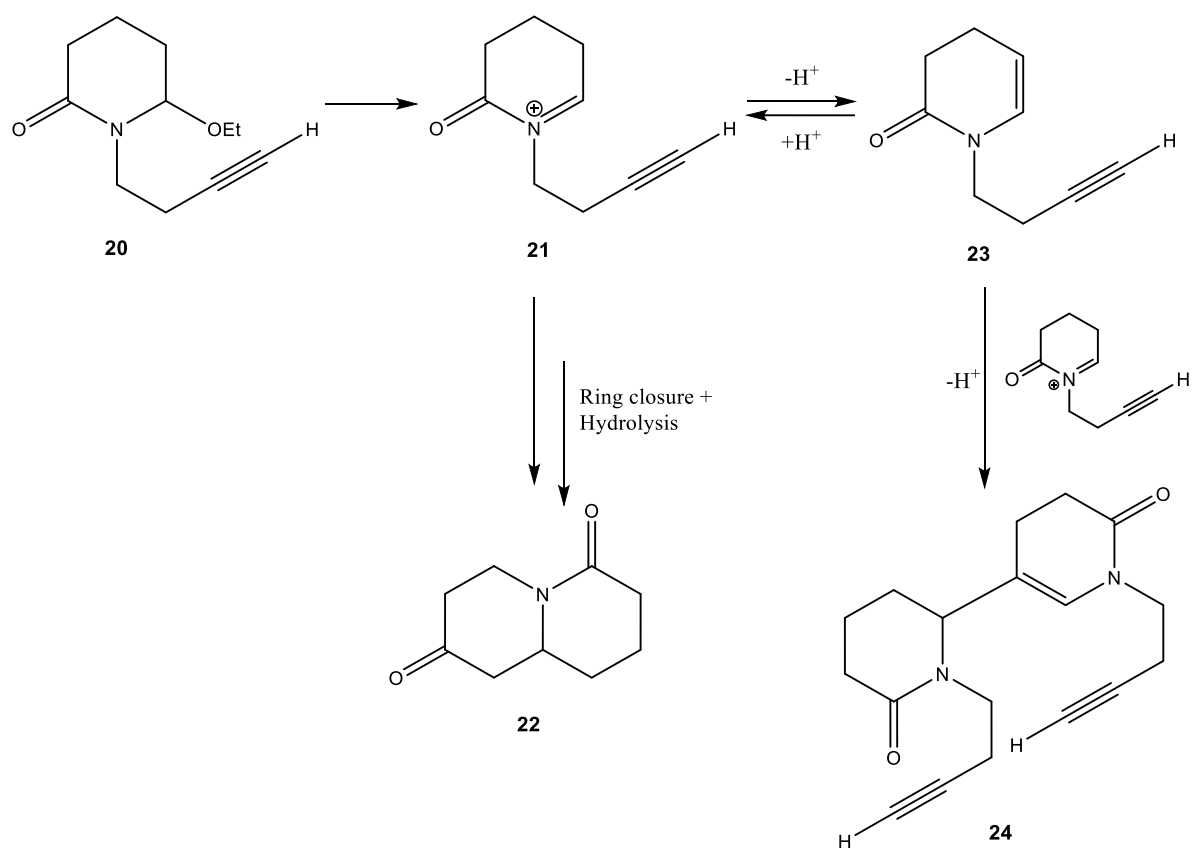
Scheme 5: Comparison of the reagents and conditions required for the successful cyclisation of electron rich (top) and unactivated (bottom) π -nucleophiles.

An important side reaction to be aware of in *N*-acyliminium ion chemistry is the formation of an enamide **18** via loss of a proton from an alpha alkyl group (Scheme 6). While this reaction is typically reversible under protic conditions, the enamides formed may further react, acting as nucleophiles with residual *N*-acyliminium ions, giving rise to dimeric structures such as **19** (Scheme 6) or even a polymerised product.



Scheme 6: Dimeric products arising from the nucleophilic nature of the enamide species.

The problems associated with enamide formation and subsequent side reactions tend to occur if nucleophilic attack on the *N*-acyliminium ion is not sufficiently fast. This can occur in cases where less reactive nucleophiles are used, or if there are large steric constraints surrounding the *N*-acyliminium centre. In the case of intramolecular reactions, stereoelectronic factors (as per Baldwin's rules²⁴) or the entropic penalty accompanying the formation of larger ring structures can also incur sluggish nucleophilic attack. An example of this phenomenon is the ring closure of the hydrolysed acetylene shown below (Scheme 7). A 5:1 mixture of the desired product **22** and dimer **24** was obtained when the reaction of 0.5 mmol of **20** was carried out in 3 mL of formic acid (ca. 0.15 M).²⁵

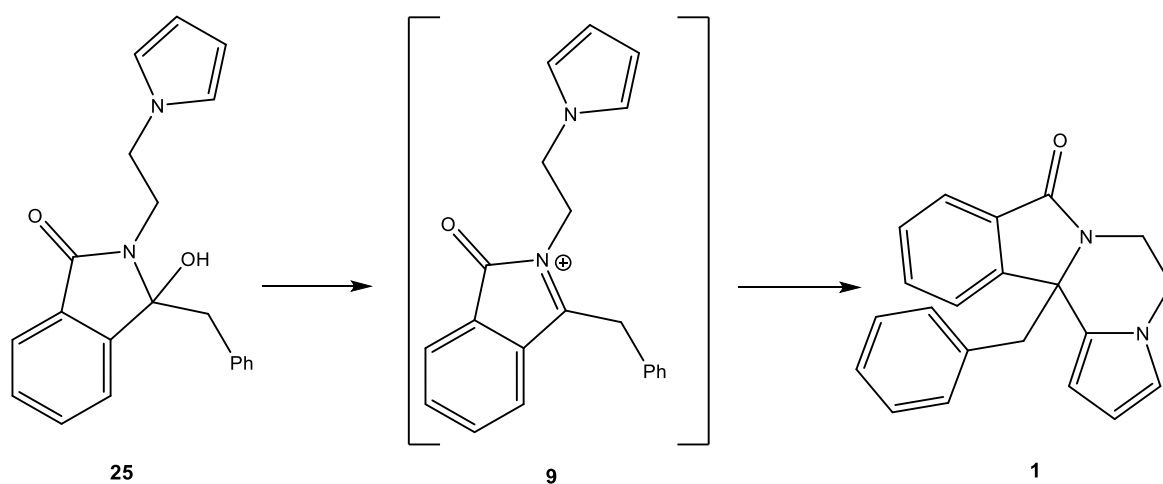


Scheme 7: Acetylene ring closure and formation of dimeric side product as described by H. E. Schoemaker et al.²⁵

However, it should be noted that simply diluting the solution causes the intramolecular reaction to become far more favourable than any dimerization reactions. Indeed, following a repetition of the above reaction in 40 mL of neat formic acid (ca. 0.01 M), formation of the dimeric product **24** was not observed, and only the desired product **22** was isolated in an 88% yield. It appears that the tendency of *N*-acyliminium ions to form enamides also depends on the nature of both the acidic catalyst and solvent.²⁶

2.1.2 Establishing a synthetic route

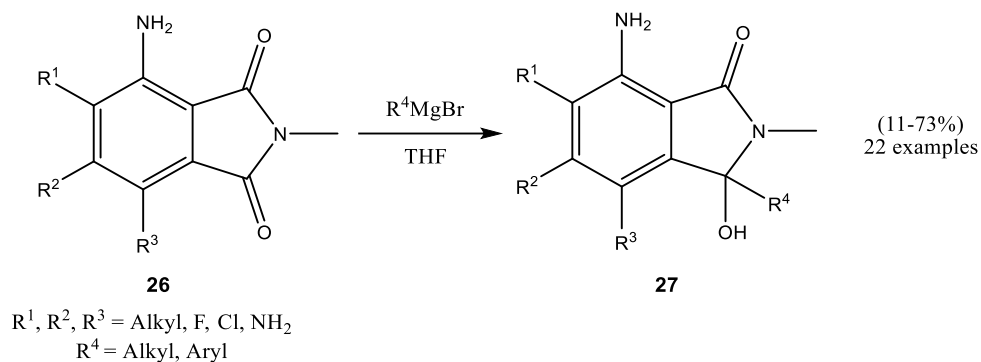
Based upon the chemistry detailed above, we deduced that a 3-hydroxyisoindolone derivative **25** could be used to furnish our target molecule **1** via an intramolecular *N*-acyliminium cyclisation (Scheme 8).



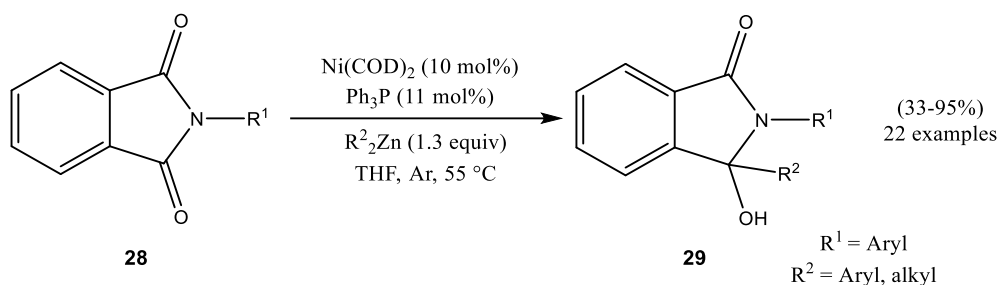
Scheme 8: Formation of the *N*-acyliminium species from the 3-hydroxyisoindolone and subsequent cyclisation.

While this cyclisation represented a novel transformation, we were reasonably confident it would work for several reasons. For one, the pyrrole ring constitutes a relatively electron-rich π system, which would serve as a reasonable nucleophile for the cyclisation reaction. Additionally, the reaction would involve a 6-*endo-trig* cyclisation, classed as stereoelectronically favoured by Baldwin's rules.²⁴

With regards to the synthesis of 3-hydroxyisoindolone **25**, several strategies have been detailed in the literature, allowing easy access to the precursor in good yield from simple and readily available substrates. One of the most documented involves the reaction of phthalimide moieties with organometallics. This was exploited by Neumann *et al.* in the synthesis of Corollosporine analogues (Scheme 9), through the reaction of *N*-methyl-4-aminophthalimides (**26**) with Grignard reagents.²⁷ Another example was presented by Dennis *et al.* (Scheme 10), who prepared γ -hydroxylactams **29** through the nickel-catalysed addition of organozinc reagents to phthalimides **28**.²⁸ There is a wealth of chemistry regarding the synthesis of phthalimide derivatives, the easiest of which simply involves the condensation of phthalic anhydride with a primary amine. However, the use of organometallics suffers from intrinsic drawbacks, such as requiring anhydrous reaction conditions and poor site selectivity.

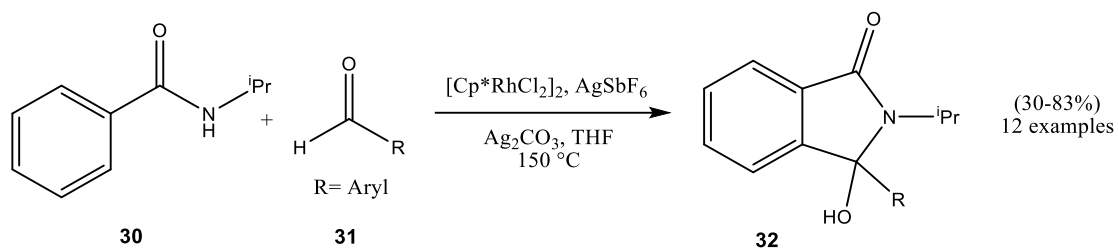


Scheme 9: 3-hydroxyisoindolones prepared by Neumann et al.²⁷



Scheme 10: Organozinc based reaction employed by Dennis et al.²⁸

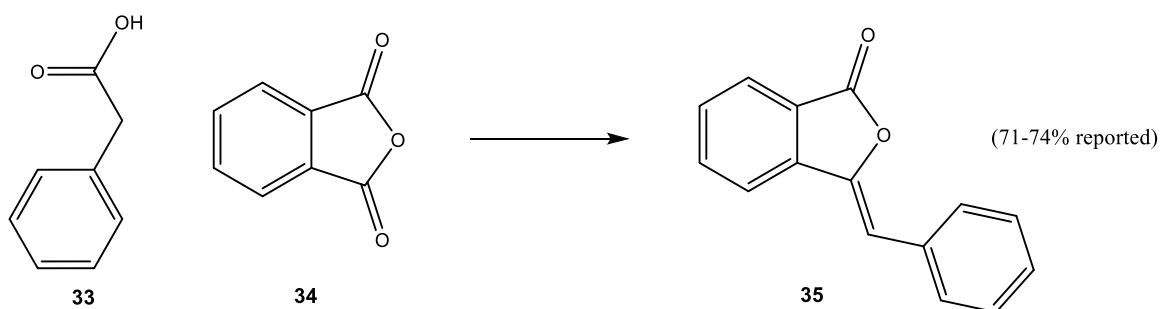
Another potential route is the transition metal-catalysed reaction of benzamides with aldehydes. This employs readily available starting materials and affords excellent yields; for example, Sharma *et al.* employed a ruthenium-based catalyst to facilitate the formation of 3-hydroxyisoindolones **32** with yields of up to 83%.²⁹ However, the use of expensive transition metal catalysts represents a significant drawback as does the issue of regioselectivity for non-symmetric benzamide starting materials.^{29,30}



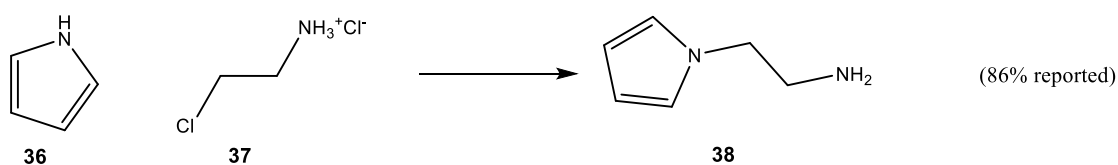
Scheme 11: Ruthenium-catalysed reaction of benzamides with aldehydes.²⁹

Fortunately, given the structure of the hydroxyisoindolone in question, we believed synthesis was possible via the simple condensation reaction of benzalphthalide (**35**) and 2-(1*H*-pyrrol-1-yl)ethanamine (**38**). The preparation of these precursor compounds was well established in literature, providing a total synthesis from phthalic anhydride (**34**), phenylacetic acid (**33**), pyrrole (**36**) and 2-chloroethylamine hydrochloride (**37**) as depicted in Scheme 12.

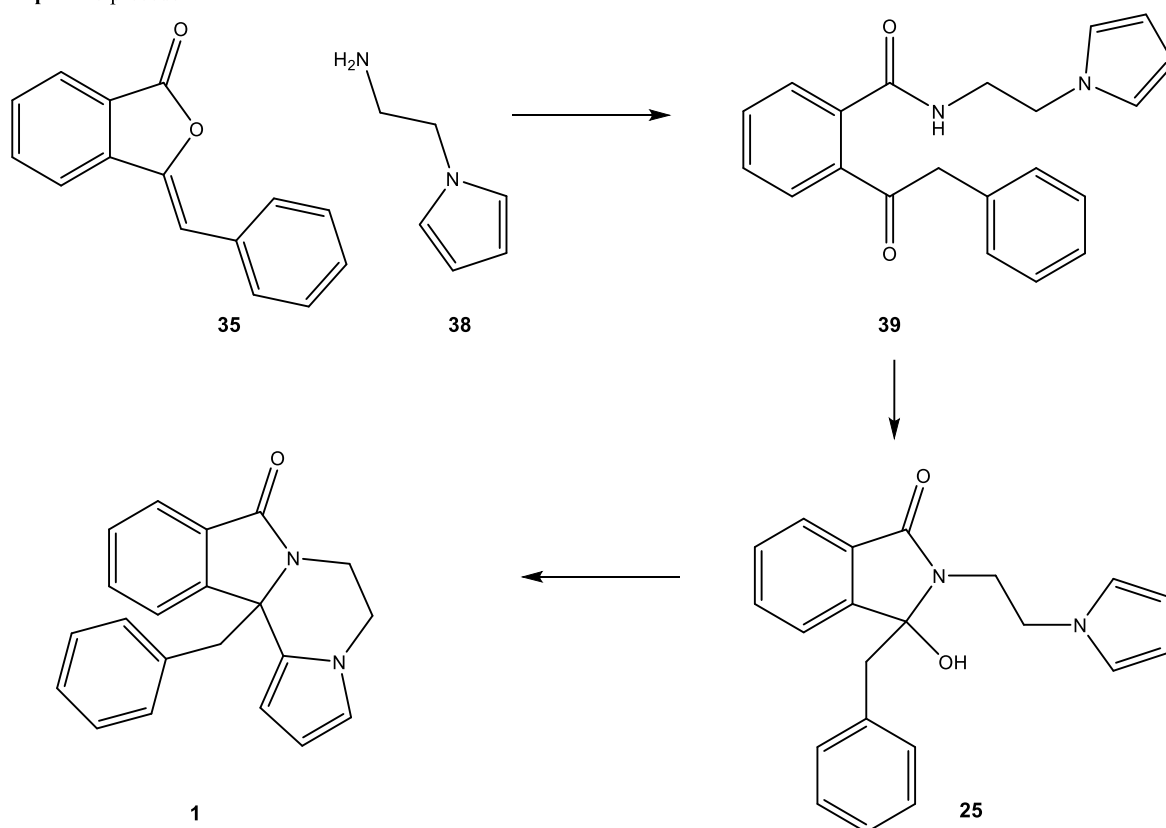
Step 1: Example precedent; R. Weiss, *Organic Syntheses*, 1933, **13**, 10.



Step 2: Example precedent; Y. He, M. Lin, Z. Li, X. Liang, G. Li and J. C. Antilla, *Org Lett*, 2011, **13**, 4490-4493.



Step 3: No precedent



Scheme 12: Total synthesis of the target isindolone product (25).

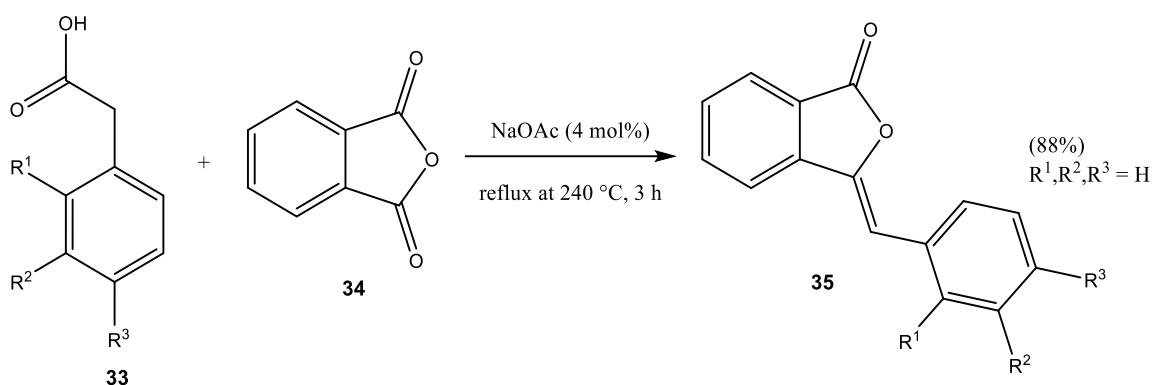
This outlined synthetic route (Scheme 12) in theory afforded several advantages - for one, all the starting materials were commercially available at low costs. The reactions to produce the intermediate products were known to be both high yielding, and as a convergent synthesis, it was expected that the final product could be achieved in a good overall yield. Additionally, all reagents were relatively

non-hazardous and stable with respect to air and moisture, resulting in an uncomplicated synthetic procedure.

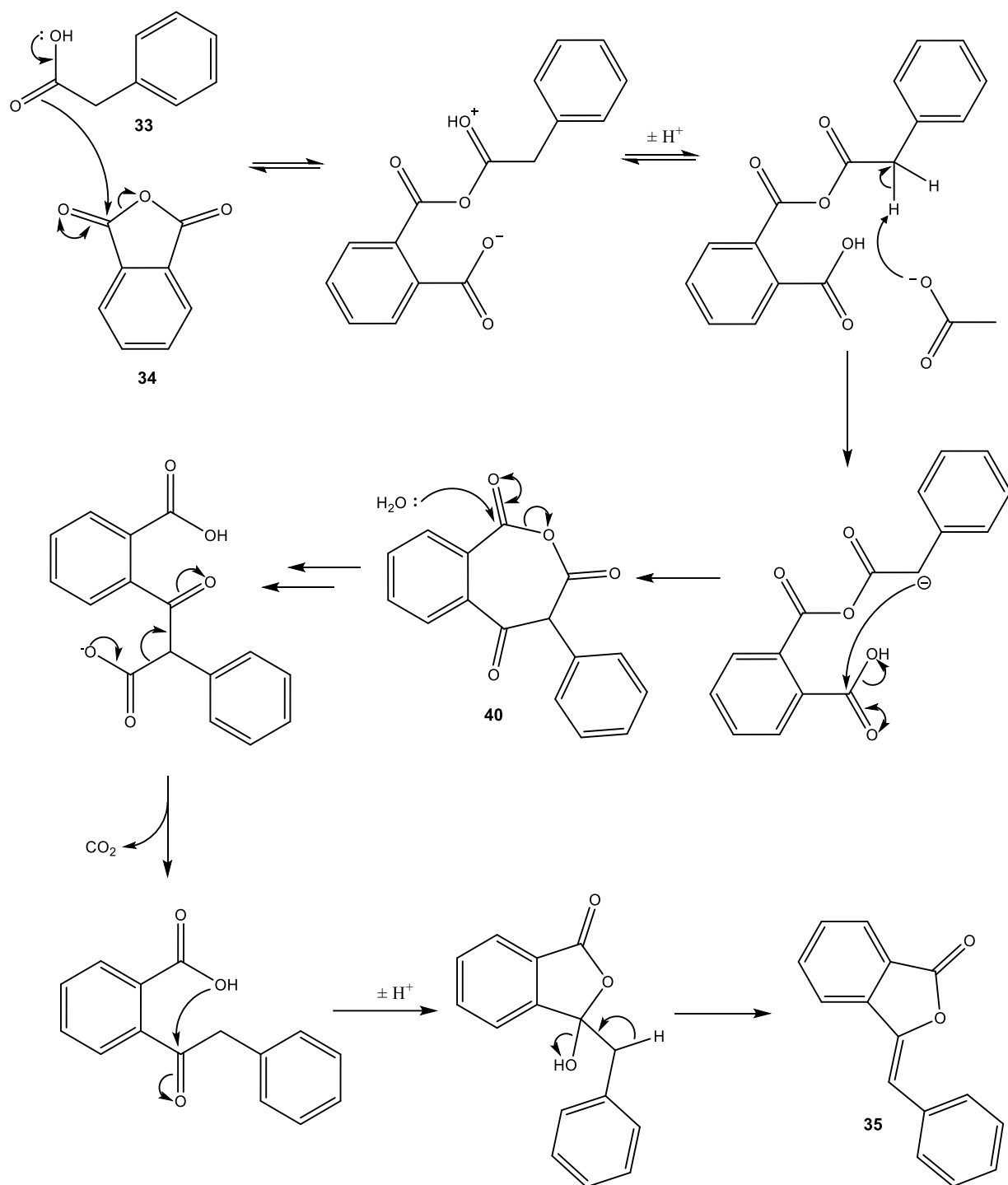
2.2 Results and discussion

2.2.1 Synthesis of benzalphthalide and its derivatives

The first synthetic transformation involves the reaction of phthalic anhydride (**34**) with phenylacetic acid (**33**). The procedure followed was that reported by Weiss, wherein the two components were heated together, in the absence of solvent and with 4 mol% sodium acetate at 240 °C for 3 h (Scheme 13).³¹ Dissolution of the resultant solid in hot ethanol and subsequent cooling yielded the desired benzalphthalide (**35**). The reaction is believed to proceed via an intermediary cyclic tricarbonyl species **40**, with the sodium acetate acting as a catalyst (Scheme 14).



Scheme 13: Reaction of phthalic anhydride with phenylacetic acid to yield benzalphthalide.



Scheme 14: Postulated mechanism for the synthesis of benzaldehyde (35).

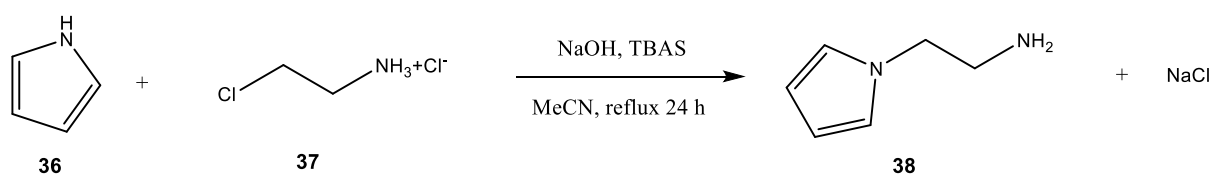
Next, additional benzaldehyde derivatives functionalised at the R¹, R² and R³ positions were synthesised (R positions as indicated in Scheme 13). An initial set of 10 derivatives was prepared, with chloro-, fluoro- and methoxy- groups substituted at the R¹, R² and R³ positions as shown in Table 1. These substituted derivatives were then used to create the correspondingly substituted final product. All the reactions were found to proceed effectively, with yields ranging from 65-91% (Table 1).

Table 1: Substituted benzaldehyde derivatives synthesised and their corresponding yields.

Derivative	R ¹	R ²	R ³	Yield/ %
35	H	H	H	88
35b	H	H	OMe	78
35c	H	Cl	H	65
35d	H	H	Cl	84
35e	Cl	H	H	68
35f	H	H	F	90
35g	H	OMe	OMe	91
35h	H	F	H	73
35i	F	H	F	77
35j	OMe	H	H	72
35k	H	OMe	H	69

2.3.2 Synthesis of amine coupling partner

Next, the synthesis of 2-(1*H*-pyrrol-1-yl)ethanamine (**38**) was performed, following the procedure detailed by Liang *et al* (Step 3, Scheme 12).³² Pyrrole (**36**) and sodium hydroxide were initially stirred in acetonitrile at room temperature for 30 minutes. Under sufficiently basic conditions, the nitrogen atom of pyrrole is deprotonated ($pK_a = 16.5^{33}$), allowing it to act as a stronger nucleophile. Tetrabutylammonium hydrogen sulfate (TBAS) was used as a phase transfer agent, ensuring that the pyrrole was effectively deprotonated by the sodium hydroxide base. Lastly, 2-chloroethylamine hydrochloride (**37**) was added and the reaction was refluxed for 24 hours to furnish the final product (Scheme 15). The reaction progress was observed by the gradual precipitation of sodium chloride as the reaction progressed.

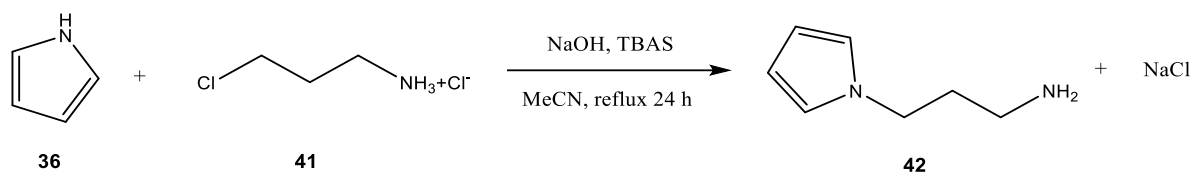


Scheme 15: Reaction of pyrrole (**36**) and 2-chloroethylamine hydrochloride (**37**) to give 2-(1*H*-pyrrol-1-yl)ethanamine (**38**)

The crude product was initially purified via column chromatography (eluent — DCM: methanol 10:1) which afforded 2-(1*H*-pyrrol-1-yl)ethanamine (**38**) as a yellow oil (45% yield). However, it was found that at a larger scale, Kugelrohr distillation served as a more convenient and efficient purification

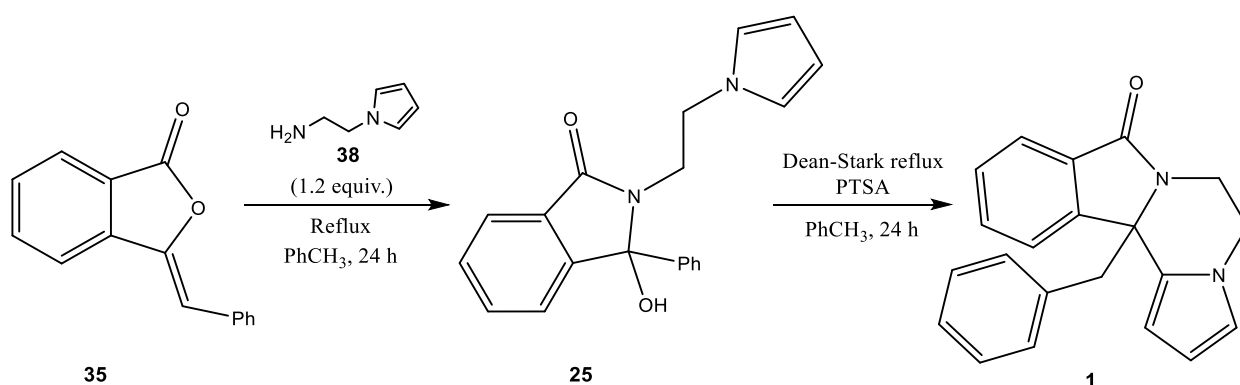
technique. The product began condensing at 190 °C and 40 mbar vacuum as a colourless oil, with an overall yield of 67%. Analysis of the ^1H NMR spectrum confirmed the high purity of the compound (>95% by ^1H NMR).

The same methodology was subsequently used to synthesise the homologue 3-(1*H*-pyrrol-1-yl)propan-1-amine (**42**) from pyrrole and 3-chloropropylamine hydrochloride, to be used in subsequent experiments. Following Kugelrohr distillation at 240 °C and 40 mbar, the product was isolated as a colourless oil, in a 79% yield.



2.3.3 Synthesis of isoindolone product

With the intermediates **35** and **38** in hand, synthesis of the final product **1** could be attempted (Scheme 16). The procedure followed was loosely based on the work of Katritzky *et al.*, who disclosed the cyclisation of similar heterocyclic structures.³⁴ Formation of the *N*-acyliminium ion intermediate was facilitated by a Brønsted acid catalyst, namely *p*-toluenesulfonic acid monohydrate (PTSA). This was chosen for its availability and high solubility in the organic solvent system. Another benefit was the availability of a resin-bound PTSA, which afforded ease of separation following the completion of the reaction. In terms of the reaction solvent, Katritzky *et al.* had primarily employed benzene for their reactions. Due to its high toxicity, we opted to use toluene instead, which was capable of dissolving all the reagents effectively. As toluene and water form an effective azeotrope, the reaction was performed using a Dean-Stark apparatus, in order to remove water from the reaction vessel as it was produced.



Scheme 16: Reaction of 2-(1*H*-pyrrol-1-yl)ethanamine (**38**) and benzaldehyde (**35**) to yield the final isoindolone product **1**.

Our initial procedure was to dissolve the benzaldehyde (**35**), 2-(1*H*-pyrrol-1-yl)ethanamine (**38**) and the acid catalyst in toluene, followed by reflux for 24 hours. An excess of the 2-(1*H*-pyrrol-1-yl)ethanamine (**38**) was used (1.2 equivalents) to ensure complete reaction of the benzaldehyde (**36**), which simplified the subsequent purification. The progress of the reaction could be conveniently monitored by the collection of water in the Dean-Stark trap. Following a wash with 1 M sodium hydrogen carbonate and water, the solvent was removed *in vacuo* and purification was carried out by column chromatography, using hexane and ethyl acetate (4:1 ratio) as the solvent system. However, the yield of the product **1** was surprisingly low (7%), with analysis by NMR spectroscopy and X-ray crystallography data instead identifying the major product as the enamide **43** (Figure 3, structure ref: 21srv467).

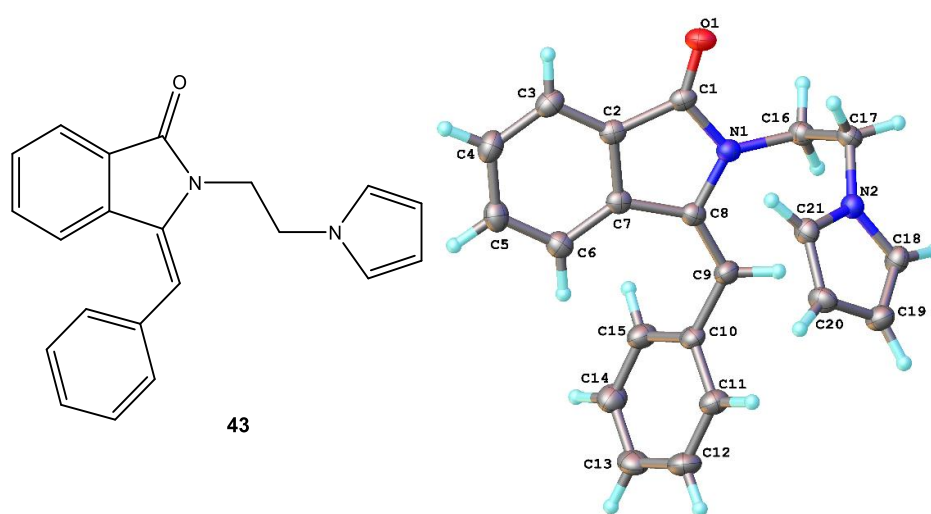


Figure 3: Enamide intermediate **43** generated from the initial procedure (left) and corresponding X-ray crystal structure (right).

As mentioned previously, formation of the enamide **43** is expected to be reversible (or an active intermediate in the cyclisation process) under protic conditions.²¹ Sure enough, NMR monitoring data suggested that the cyclisation of **43** was completed following further reflux with PTSA to yield the desired product **1** (Figure 4).

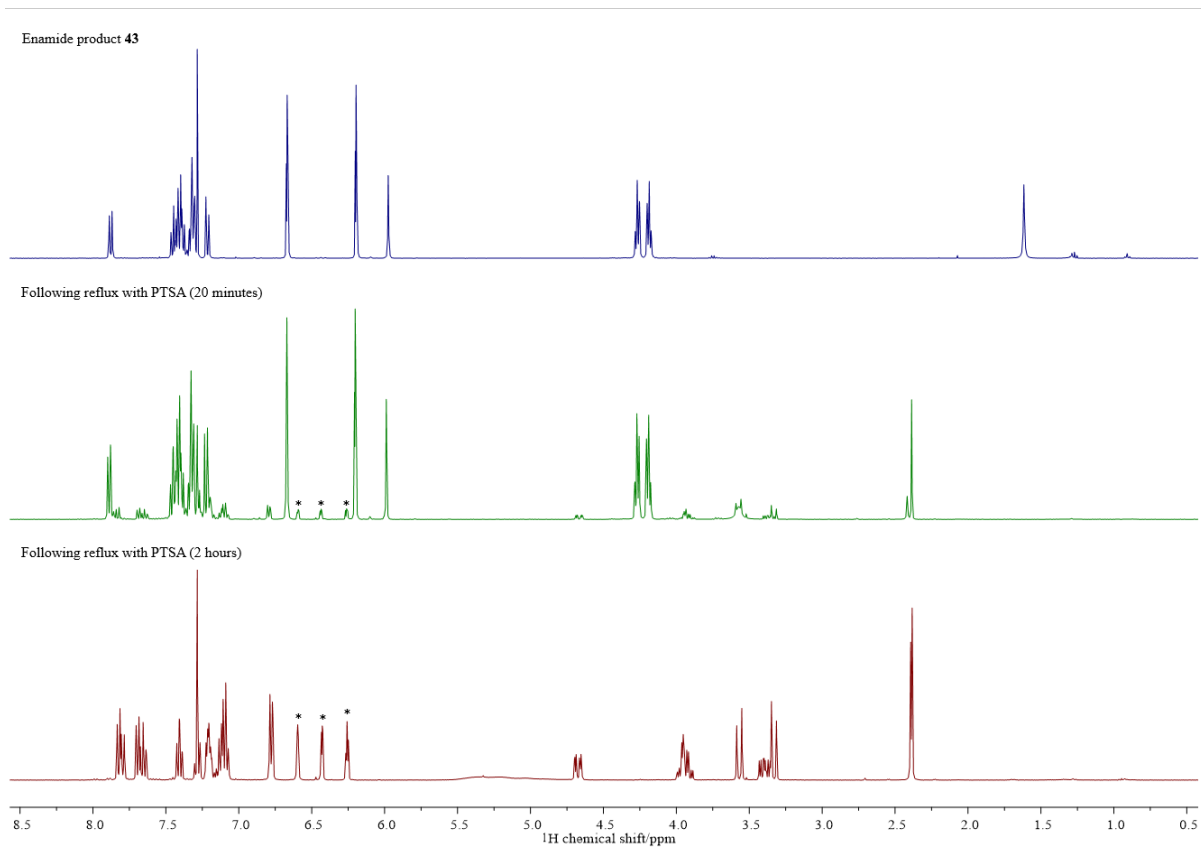


Figure 4: Conversion of the enamide **43** into the fully cyclised product **1**. The 3 pyrrolic peaks (marked with *) are indicative of successful cyclisation.

The product was shown to be the desired heterocyclic structure following NMR characterisation and confirmed by X-ray crystallography (Figure 5, structure ref: 22srv006).

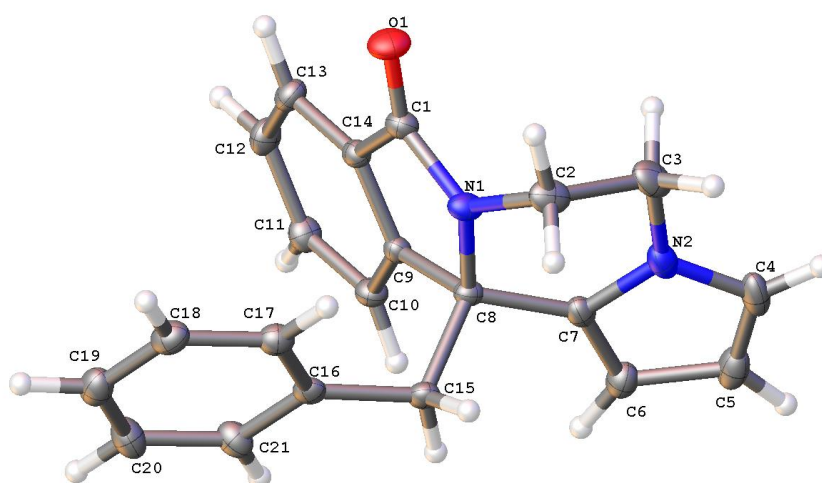


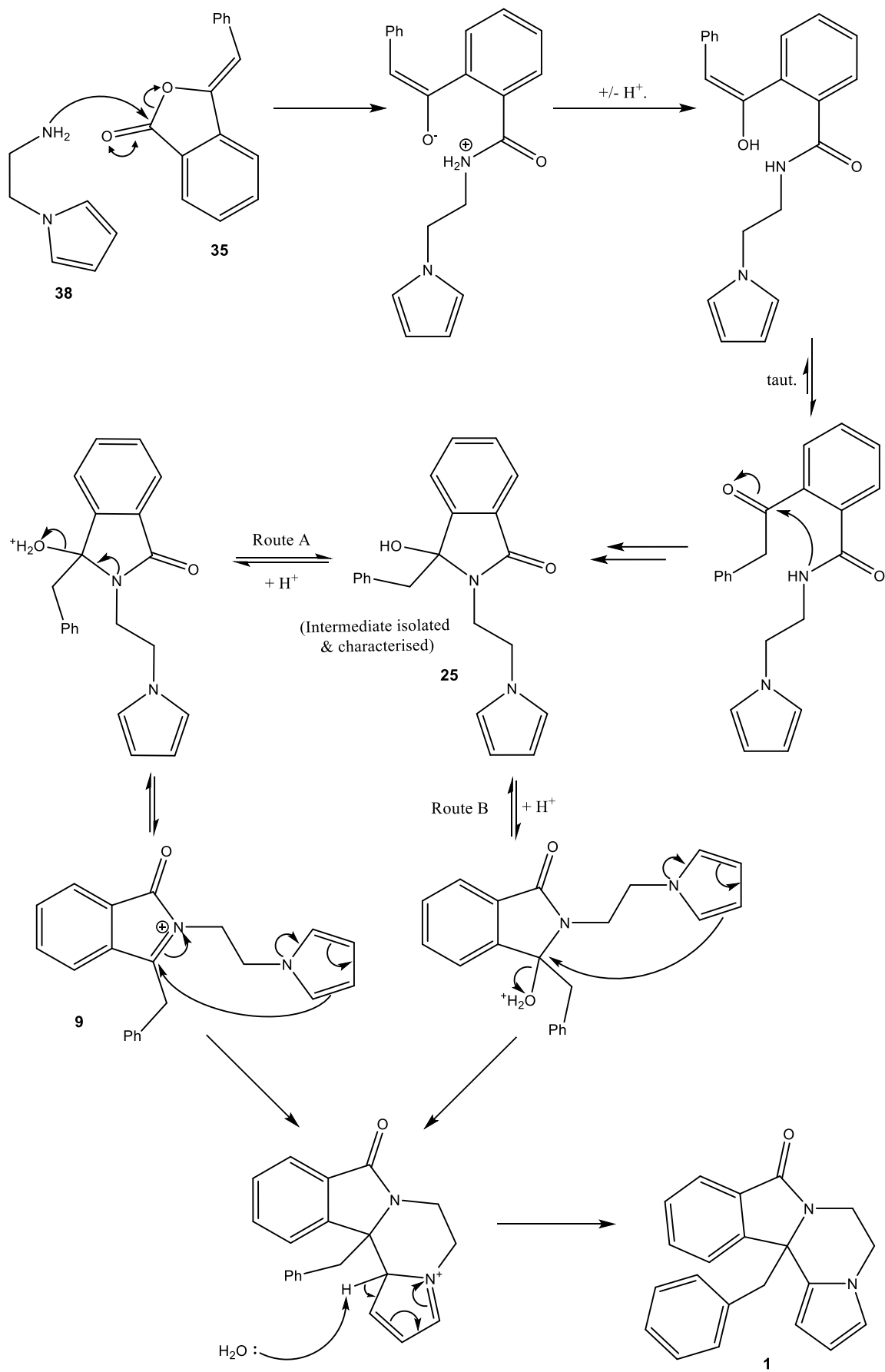
Figure 5: X-ray crystal structure of the final cyclised product, demonstrating the successful synthesis of the product **1**.

Based upon the test reaction, the second attempt involved some slight modifications to our initial procedure. Benzaldehyde (**36**, 10 mmol) and 2-(1*H*-pyrrol-1-yl)ethanamine (**38**, 1.2 equivalents) were initially refluxed in toluene for 24 hours, resulting in essentially quantitative conversion to the 3-hydroxyisoindolone intermediate **25** as determined by NMR spectroscopy. At this stage a portion of PTSA (13 mol%) was added, and the solution was refluxed for a further 24 hours. During this time, a colour change from clear to orange was observed. Following the same workup and purification procedure as detailed before, a yield of 86% of **1** was obtained, with almost complete conversion to the fully cyclised product. It was observed that the amount of PTSA used appeared to strongly influence reaction outcome; quantities less than 13 mol% typically failed to induce complete cyclisation, while larger quantities caused the reaction mixture to darken significantly and generate a deep red/black residue/tar that coalesced upon washing. It is well known that pyrrole and its corresponding compounds can readily polymerise under strongly acidic conditions,³³ and it was assumed that a similar reaction was occurring at the pyrrole ring in the intermediate. It was also discovered that the product could be readily isolated by crystallisation. Consequently, for all future reactions, recrystallisation from isopropyl alcohol was used in lieu of column chromatography as the standard purification technique, which afforded the product as clear orange crystals. This was due to the greater speed and convenience afforded by recrystallisation, at the cost of a slightly reduced yield of 72 versus 86%.

Proposed reaction mechanism

With regards to the reaction sequence, it is believed that primary amine group of **38** initially attacks the carbonyl centre of the benzaldehyde (**35**) (Scheme 17). Proton transfer, subsequent tautomerisation, and attack of the amine group at the newly revealed carbonyl afford the 3-hydroxyisoindolone intermediate **25**. Following addition of the acid catalyst (PTSA) to the mixture, two forward reaction routes are possible (Route A and B). In the first (Route A), elimination of the hydroxyl group affords the *N*-acyliminium ion intermediate **9**, which is subsequently attacked by the electron rich pyrrole ring to furnish **1**. Alternatively, a concerted displacement process may occur (Route B) in which there is concerted substitution of the protonated hydroxyl group by the pyrrole ring. Currently it remains unclear which of these two mechanisms is correct; it is also worth noting that the two are not necessarily mutually exclusive.

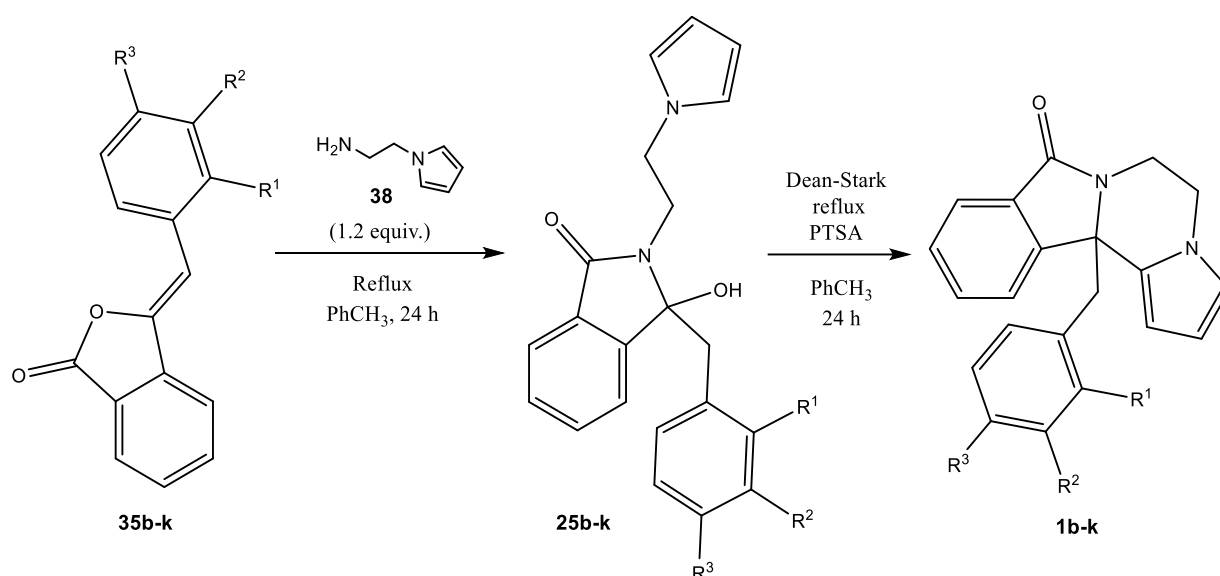
Having established a suitable procedure for the final synthesis of the isoindolone product **1**, we next wanted to establish the scalability of the reaction. The same procedure was followed, this time on a 40 mmol scale. To our delight, very similar yields were obtained following crystallisation (8.81 g, 70%), confirming the scalability of the reaction with the use of simple crystallisation purification, again being much simpler at larger scales.



Scheme 17: Proposed mechanism for the reaction of benzaldehyde (35) with 2-(1H-pyrrol-1-yl)ethanamine (38).

2.3.4 Preparation of substituted derivatives

Having developed a successful synthetic route, we turned our attention to generating various substituted derivatives of the isoindolone product **1**. Although it is inevitable that some variation in yield will be observed, we expected the performance of the reactions involving the substituted reagents to be broadly the same. For one, the position of the planned substitutions was remote to the reactive centre, mitigating any electronic effects the substituents might impart. Additionally, it was believed that any steric effects would be minimal; as seen in the X-ray crystal structure of the unsubstituted product (Figure 5), any substitutions at R¹, R² and R³ positions were remote from the newly forming reactive centre.



Scheme 18: Preparation of substituted derivatives with R¹, R² and R³ positions shown.

Each of the previously substituted benzaldehyde derivatives **35b-k** (10 mmol, Table 1) was reacted with 2-(1H-pyrrol-1-yl)ethanamine (**38**, 1.2 equivalents) under the same reaction conditions as detailed at section 2.3.3. The recrystallisations of products **1b-k** were performed from various solvents that depended on the derivative in question; acetonitrile, isopropyl alcohol, toluene and hexane/ethyl acetate were all found to be suitable candidates depending on the product (Table 2).

Table 2: Yields obtained for the substituted isoindolone derivatives.

Derivative	R ¹	R ²	R ³	Recrystallisation solvent	Yield/ %
1	H	H	H	isopropyl alcohol	72
1b	H	H	OMe	acetonitrile	32
1c	H	Cl	H	isopropyl alcohol	51

1d	H	H	Cl	isopropyl alcohol	22
1e	Cl	H	H	isopropyl alcohol	46
1f	H	H	F	isopropyl alcohol	21
1g	H	OMe	OMe	toluene	61
1h	H	F	H	isopropyl alcohol	66
1i	F	H	F	isopropyl alcohol	57
1j	OMe	H	H	hexane/ethyl acetate	61
1k	F	OMe	H	isopropyl alcohol	64

The performance of the reactions tended to be lower compared to the unsubstituted product, with yields ranging from 21-66%. Most notably, the isolated yields of derivatives **1d** and **1f** were consistently the poorest, even following the repetition of each experiment. An examination of the crude NMR spectra showed that the conversion levels of the cyclisation step appeared to be lower in these cases. The ^1H NMR spectrum of the crude product of **1d** is shown (Figure 6) in which the peaks of the corresponding enamide intermediate are clearly visible. One possible explanation could be that the chloro- and fluoro- groups deactivate the enamide intermediate through an inductive electron withdrawing effect, inhibiting protonation of the olefin and subsequent cyclisation.

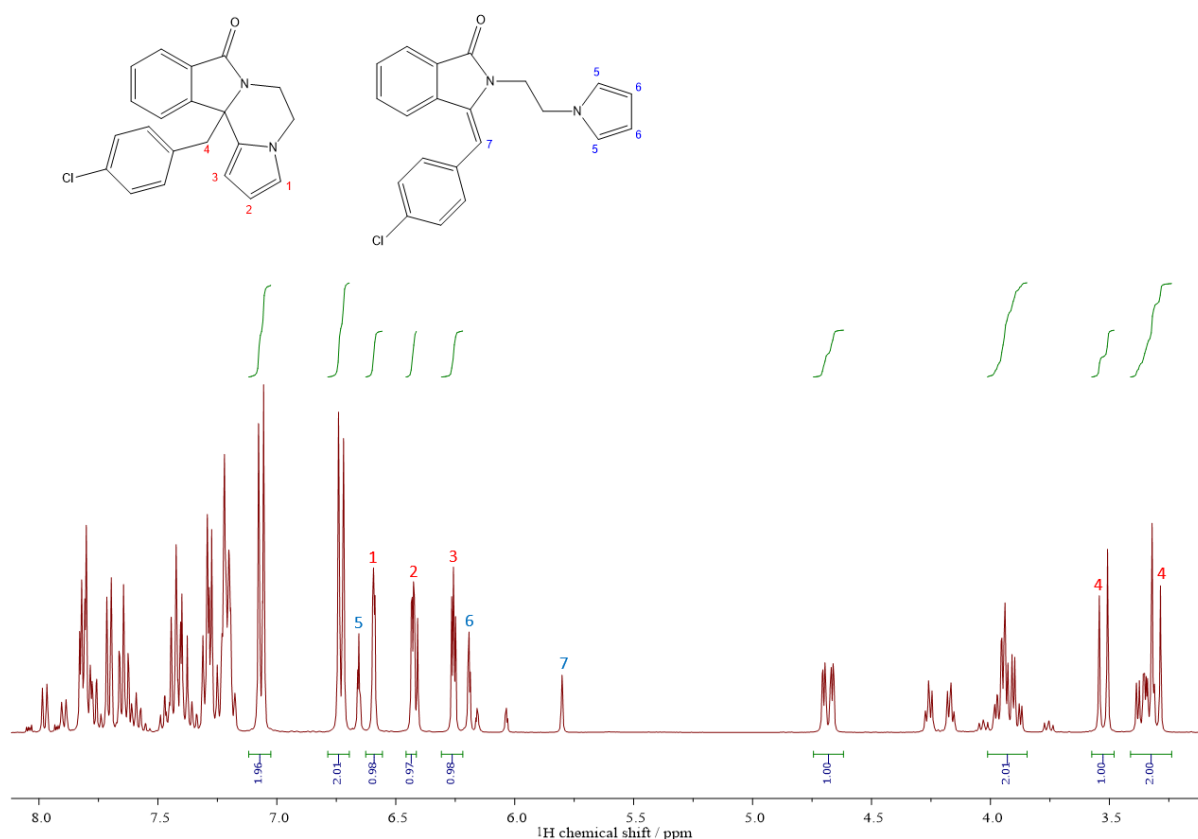


Figure 6: ^1H NMR spectrum of the crude 5D product, with peaks corresponding to the product **1d** the enamide intermediate **43d** labelled.

Additionally, we repeated the reaction of the 4-chloro substituted benzaldehyde **35d** with 2-(1H-pyrrol-1-yl)ethanamine (**38**) (one of the lowest yielding reactions). The reaction mixture was examined via ^1H NMR spectroscopy after the initial reflux in toluene. Interestingly, a conversion of only 40% to the hydroxy intermediate was observed (Figure 7, enamide peak of **35d** used for reference). This is in direct contrast to the corresponding unsubstituted reaction, in which virtually complete conversion was achieved. Furthermore, 3 separate pyrrolic peaks, each of integral ≈ 0.9 , were observed within the spectrum, suggesting that a reaction had occurred on the pyrrole ring. Analysis via LCMS only indicated the hydroxy intermediate and starting material as identifiable species. Consequently, we are still uncertain as to the reason behind the lower conversion to the hydroxy intermediate.

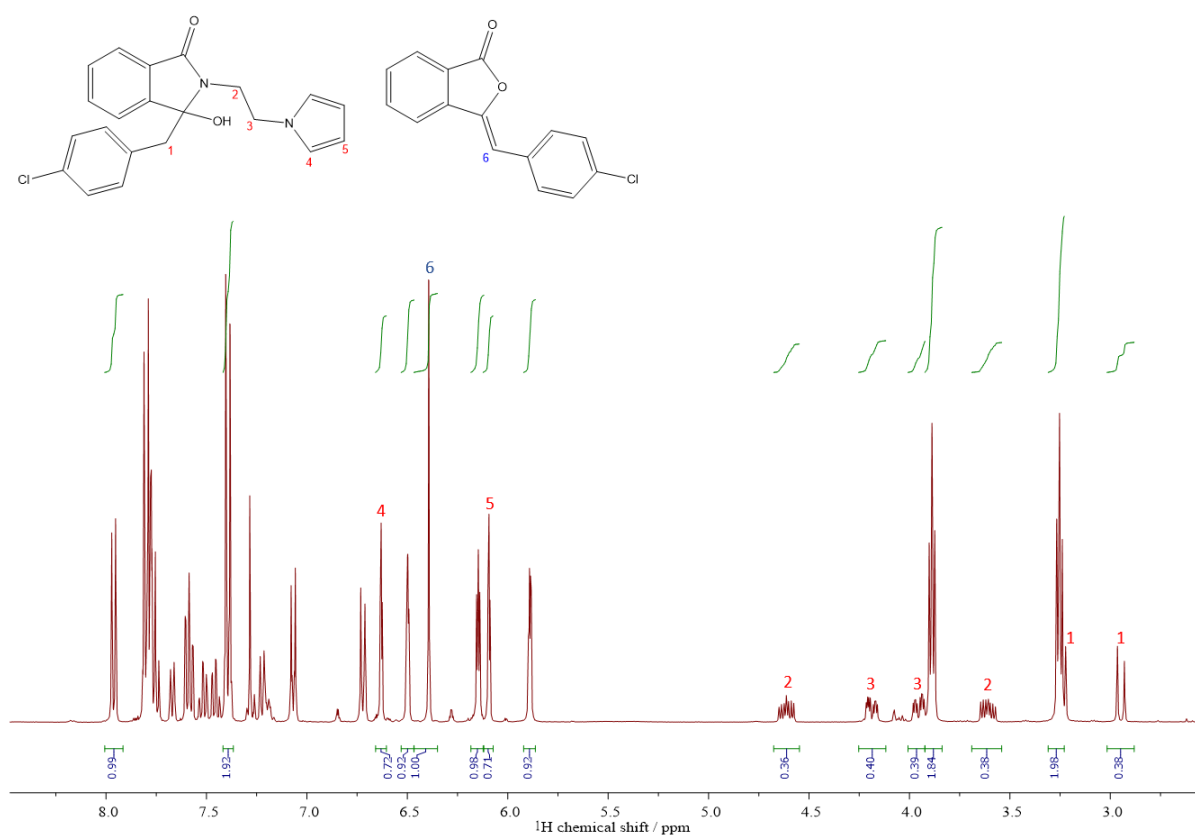


Figure 7: ^1H NMR spectrum of the reaction of 4-chloro substituted benzaldehyde **35** with 2-(1H-pyrrol-1-yl)ethanamine (**38**), after reflux in toluene for 24 hours.

2.3 Summary

The objective addressed in this chapter was to establish a synthetic route to our isoindolone product **1**. To this end, we successfully prepared the target molecule in a reasonable overall yield (57%, 3 steps), from readily available starting materials. We were also able to prepare substituted derivatives **1b-1k**, although in significantly reduced yields in some cases. It is possible that greater performance could be achieved simply by individually tailoring the reaction conditions to the derivative in question. In this respect, there are many examples in the literature of different solvents and acid catalysts

employed effectively to furnish equivalent cyclisations. For example, trifluoroacetic acid, dichloromethane and dioxane have all been employed effectively as solvents for similar reactions, and could pose as suitable replacements for toluene to improve conversion and therefore isolated yields.

3: Use of alternative nucleophilic components

3.1 Background

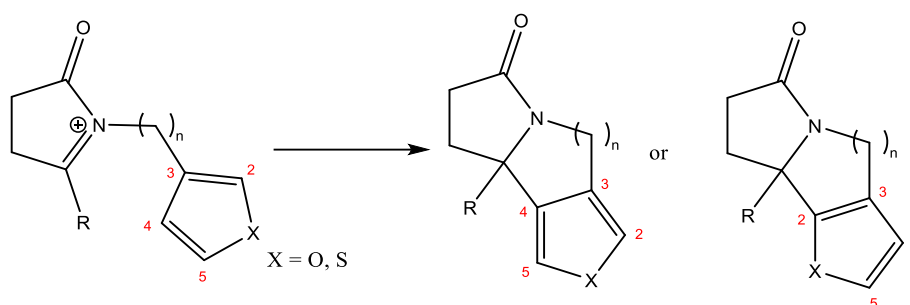
Having established a successful synthetic route for the synthesis of our desired heterocyclic compound **1** and its derivatives **1b-k** in chapter two, we wished to investigate the feasibility of expanding the range of nucleophilic components in the *N*-acyliminium cyclisation. Although the use of other nucleophiles in related systems is documented (see below), the apparent novelty of our 3-hydroxyisoindolone framework represented an unexplored area. The *N*-acyliminium ion is formed at a benzyl-substituted tertiary carbon, which constitutes a relatively hindered reacting centre. While the formation of a 6 membered ring with an electron-rich pyrrole nucleophile had worked well (arguably the most straightforward reaction), we were interested to see how tolerant the reaction was toward less electron-rich species. Furthermore, the potential to form different ring sizes was also of interest. In particular, 7-membered rings are a common structural feature of both natural products and pharmaceuticals, yet their synthesis remains challenging. Finally, we wished to explore some less-common nucleophiles in *N*-acyliminium ion cyclisations. Imidazole is one example for which there are relatively few studies concerning its use. Additionally, while the use of π -based nucleophiles is well documented, there are very few examples of σ -based nucleophiles being employed. Investigating these variables would thus allow us to demonstrate the versatility of the reaction, while increasing the library of compounds available for structure-activity testing through our collaborations.

3.1.1 Reactivity of heterocyclic aromatic systems- pyrrole, thiophene and furan

As mentioned in chapter 1, the scope of the *N*-acyliminium cyclisation extends far beyond the use of the pyrrole-based nucleophiles we initially employed. The first related examples of this reaction by Belleau *et al.* employed an unsubstituted aryl species as the nucleophile, albeit requiring heating for 24 hours in excess polyphosphoric acid at a temperature of 100 °C.¹⁵ The efficacy of the nucleophilic cyclisation depends on its propensity to donate electron density; in the case of aromatic π -systems, this in turn depends on how electron rich the aromatic ring is. Heterocyclic systems such as pyrrole, thiophene and furan contain nitrogen, sulfur, and oxygen respectively in the aromatic ring. The electron donating heteroatoms increase the electron density and thus the rings' nucleophilic character. The degree of this electron donating effect is determined by several factors. Both pyrrole's and furan's lone pairs of electrons reside in 2p orbitals, providing good energy matches for the 2p orbitals of the remaining 4 carbon atoms. However, the nitrogen atom of pyrrole is less electronegative than furan's oxygen atom, leading to a greater electron-donating effect. By contrast, thiophene's lone pair resides in a 3p orbital, and is therefore a poorer energy match to the rest of the

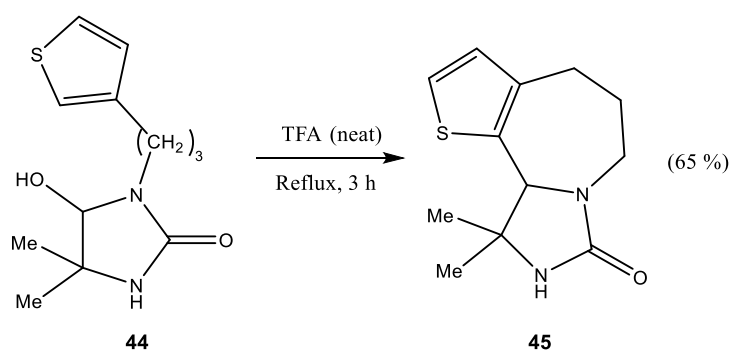
carbons' 2p orbitals. The order of nucleophilicity (in decreasing order) is therefore pyrrole, then furan, then thiophene.³³

The use of thiophene and furan in particular poses an interesting issue not observed in the case of *N*-substituted pyrroles. Direct substitution (tethering) at the heteroatom position is impossible for either thiophene or furan, and so the tether for intramolecular reactions must be attached at the 2 or 3 position (Scheme 19). This gives rise to the potential for varying regiochemical outcomes of the ensuing intramolecular cyclisation, depending on where the new carbon-carbon bond is formed.



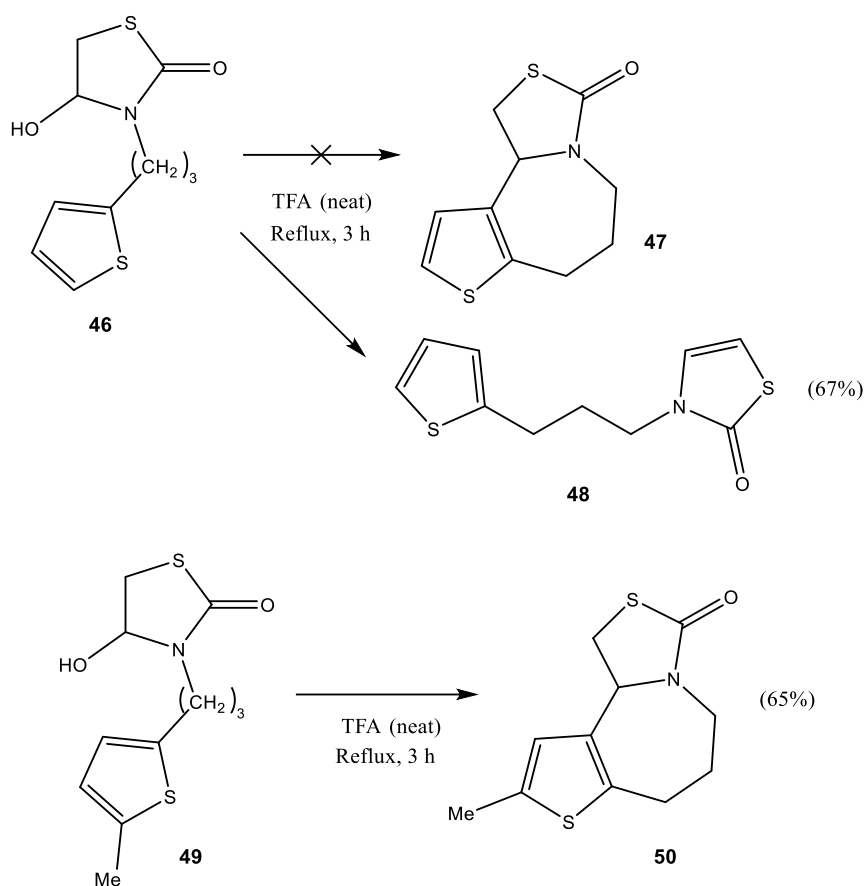
Scheme 19: Example *N*-acyliminium cyclisation of furan or thiophene. The numbering of the aromatic ring shown is the convention adopted in this text.

For thiophene, reaction outcomes are typically straightforward to predict. In the following illustrative example provided by Kano *et al.* (Scheme 2), the use of a 3-substituted thiophene component **44** resulted in the exclusive formation of a single 2-alkylated regioisomer **45** in a 65% yield.³⁵ In the case of 3-substituted thiophenes, cyclisation at the 2-position is typically most favourable.^{36,37}



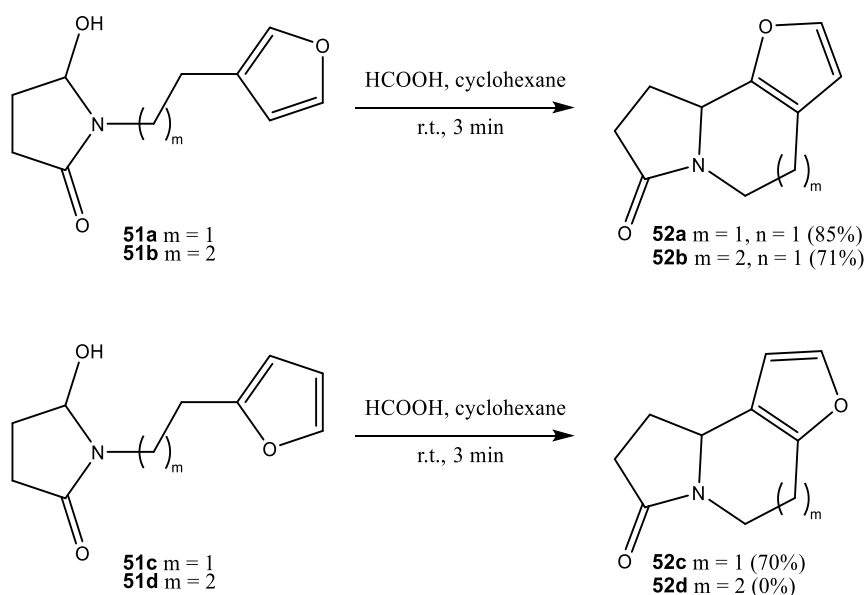
Scheme 20: Cyclisation of a thiophene ring tethered at the 3-position, demonstrating the single regiochemical outcome.³⁵

Interestingly, attempts by Kano *et al.* to cyclise a similar species **46** with a tether at the 2-position were unsuccessful, instead leading to the dehydration product **48** (Scheme 21). This reflects the lower reactivity observed by the thiophene ring as a nucleophilic species. By contrast, the same reaction performed with the alkyl-substituted thiophene **49** (a weakly electron donating substituent) successfully cyclised to give the desired product **50** as a single regioisomer.³⁵



Scheme 21: Top: generation of the alternative enamide product **48** from a thiophene tethered at the 2-position **46**. Bottom: successful cyclisation to an alkyl-substituted thiophene ring **50**.³⁵

Related examples of furan's nucleophilic use in *N*-acyliminium cyclisations are limited, with work predominantly carried out by Tanis *et al.*^{38,39} The reaction outcome is highly dependent on a multitude of factors, including the position of the furan tether, the tether length, and the presence of any substituents on the furan ring. Furans linked at the 3-position are capable of cyclising to potentially form 6 and 7 membered rings (Scheme 22), however, the products were found to exclusively cyclise at the 2-position.³⁸ By contrast, furan-based species with a tether at the 2-position were only found to cyclise in the case of 6-membered rings under the same conditions.



Scheme 22: Examples of furan-based N-acyliminium cyclisations performed by Tanis et al.³⁸

One possible explanation for the reactive tendencies of these heterocycles could be derived from examining their respective HOMOs (highest occupied molecular orbitals). In each case, the largest contribution to the HOMO (and correspondingly the greatest electron density) is found at the C-2 position; this is therefore the preferential site of reaction in the case of electrophilic substitution (Figure 8). Of course, this argument only considers the ground state of these heterocycles, and therefore assumes that the HOMOs of the respective transition states would be similar.

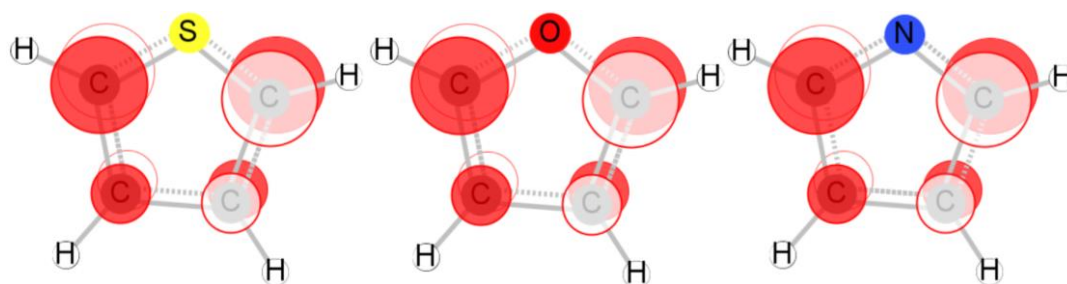
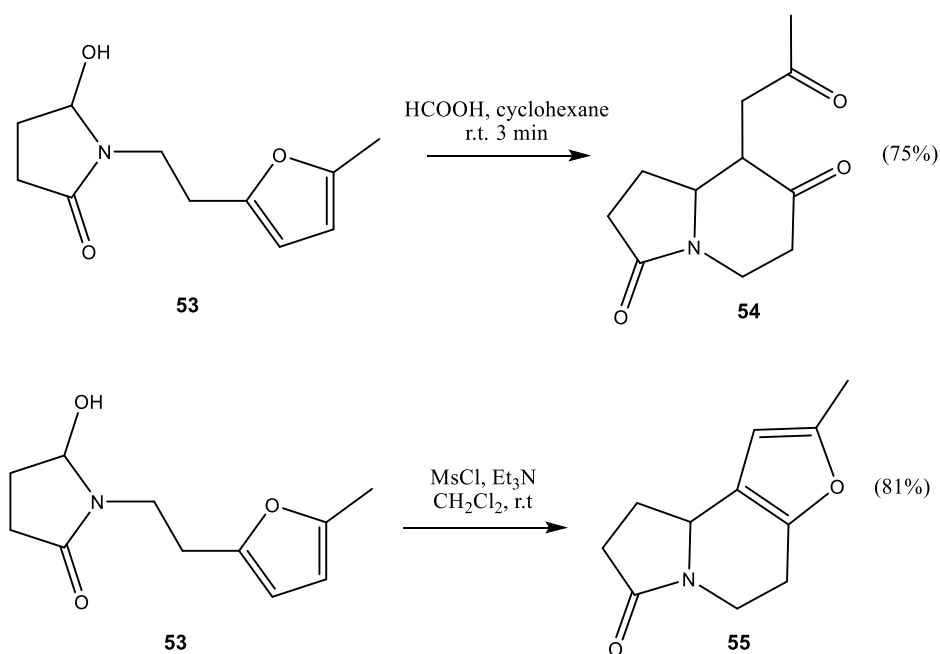


Figure 8: HOMOs of thiophene (left), furan (middle) and pyrrole (right). Molecular orbitals calculated with HuliS version 3.3.6.⁴⁰

The use of furan in *N*-acyliminium cyclisations is accompanied by another problem not observed for either thiophene or pyrrole systems; the furan ring is susceptible to degradation under the acidic conditions commonly employed to generate the *N*-acyliminium ion. In the following example, treatment of the furan **53** with formic acid in cyclohexane leads to hydrolysis of the furan ring to afford the diketone **54**. This necessitates the use of alternative conditions to generate the *N*-acyliminium ion

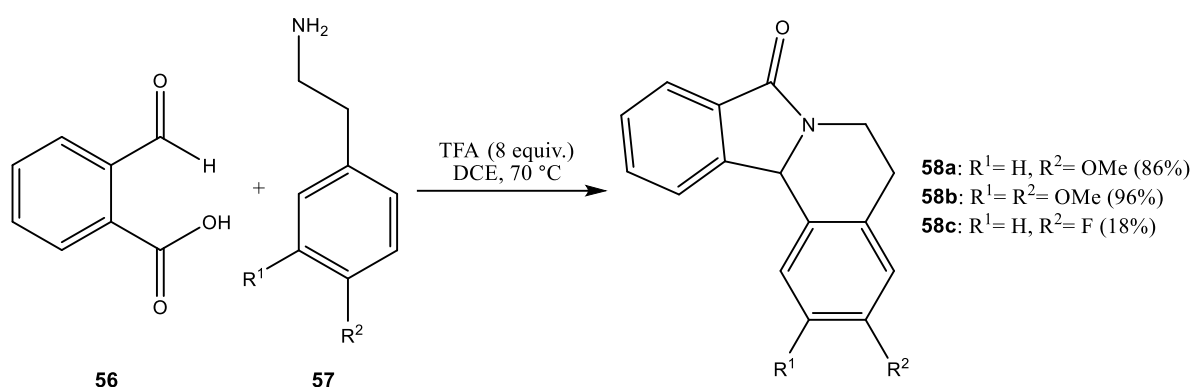
and subsequently furnish the desired heterocycle **55**, namely mesityl chloride and triethylamine as the activation method (Scheme 23).³⁸ As a consequence, cyclisations involving a furan moiety are typically performed under anhydrous conditions with a short reaction time, to avoid a reduced yield and potential side product formation.



Scheme 23: Top: hydrolysis of furan **53**, leading to diketone **54**. Bottom: use of alternative reagents to furnish the desired heterocycle **55**.³⁸

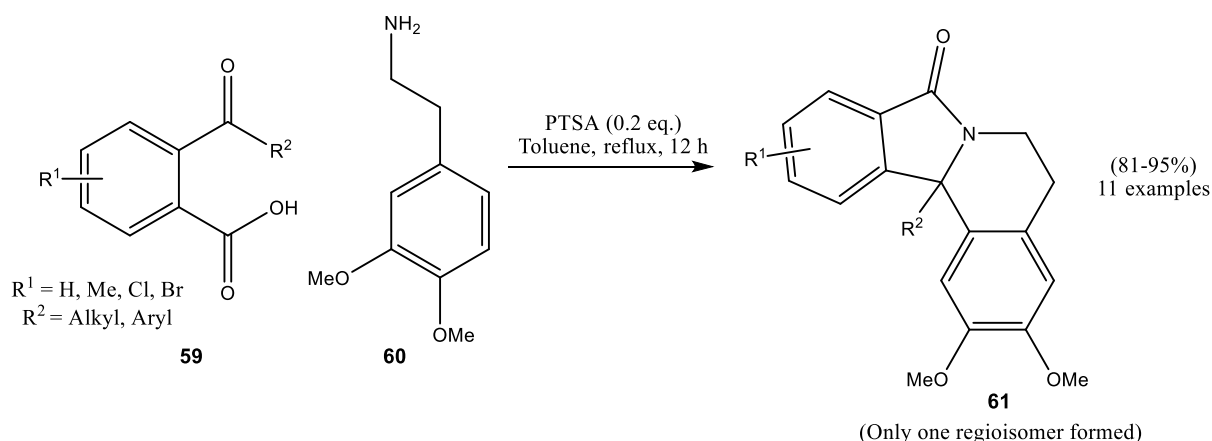
3.1.2 Reactivity of aryl-based nucleophiles

In the case of aryl species, electron donating substituents can be used to activate the aromatic ring, providing a similar order of reactivity to the heterocycles mentioned above. The degree of substitution influences the nucleophilicity of the aromatic ring, but in most instances cyclisation nonetheless occurs with no appreciable difference in performance, provided the substituents are electron donating. For example, Huang *et al.* detailed the cyclisation of mono- and dimethoxy-phenyl species and reported yields of 86% and 96% respectively (Scheme 24); by contrast, replacement of the methoxy substitutions with a para-fluoro group (σ_m : +0.337, σ_p : +0.062) resulted in a considerably reduced yield of 18%.⁴¹



Scheme 24: Cyclisations of substituted aryl species performed by Huang et al.⁴¹

The use of substituted aryl derivatives in these cyclisation reactions is also accompanied by the potential for different regiochemical outcomes. In the example below, the 3,4-dimethoxyphenyl component **60** could feasibly react at either the 2 or 6 position, giving rise to 2 regioisomers. However, attack occurs exclusively at the 6-position to give product **61** (Scheme 25).⁴² Such an outcome can likely be attributed to the steric effects of the methoxy groups **Error! Reference source not found.**



Scheme 25: N-acyliminium cyclisations employing 3,4-dimethoxybenzene as a nucleophile.⁴²

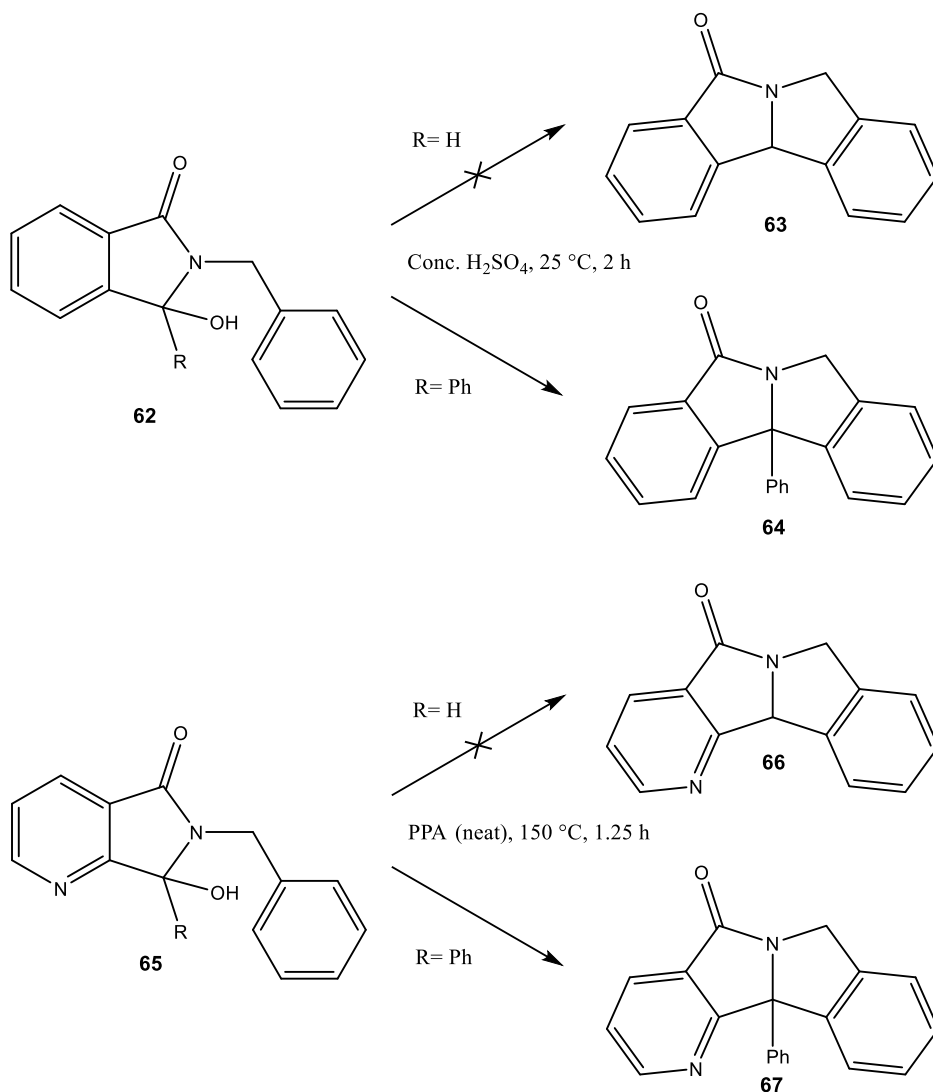
3.1.3 Impact of the forming ring size

While the nature of the nucleophile plays an important role in the success of the intramolecular *N*-acyliminium cyclisation, it is also necessary to consider the size of the newly forming ring. In general, the scope of the reaction is reasonably broad; the syntheses of 5, 6, 7 and 8 membered rings have all been previously detailed in literature.³⁶ However, difficulties arise toward both ends of this scale, particularly for weaker nucleophiles.

Formation of 5-membered rings

The formation of 5-membered rings is inherently challenging via the *N*-acyliminium pathway, as these reactions tend to be examples of 5-*endo-trig* cyclisations (disfavoured according to Baldwin's rules²⁴).

In the example provided by Winn *et al.*, the 3-hydroxyisoindolone species **62** was incapable of forming a 5-membered ring when R = H, even in concentrated sulfuric acid.⁴³ These findings were mirrored by Hitchings *et al.*, who undertook a similar cyclisation except with *N*-substituted hydroxyphthalimidines **65** in polyphosphoric acid (Scheme 26).⁴⁴ Interestingly, however, the same cyclisations were possible in each case when the R group was changed from hydrogen to phenyl.



Scheme 26: Work performed by Winn *et al.*⁴³ (top) and Hitchings *et al.*⁴⁴ (bottom), demonstrating the discrepant reactivities with H and phenyl R-groups.

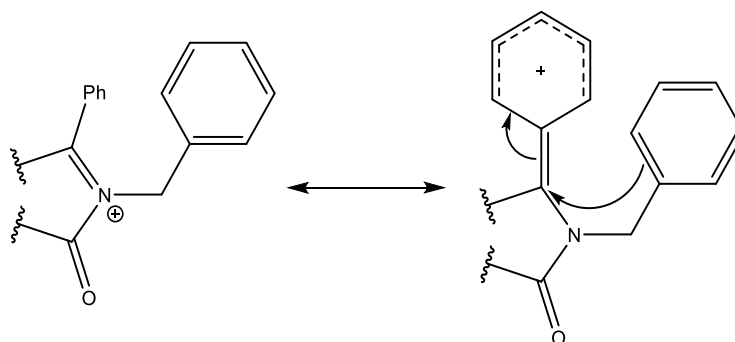
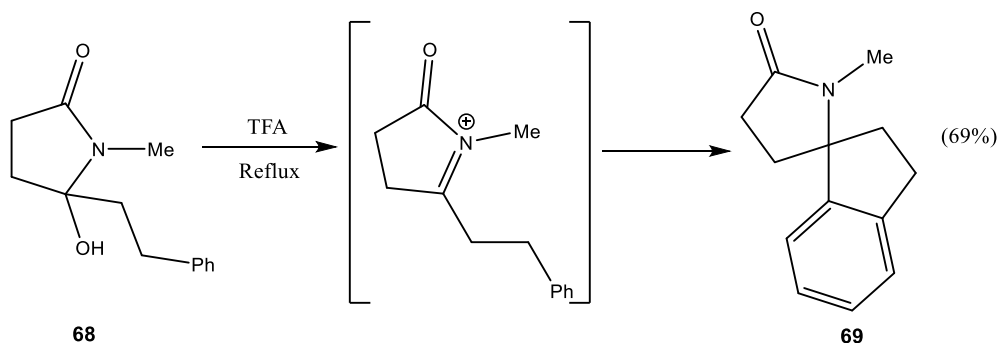


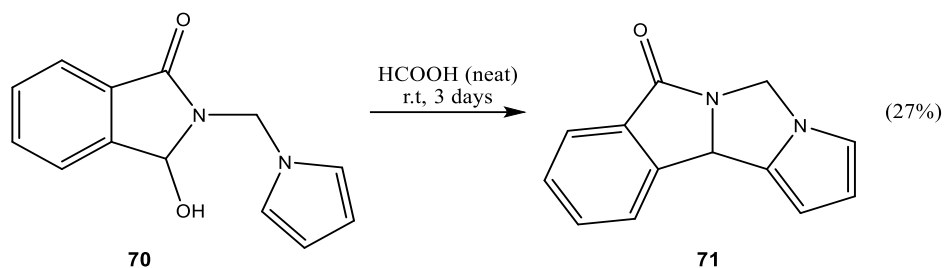
Figure 9: Resonance canonicals of the phenyl-substituted *N*-acyliminium intermediates described in Scheme 26.

One possible explanation is the increased stability of the *N*-acyliminium ion through resonance effects when there is a phenyl ring attached to the α -carbon. Additionally, the phenyl group may facilitate ring-closure by conferring 5-*exo-trig* character on the cyclisation step, which then becomes a favoured cyclisation process (Figure 9). This latter argument is further supported by the fact that aryl nucleophiles can readily form 5-membered rings in *N*-acyliminium cyclisations when the ring in question is spirocyclic.^{45,46} In the following example (Scheme 27), **68** was successfully cyclised to the spirocyclic structure **69** in a 69% yield following reflux in trifluoroacetic acid.



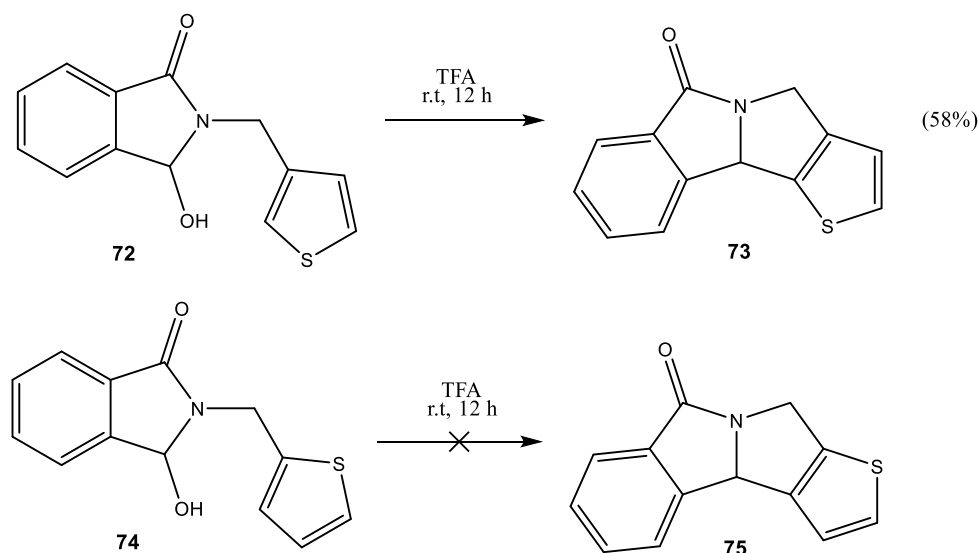
Scheme 27: Successful 5-*exo-trig* spirocyclic ring closure performed by Bailey et al.⁴⁵

By contrast, more electron-rich heterocyclic systems have far less trouble forming 5-membered ring systems in *N*-acyliminium cyclisations. For example, the electron-rich pyrrole ring in **70** is a sufficient nucleophile to offset the unfavourable 5-*endo-trig* cyclisation, albeit in a reduced yield of 27% (Scheme 28).^{47 48}



Scheme 28: Successful 5-membered cyclisation of a pyrrole nucleophile.⁴⁷

Equivalent thiophene based systems are also capable of cyclising, though only when the more reactive 2-position is available for reaction. Othman *et al.* documented the successful cyclisation of **72** to **73** in trifluoroacetic acid in a 58% yield, however, the same reaction did not proceed for the equivalent 2-substituted thiophene **74** (Scheme 29).⁴⁸

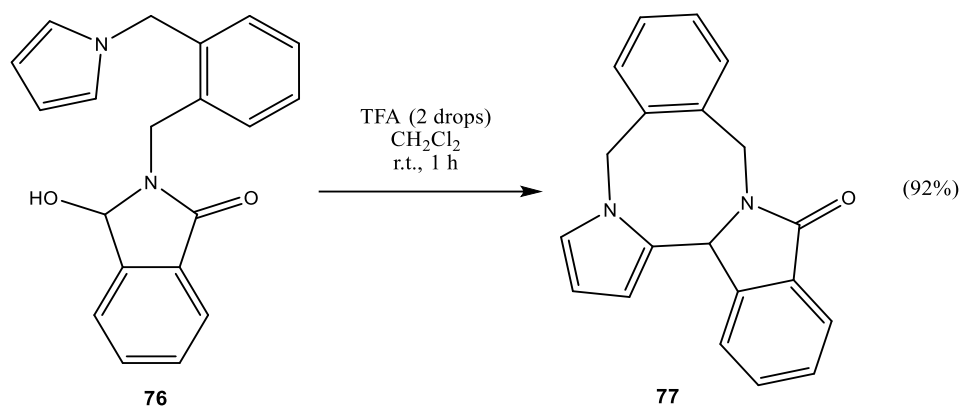


Scheme 29: 5-membered cyclisation of thiophene derivatives.⁴⁸

Formation of 7 and 8-membered rings

The formation of larger ring systems also poses challenges, for different reasons. Transannular ring strain, and the longer length of the connecting tether means that such cyclisations can incur significant enthalpic and entropic penalties. In terms of *N*-acyliminium ion cyclisations, the trend of larger ring systems is the same as the 5-membered cyclisations detailed above; less reactive nucleophiles pose more difficulty than their electron rich counterparts. The formation of 7-membered rings in arene cyclisations can be troublesome, but several successful examples have been documented.^{49,50} In general, it appears that a stronger acid catalyst or a more reactive acyliminium centre are instrumental to the success in these cases. More examples exist for nucleophiles such as thiophene (as seen in Scheme 20) and pyrrole; most remarkably, formation of an 8-membered ring from **76** was documented by Othman *et al.*⁵¹ The compound was isolated in a 92% yield on a 0.36 mmol scale,

using 2 drops of trifluoroacetic acid as the activation catalyst. Obviously, the integration of the aromatic system into the tethering chain, significantly helps with conformational inflexibility and thus probability of cyclisation.



Scheme 30: Successful cyclisation of a tethered pyrrole nucleophile to afford an 8-membered ring.⁵¹

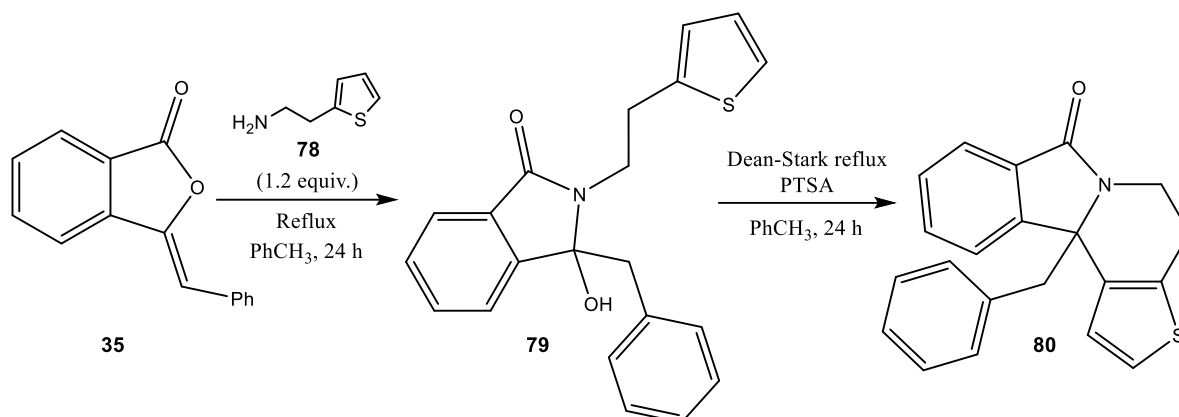
3.2 Results and discussion overview

To examine the varying stereoelectronic effects of changing the nucleophile, we sourced a variety of structural analogues of the 2-(1*H*-pyrrol-1-yl)ethan-1-amine (**38**) coupling partner as employed in chapter 1, with pyrrole replaced by alternative nucleophilic components in each case. The compounds were chosen for their commercial availability and their low cost, while maximising the structural diversity in order to investigate the reaction scope. Additionally, we used the 3-(1*H*-pyrrol-1-yl)propan-1-amine (**42**) prepared in chapter 2, together with 1-(3-aminopropyl)imidazole (**94**), to investigate the feasibility of forming 7-membered rings within our heterocyclic system.

The synthetic procedures were analogous to those used in chapter 1, with the reactions being each performed on a 10 mmol scale. Benzaldehyde (**35**) and the nucleophilic component (1.2 equivalents) were initially heated at reflux for 24 hours to afford the corresponding 3-hydroxyisoindolone adduct. PTSA was subsequently added, and the reaction was again heated at reflux under Dean-Stark conditions for a further 24 hours. Workup consisted of washing with water and sodium hydrogen carbonate, followed by recrystallisation to purify the crude material. Crude conversion was monitored by ¹H NMR spectroscopy; in the case of unsuccessful cyclisation and enamide formation, the quantity of PTSA used was increased, up to a maximum of 1 g (equating to 50 mol%). In some cases, the lower reactivity of the nucleophile necessitated the use of Eaton's reagent as an acid catalyst in lieu of PTSA. This consists of a 10% by weight solution of phosphorous pentoxide dissolved in methanesulfonic acid (formula weight: 142.0 g mol⁻¹). The reactivity of Eaton's reagent is comparable to that of polyphosphoric acid, but its lower viscosity results in far easier handling.

3.2.1 Reaction of heterocyclic aromatics

Thiophene-2-ethylamine

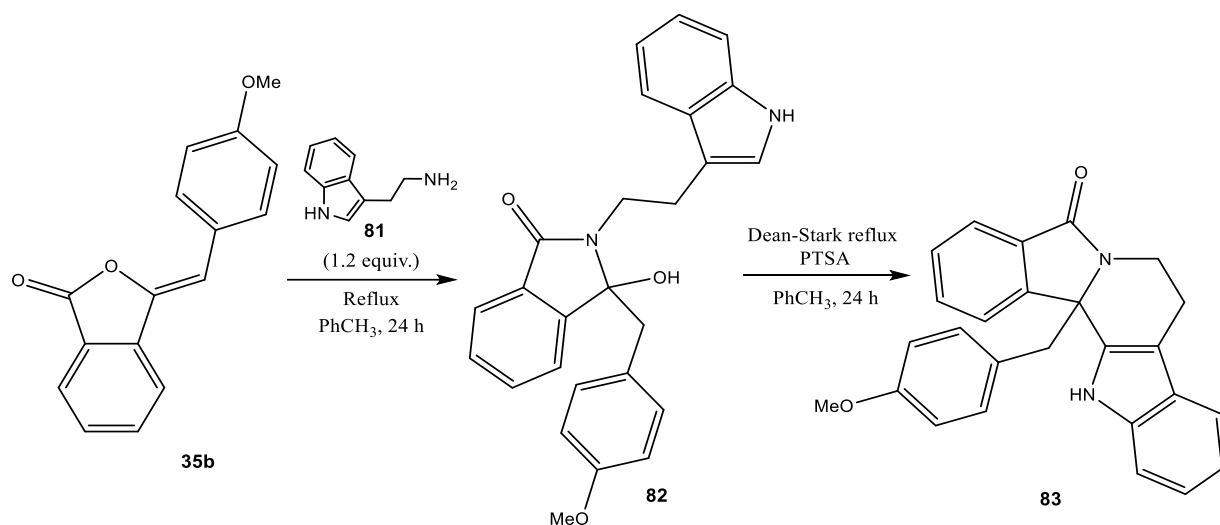


Scheme 31: Reaction of thiophene-2-ethylamine (78) with benzalphthalide (35).

For our first attempt at utilising an alternative nucleophilic component, we examined the reaction of thiophene-2-ethylamine (**78**) with benzalphthalide (**35**). Post-reaction analysis via ¹H NMR indicated that the cyclisation had not been successful and instead the corresponding enamide product had been recovered. This outcome was not entirely surprising; as mentioned above, thiophene is a less reactive nucleophile than pyrrole, particularly when the more reactive 2-position is blocked.

The reaction was repeated again, this time using an increased quantity of PTSA (16 rather than 13 mol%). To our delight, the NMR spectrum suggested the cyclisation was successful, with virtually 100% conversion to the desired product **80**. Recrystallisation from isopropyl alcohol afforded the purified product as light brown needles in a 60% yield. This outcome marked an interesting contrast to the findings of Kano *et al.*, as their 2-substituted thiophene system failed to undergo cyclisation (Scheme 21).³⁵ The cause of this discrepancy is likely to be due to the differing sizes of the rings being formed; additionally, it may be that TFA affords less forcing reaction conditions than PTSA.

Tryptamine



Scheme 32: Reaction of tryptamine (81) with benzaldehyde (35).

Indole systems can be considered similar to pyrrole in terms of reactivity, and so we expected the reaction of tryptamine (81) with benzaldehyde (35) to proceed smoothly to yield the polycyclic heterocycle 83. In the case of the indole systems, there is ambiguity as to whether cyclization takes place via a simple S_N1-type mechanism (Path A), or via alkyl migration of a spiroindoline intermediate (Path B) (Figure 10).⁵² Regardless, the anticipated product was isolated following our standard experimental procedure in a 91% yield.

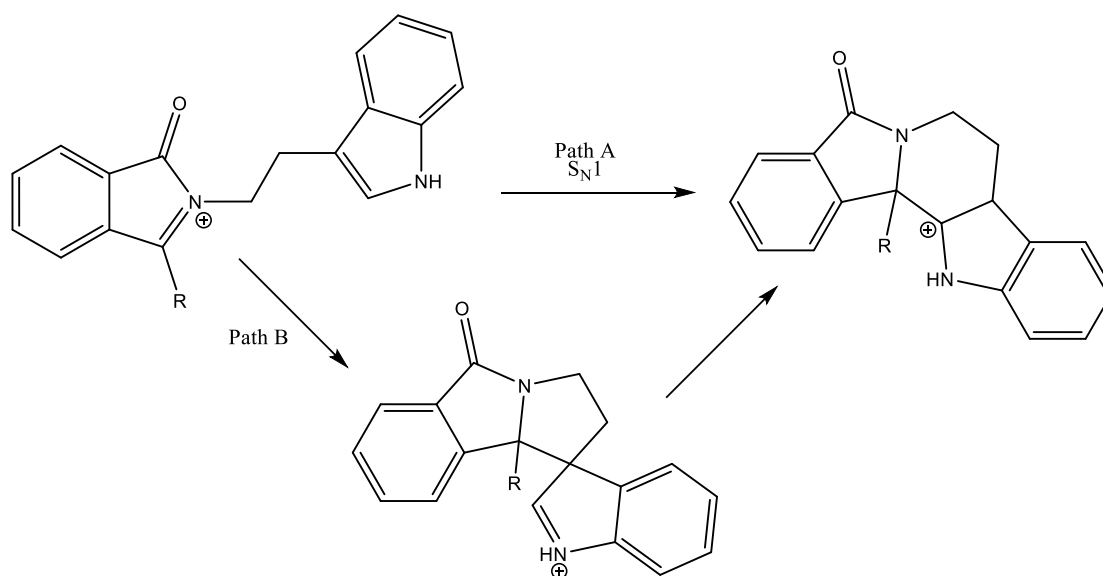
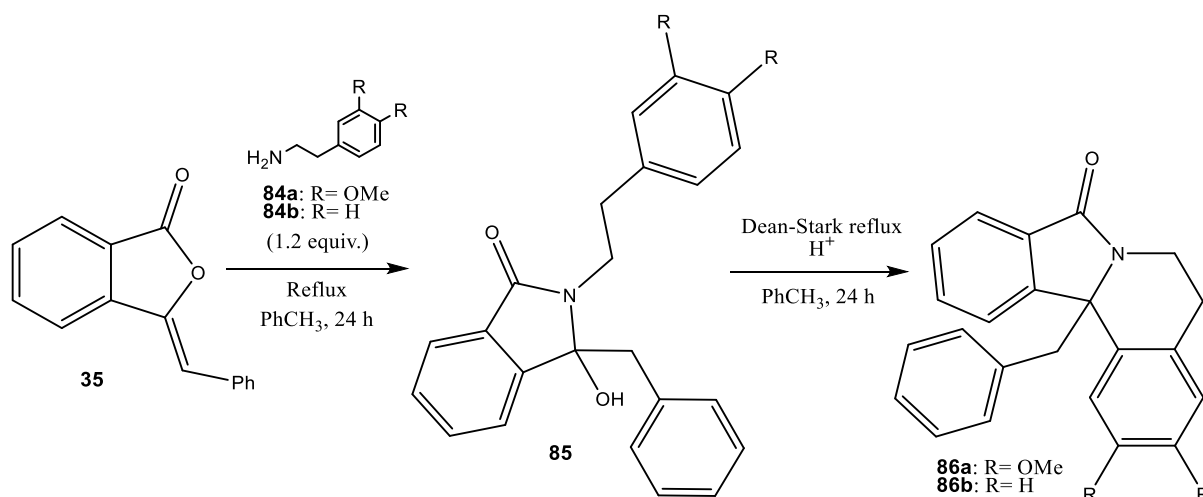


Figure 10: potential reaction mechanisms for the acyliminium cyclisation of indole systems.

3.2.2 Reactions of aryl nucleophiles



Scheme 33: Reaction of phenylethylamine (84b) and 3,4-dimethoxyethylamine (84a) with benzalphthalide (35).

Next, we turned our attention to examining aryl-systems as potential nucleophiles. 3,4-dimethoxyphenylethylamine (**84a**) and phenylethylamine (**84b**) are commercially available at a relatively low cost, and so both compounds were sourced to investigate their propensity for cyclisation within our *N*-acyliminium system. Cyclisation with the 3,4-dimethoxy moiety **84a** was attempted first, initially employing 13 mol% PTSA for the second stage catalysis. Analysis of the crude ¹H NMR spectra indicated the formation of multiple products; once again however, the enamide species was the only easily identifiable intermediate. Repeating the experiment with 16 mol% PTSA yielded the fully cyclised species, which was subsequently recrystallised from ethyl acetate to afford the purified product as light-yellow crystals (57% yield). All collected spectral data (NMR, LCMS, X-ray crystallography) indicated the formation of a single regioisomer **86a**, arising from attack from the 6-position, in agreement with the prior analogous literature (section [3.1.2](#)).

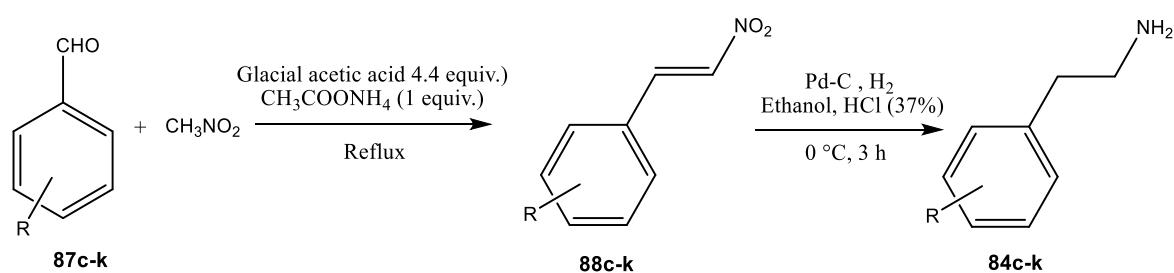
Following this success, we attempted the same procedure with the unsubstituted phenylethylamine **84b**. However, only the enamide product was obtained even when employing up to 50 mol% PTSA. As such we attempted more forcing conditions, employing 1 equivalent of Eaton's reagent as an alternative stronger acid catalyst and dehydrating reagent. Following reflux for 24 hours, analysis of the NMR spectral data indicated the cyclisation had been successful to form **86b**. This was confirmed by X-ray crystallography following recrystallisation from isopropyl alcohol (52% yield). The discrepancy between the reactivities of the unactivated and methoxy substituted aryl nucleophiles agrees with prior literature - as mentioned previously (section [3.1.1](#)), the degree of nucleophilicity is a major factor in how easily the intramolecular cyclisation occurs.

To further investigate the electronic effects of substituents on the aromatic ring, we sought to synthesise a greater range of aryl-based nucleophiles in a two-step synthesis from substituted benzaldehydes **87c-k** (Table 3).

Table 3: substituted benzaldehydes 87c-k

Compound	Structure	Compound	Structure
87c		87h	
87d		87i	
87e		87j	
87f		87k	
87g			

A Henry reaction with nitromethane would afford the corresponding β -nitrostyrenes, which could then be reduced via sequential hydrogenation to our desired substituted phenylethylamines **84c-k** (Scheme 34).



Scheme 34: 2 step synthesis of substituted phenylethylamines from the corresponding benzaldehydes.

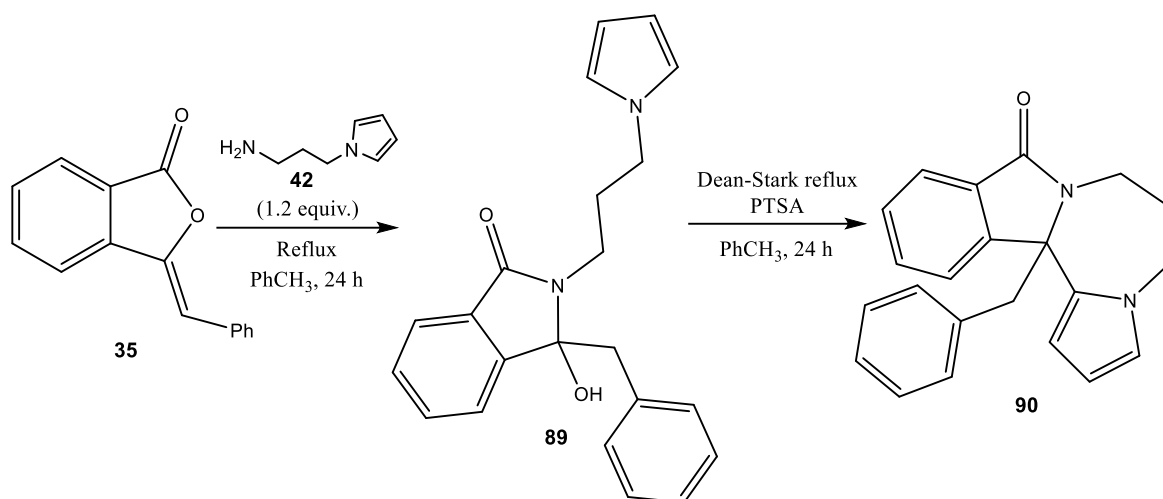
The initial Henry reaction was carried out following a procedure disclosed by Agarwal *et al.*⁵³ Equimolar quantities of the arylaldehyde and $\text{CH}_3\text{COONH}_4$ in glacial acetic acid were reacted with an excess of nitromethane under reflux. This approach allowed the synthesis of a range of β -nitrostyrenes **88c-k** which were isolated following recrystallization from ethanol in yields of 65-82%.

Next, we attempted the hydrogenation of the nitrostyrenes, using a procedure documented by Kohno *et al.*⁵⁴ using ethanol, 37% HCl and 5% palladium on charcoal (10 mol% Pd). Unfortunately, despite repeated attempts none of the desired reduced material could be isolated. One potential reason could

be the precise nature of the catalyst employed; as examined by Crawford *et al.*, the exact properties of the catalyst can have a major effect on reaction efficacy.⁵⁵ Due to time constraints on the project we decided to place further work on this aspect of the chemistry on hold until this could be more comprehensively explored.

3.2.3 Formation of 7-membered heterocycles

3-(1*H*-pyrrol-1-yl)propan-1-amine



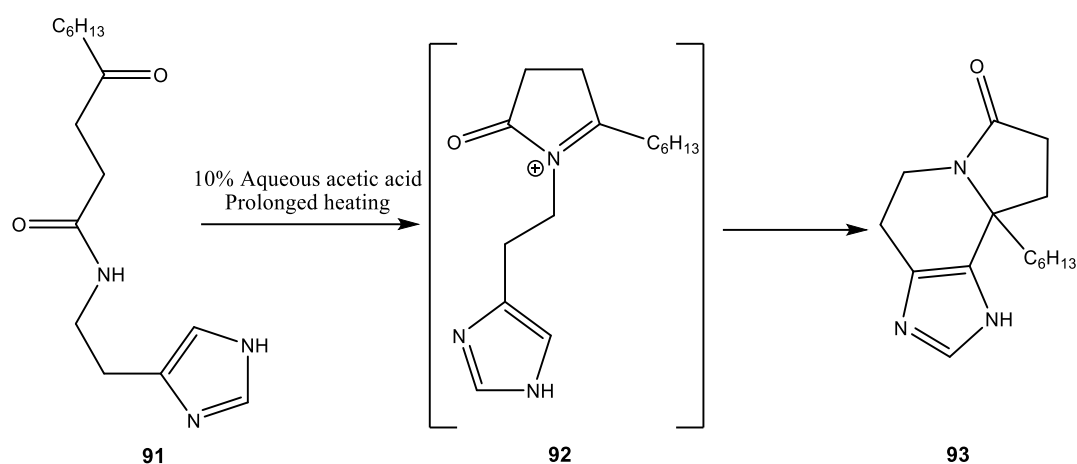
*Scheme 35: Reaction of 3-(1*H*-pyrrol-1-yl)propan-1-amine (42) with benzaldehyde (35).*

To investigate the effect of larger ring formation, 3-(1*H*-pyrrol-1-yl)propan-1-amine (42) was prepared according to the method described in chapter 1. It was expected that the electron-rich pyrrole would be able to offset the less favourable entropic cyclisation conditions. Following essentially quantitative conversion to the hydroxy intermediate 89, reflux with 16 mol% PTSA resulted in a darkening of the solution from colourless to a deep red. Analysis of the ¹H NMR of the resulting crude material indicated complete conversion to the desired product, illustrating that the electron-rich pyrrole system was more than enough to offset the greater entropic penalty. The solution was washed, and the solvent removed *in vacuo*. Recrystallisation from isopropyl alcohol afforded the purified product 90 as yellow, needle-like crystals in a yield of 45%.

1-(3-Aminopropyl)imidazole

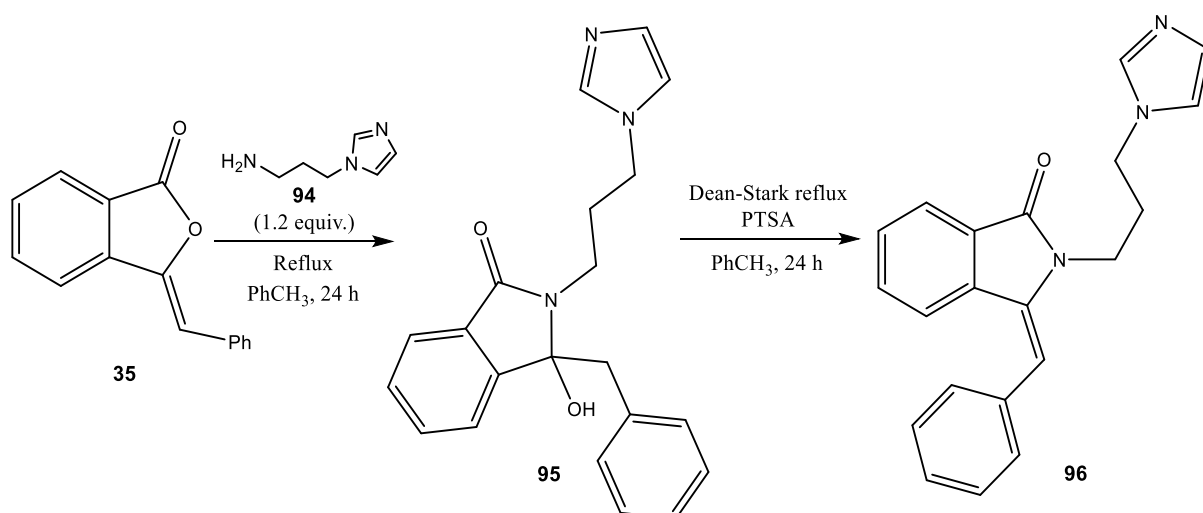
Encouraged by the success achieved with the 7-membered ring we elected to evaluate the corresponding imidazole variant. Examples of imidazole based cyclisations are extremely rare in the literature, and we were intrigued as to whether the commercially available 1-(3-aminopropyl)imidazole (94) would be capable of undergoing cyclisation. We expected the reactivity to be somewhat lower than pyrrole; the lone pair of the second nitrogen atom of imidazole is not delocalised, and its electronegative character reduces the energy of the HOMO. This in turn reduces

the nucleophilicity of the aromatic ring. One of the few documented works is by Lambertson *et al.* on histamine-based alkaloids (Scheme 36).⁵⁶ This work details the transformation of starting material **91** into heterocycle **93** (presumably through intermediate **92**) in an undisclosed yield when subjected to prolonged heating in 10% aqueous acetic acid.



Scheme 36: Imidazole-based *N*-acyliminium cyclisation as described by Lambertson *et al.*⁵⁶

Following essentially quantitative conversion to the hydroxyisoindolone intermediate **95**, addition of 13 mol% PTSA catalyst resulted in a gradual colour change of the initially clear solution to dark brown. Analysis of the crude product indicated that the enamide species **96** was the only species formed (Scheme 37).



Scheme 37: Reaction of 1-(3-aminopropyl)imidazole (**94**) with benzaldehyde (**35**).

Consequently, the reaction was repeated with increased quantities of PTSA. However, no change to the product was observed, even with PTSA catalyst loading of up to 50 mol% (Analysis by ¹H NMR, X-ray crystallography). The same result was obtained with both Eaton's reagent and 10% aqueous acetic

acid. This outcome was presumed to be due to the basic nature of the second nitrogen in the imidazole ring- protonation at this location under the acidic conditions of the cyclisation step would likely further inhibit the imidazole's nucleophilic behaviour. Nonetheless, it would be interesting to reattempt the reaction with 1-(2-aminoethyl)imidazole (**94b**) to form a 6-membered ring to rule out the effect of the longer tether length. It might also be possible to facilitate cyclisation by using mesyl chloride and triethylamine in place of PTSA, thereby eliminating the potential for protonation of the imidazole.

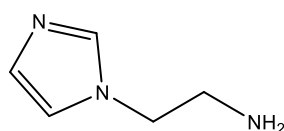
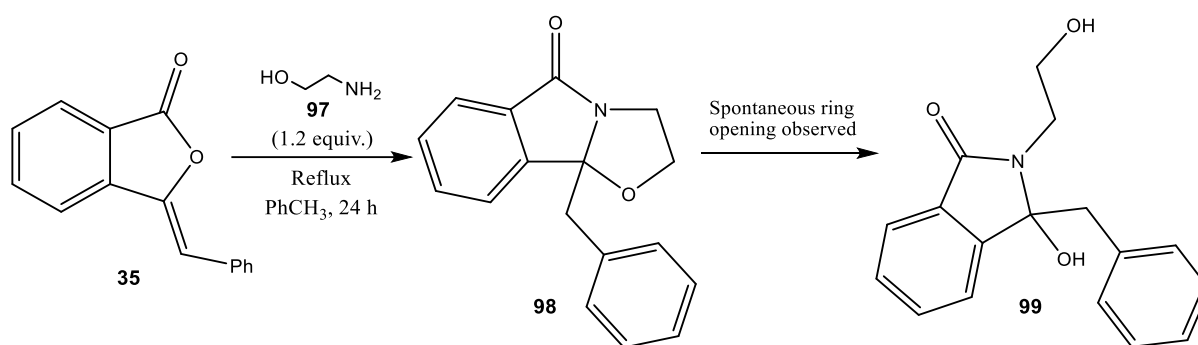


Figure 11: 1-(2-aminoethyl)imidazole **94b**.

3.2.4 Reaction of other nucleophiles

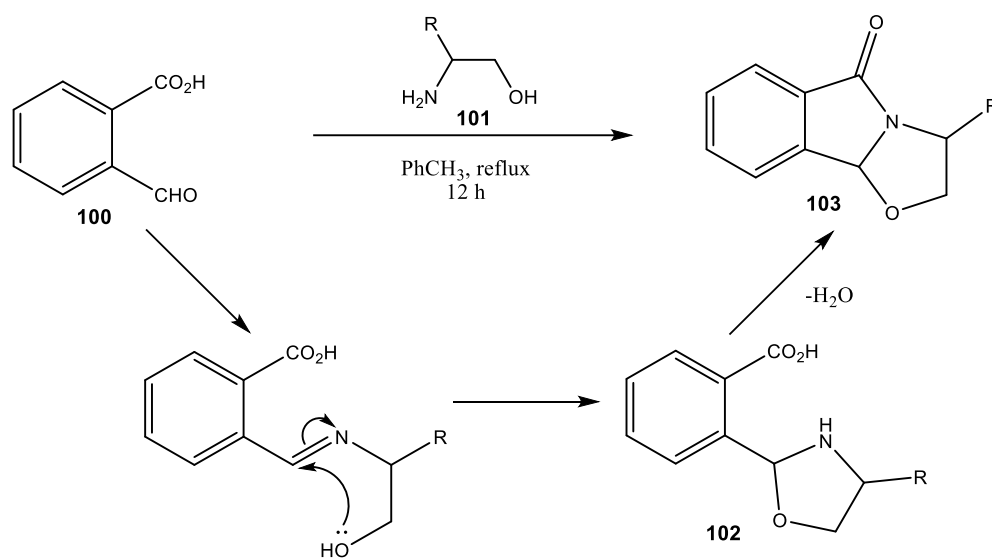


Scheme 38: reaction of ethanolamine (**97**) with benzaldehyde (**35**).

In contrast to all previously attempted reactions, the reaction of ethanolamine (**97**) with benzaldehyde (**35**) involves a σ -nucleophile in the form of a hydroxy group. This represents a largely unexplored area of research in terms of *N*-acyliminium cyclisations. Following the initial reflux of the 2 components in toluene, a crude ^1H NMR analysis of the material was performed. Interestingly, it appeared that the material had completely cyclised even in the absence of an acid catalyst. We therefore attempted to work up the material; the solvent was removed *in vacuo*, and the product was crystallised from isopropyl alcohol. However, when we attempted the characterisation it was clear that the product had been transformed. We concluded the new species was the hydroxyisoindolone **99**, based upon the NMR spectra, MS data including a characteristic $[\text{M}+\text{H}]$ peak of 284 Da, and the X-ray crystallography data from single crystal analysis.

The propensity for cyclisation, together with the apparent reversibility of the reaction, suggested to us that the cyclisation of **97** with benzaldehyde likely proceeded via an alternative reaction mechanism instead of the *N*-acyliminium pathway. Allin *et al.* described similar reactions of amino alcohols and proposed a mechanism in which the reaction proceeds via an oxazolidine intermediate

102 (Scheme 39).⁵⁷ This pathway excludes the *N*-acyliminium intermediate, and thus can proceed without a catalyst. An equivalent mechanism could occur in the case of our reaction if the benzaldehyde underwent hydrolysis and a subsequent ring opening to yield the corresponding 2-(benzoyl)benzoic acid.

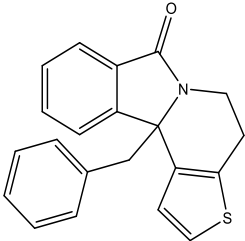
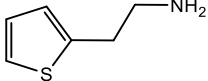
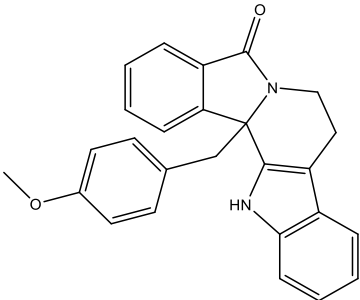
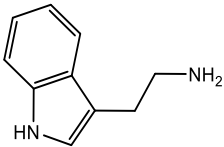
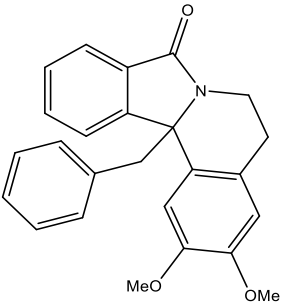
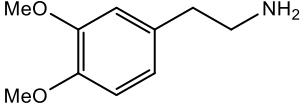
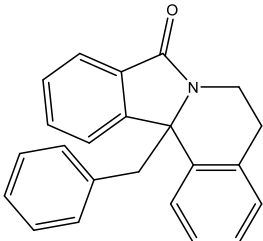
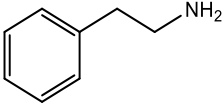


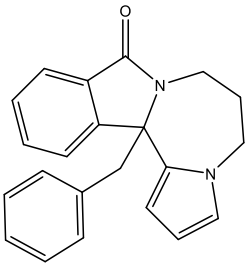
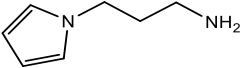
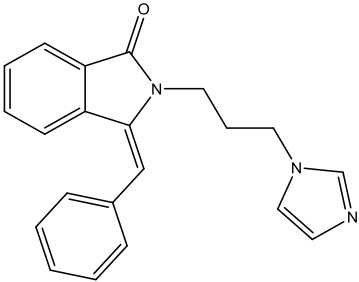
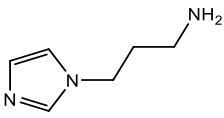
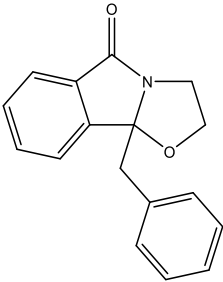
Scheme 39: Formation of tricyclic lactams via formation of an oxazolidine intermediate proposed by Allin et al.⁵⁷

3.3 Tabulated summary of results

Overall, while not all the reactions attempted were successful, the majority of amine components cyclised via our general experimental protocol. We therefore concluded that the acyliminium cyclisation is highly tolerant toward many different nucleophiles, even in the case of a hindered reacting centre such as ours. In the context of drug design, the ability to form these quaternary carbon centres is integral to inciting molecular complexity and moving away from the sp^2 -dominated chemistry of historical pharmaceutical structures. Further work examining other potential nucleophiles, such as furans and the substituted phenylethylamines (from the Henry reaction/hydrogenation route) will help to expand this area.

Table 4: Tabulated results of each amine component, including the acid catalyst employed, conversion and isolated yield.

Product	Amine component	Acid catalyst	% Product yield
 <p>80</p>		PTSA	60
 <p>83</p>		PTSA	91
 <p>86a</p>		PTSA	57
 <p>86b</p>		Eaton's reagent	52

Product	Amine component	Acid catalyst	% Product yield
 <p>90</p>		PTSA	45
 <p>96</p>		PTSA Eaton's reagent 10% AcOH _(aq)	63
 <p>98</p>		No catalyst	96 (Product subsequently degraded into hydroxyisoindolone 99)

4: Mechanistic considerations & asymmetric synthesis

4.1 Background

Each of the isoindolone products synthesised thus far contain a quaternary chiral carbon centre, with the product being obtained as a racemic mixture (Figure 12).

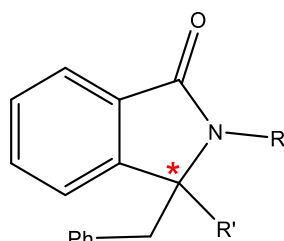


Figure 12: General structure of synthesised isoindolone products, with quaternary centre marked with *

However, it is well known that the specific chirality of a molecule can play an integral role in its potential biological activity. One key example is the drug 3,4-dihydroxyphenylalanine (DOPA) (Figure 13); the (*S*)-enantiomer **104** is used to treat Parkinson's disease, while the (*R*)-enantiomer **105** is ineffective and also highly toxic.⁵⁸

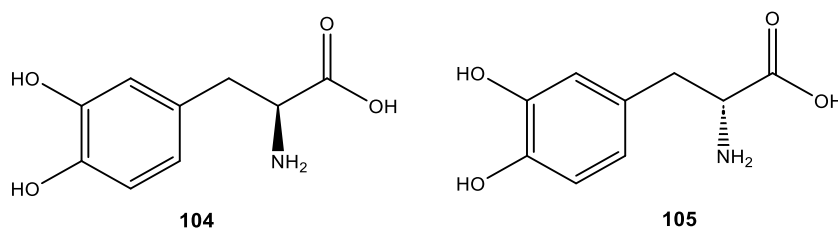


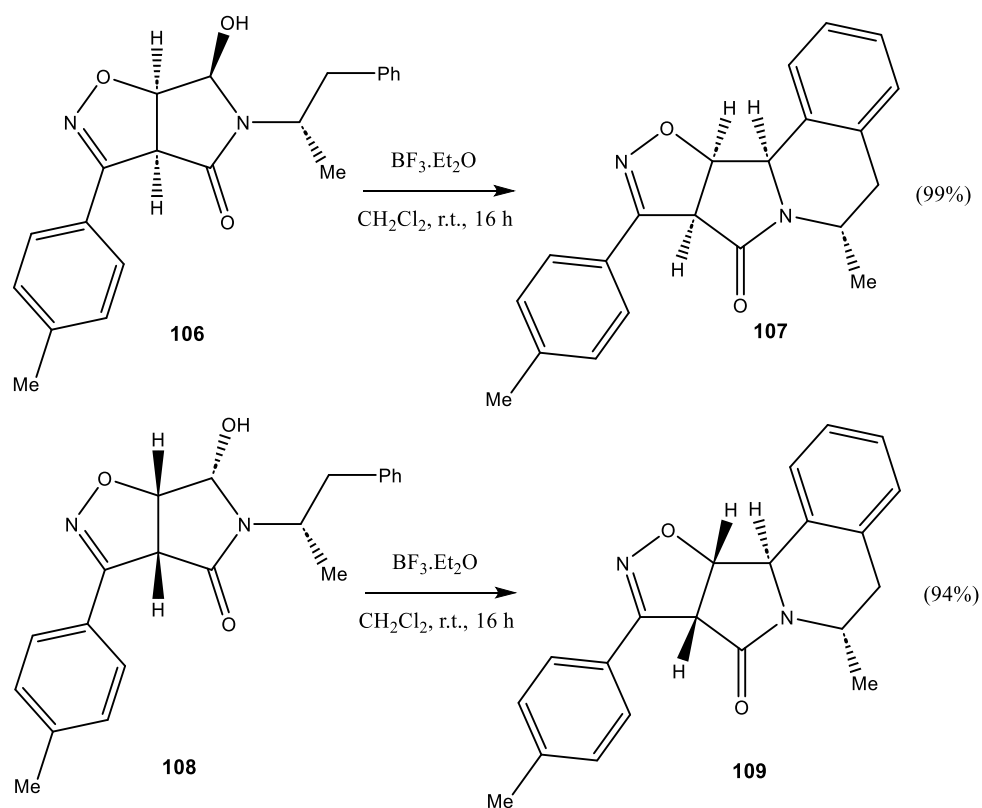
Figure 13: Structures of L-DOPA (**104**) and D-DOPA (**105**).⁵⁸

This is due to the chiral nature of biological systems; the receptors and enzymes adopted as pharmaceutical targets are inherently asymmetrical thanks to the chirality of the component amino acids and sugars. We therefore wanted to acquire the separated enantiomers of our products (or at least establish a means of separation) for structure-activity relationship (SAR) testing, such that any discrepancies in biological activity could be identified and utilised.

Ideally, we wanted to establish an enantioselective synthesis of our isoindolone products. This in turn required a more thorough understanding of the mechanistic implications of the reaction. As mentioned in chapter one, cyclisation of the hydroxylactams **25** could feasibly proceed via either a S_N1 or S_N2 -type process to furnish the final product. Depending on which was the case would determine what synthetic strategy we adopted to acquire the separated enantiomers. Consequently, we sought to investigate the wider stereochemical implications of *N*-acyliminium ion cyclisations, to gain a better understanding of the reaction pathway.

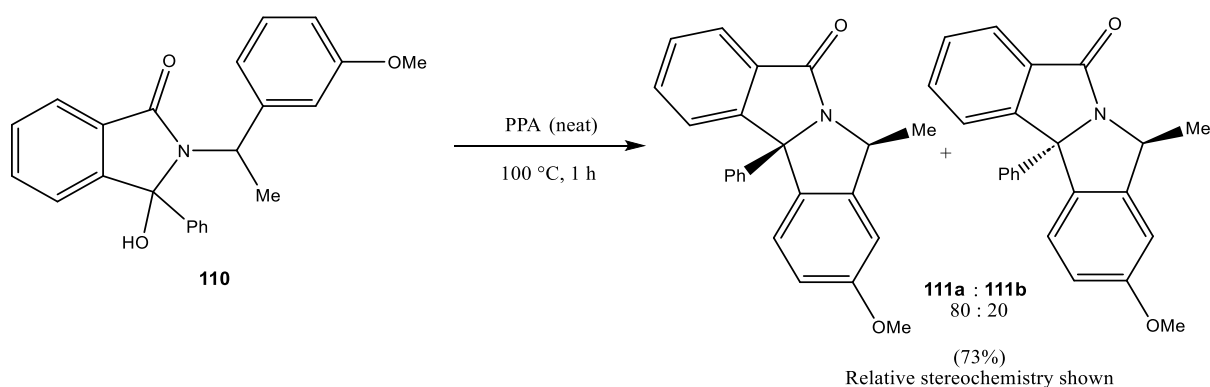
4.1.1 Precedent for Stereoselective cyclisations

Examples of stereoselective *N*-acyliminium ion cyclisations are numerous, with excellent stereocontrol observed in many cases.^{59–63} Most favourable results tend to arise from simple stereoelectronic factors, such as constraints on approach of the nucleophile to the reacting centre. A representative example is provided by Ledovskaya *et al.* for the synthesis of substituted isoxazopyrroloisoquinolines (Scheme 40).⁶² Here, species **106** and **108** were cyclised in the presence of 3 equivalents of $\text{BF}_3 \cdot \text{Et}_2\text{O}$, in yields of 99% and 94% respectively. In each case, formation of a single diastereomer was observed.



*Scheme 40: Diastereoselective cyclisations performed by Ledovskaya et al.*⁶²

These findings are mirrored in experiments performed by Bahajaj *et al.*, who detailed the stereoselective cyclisation of a similar structure **110**, acquiring products **111a** and **111b** in an 80:20 ratio in a 73% yield (Scheme 41).⁶¹ The observed diastereoselectivity in these two examples is thought to be due to the conformational effects in the transition state; $A^{(1,3)}$ strain between the α -methyl and carbonyl groups inhibits the formation of the minor diastereomer (Figure 14).^{62,64} It can therefore be concluded that substituents located at the α -position to the nitrogen can play an integral role in the stereochemistry of the cyclised product. By contrast, the stereochemistry at the reacting carbon centre of the hydroxy lactam intermediates was found to have no effect on the stereochemical outcome, supporting a more carbocation like transition state.



Scheme 41: Preferential formation of the *cis*-cyclised product documented by Bahajaj et al.⁶¹

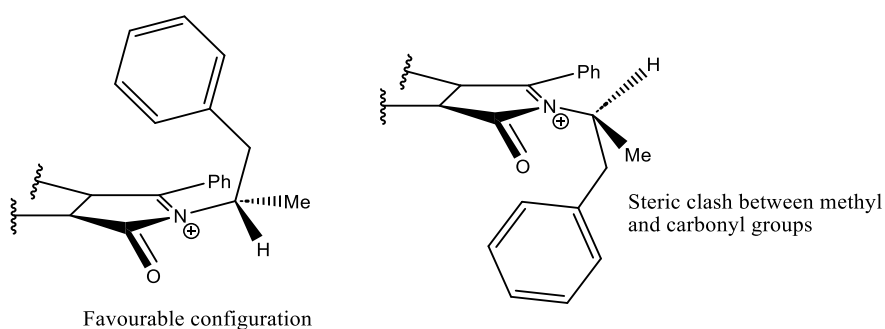
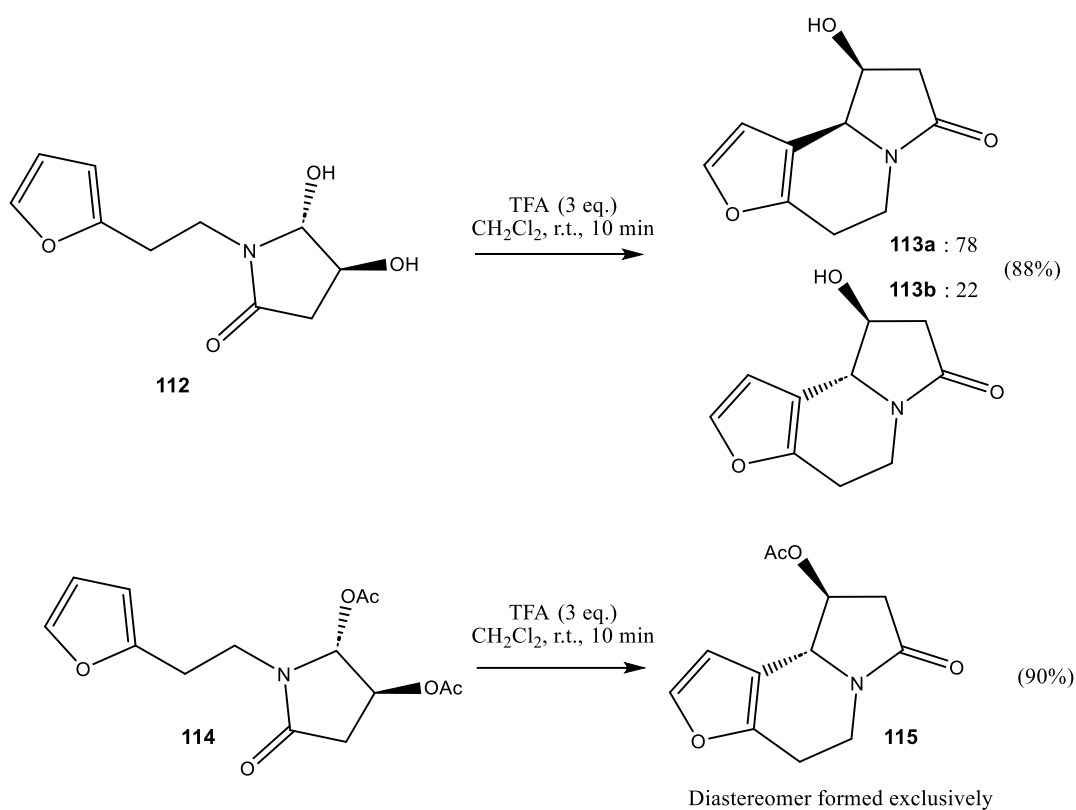
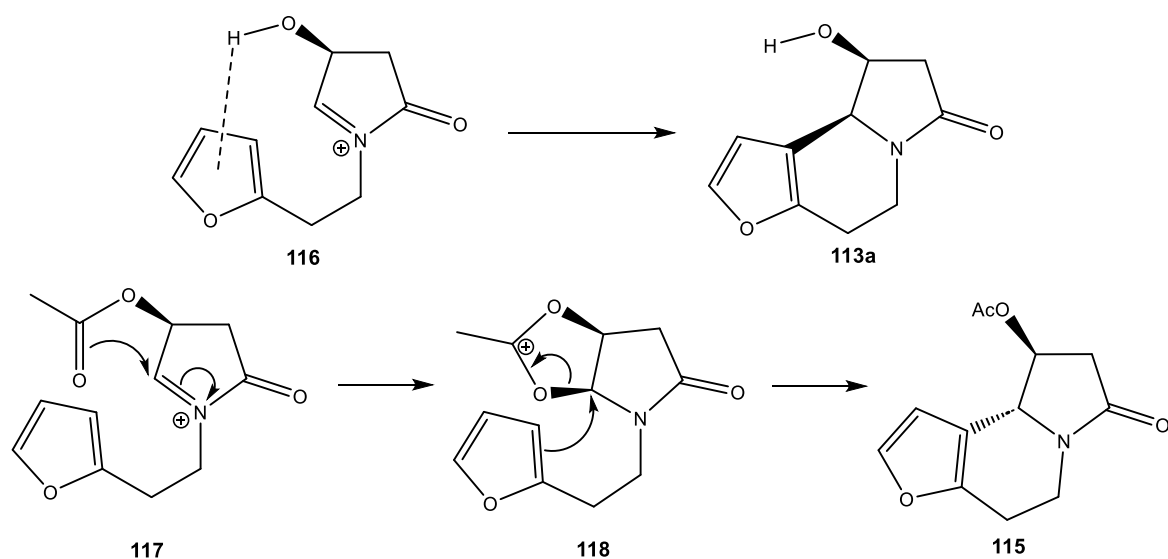


Figure 14: $A^{(4,3)}$ strain arising from the conformation of *N*-acyliminium transition state.

In addition to steric constraints, the electronic effects of neighbouring groups can also play an important role in generating the resultant stereoselectivity. In the following example (Scheme 42), the tethered furan species **112** underwent cyclisation to yield diastereomers **113a** and **113b** in a 78:22 ratio.⁶³ The preference for the *cis* relationship (first example) was attributed to intramolecular hydrogen bonding in the cyclisation intermediate **116** (Scheme 43). By contrast, protection of the hydroxy groups with an acetate gave formation of **115** as a single diastereomer, potentially due to formation of an acetoxonium intermediate **118** (Scheme 43). Assuming this to be the case, the latter reaction represents an interesting example of an *N*-acyliminium cyclisation proceeding via a concerted displacement type mechanism (invoking neighbouring group participation), with inversion of stereochemistry occurring at the reacting centre.



Scheme 42: Tethered furan cyclisations performed by Shengule et al.⁶³



Scheme 43: Influence of electronic effects of neighbouring substituents on diastereoselectivity.⁶³

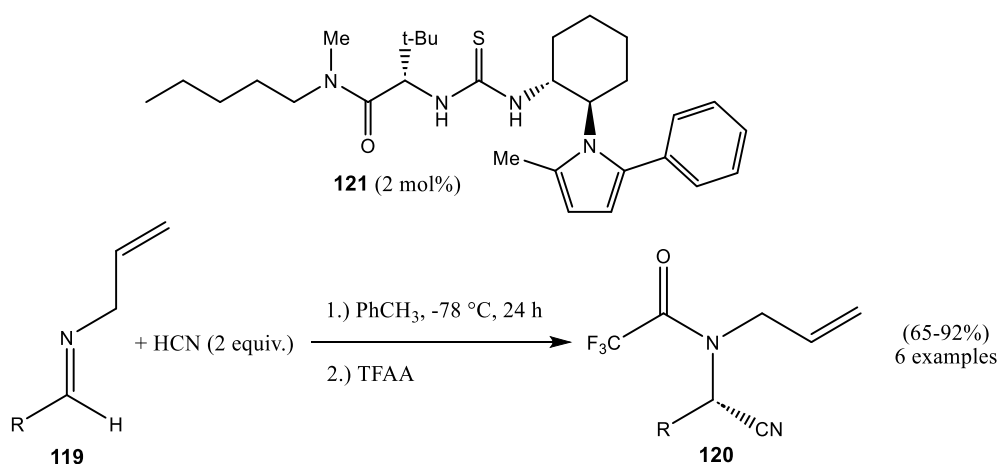
4.1.2 Asymmetric synthesis

While the stereoselectivity of *N*-acyliminium ion cyclisations has been well documented since the 1960's,^{36,65} enantioselective syntheses using chiral catalysts represents a relatively new field of research in this area. The reactive nature of the electrophile necessitates relatively mild conditions to generate an appreciable enantiomeric excess. Consequently, two classes of catalyst have become

predominant; 1,1'-bi-2-naphthol (BINOL) derived Brønsted and Lewis acids, and thiourea derivatives.^{52,66–69} The mechanistic implications of many of these reactions are still not fully understood, but in both cases it is believed that a complex forms between the catalyst and the reacting *N*-acyliminium centre that directs subsequent nucleophilic attack.^{52,70} Consequently, the catalyst must be capable of forming a tight complex (ion pair) with the *N*-acyliminium ion to effectively influence the reaction's stereochemistry.

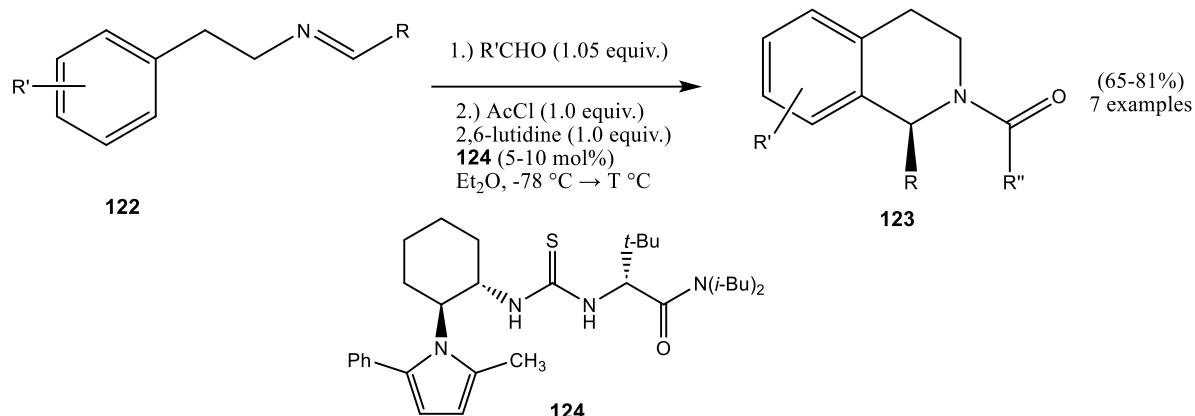
Thiourea catalysis

The concept of bidentate, hydrogen bond-based catalysis stems from the work of Kelly⁷¹ and Jorgensen⁷², with the use of urea or thiourea derived organocatalysts first documented by Curran *et al.* in 1995.⁷³ However, it was only in 1998 that their potential as enantioselective catalysts was realised by Jacobsen *et al.*, who successfully demonstrated their use in an asymmetric Strecker reaction (Scheme 44). By employing the chiral catalyst **121**, enantioselectivities from 70-91% and yields of 65-92% were achieved.⁷⁴



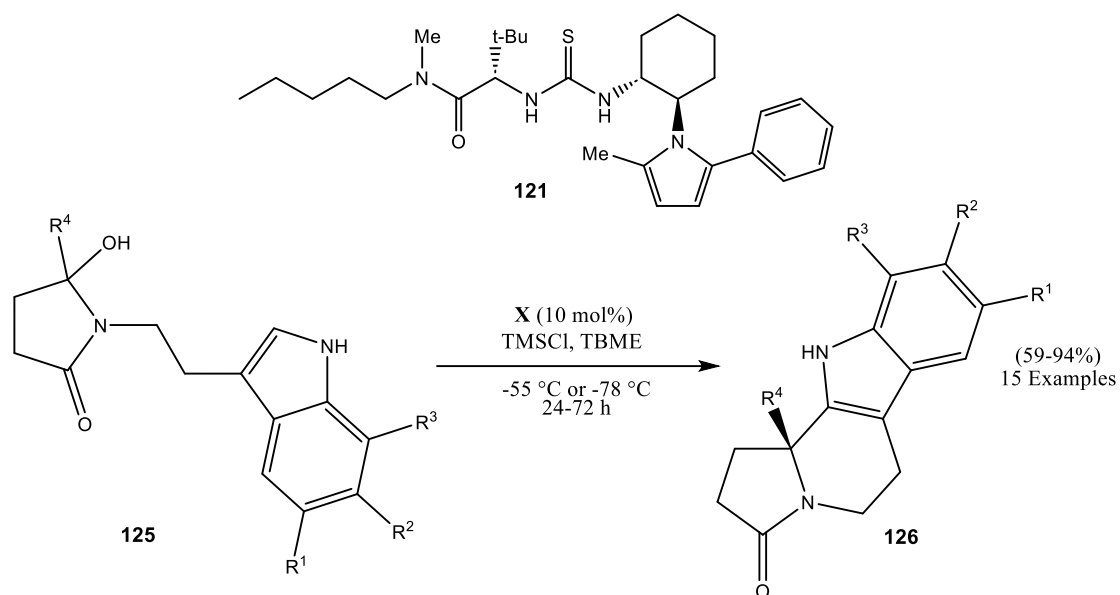
Scheme 44: Asymmetric Strecker reaction disclosed by Jacobsen *et al.*⁷⁴

Since then, thiourea catalysts have been widely applied to various organic reactions as hydrogen bond-mediated catalysts, including *N*-acyliminium cyclisations.⁷⁵ In this respect, Jacobsen and Taylor initially reported several enantioselective examples of intramolecular cyclisations in 2004.⁷⁶ The *N*-acyliminium species was exploited as a more reactive alternative to imine substrate in a Pictet-Spengler reaction, which allowed the use of milder reaction conditions and lower temperatures. Consequently, a greater degree of enantioselectivity (85-93% enantiomeric excess) was observed compared to imine-based reactants. Nonetheless, performance was highly dependent on the choice of solvent and structure of the acylating agent.

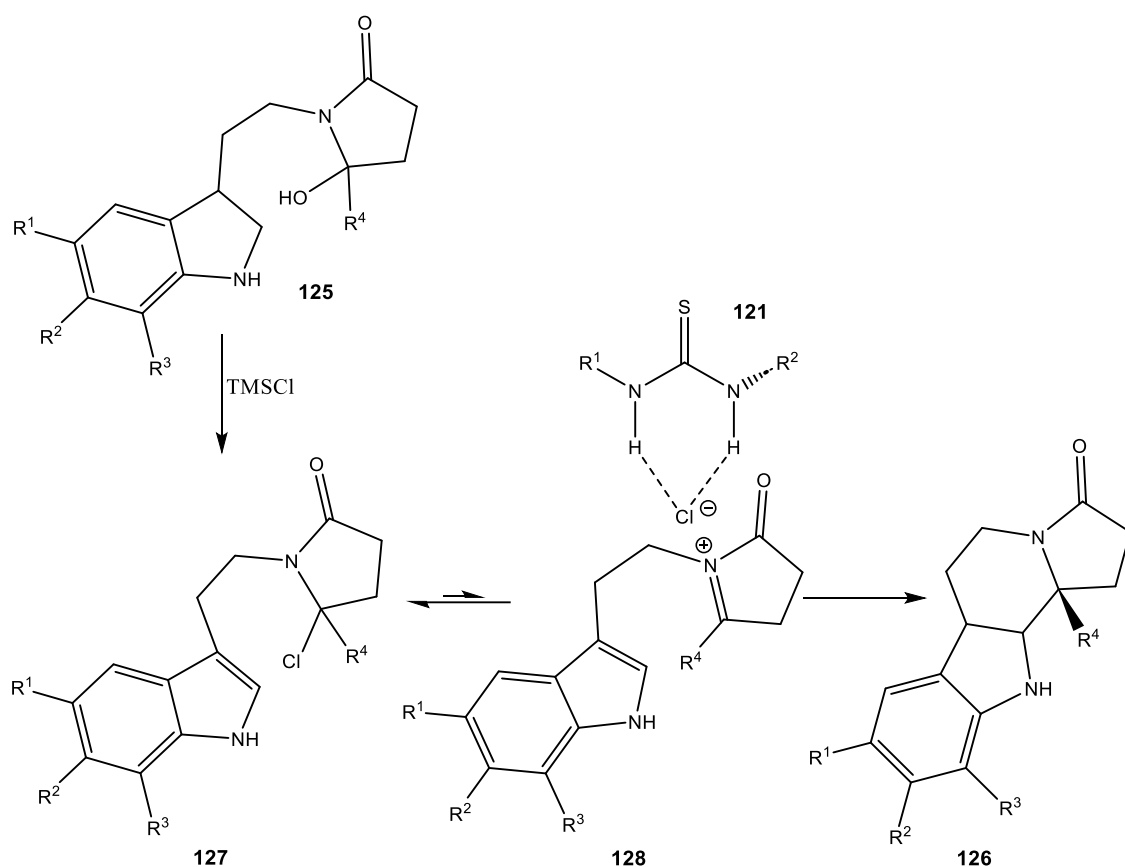


Scheme 45: Asymmetric acyl Pictet-Spengler reaction documented by Jacobsen et al.⁷⁶

Three years later, the same methodology was shown to be applicable for the reaction of β -indolyl ethyl hydroxylactams **125** (Scheme 46), obtaining enantiomeric excesses of 81-99%. This work included the preparation of the natural product (+)-Harmicine (R^1 , R^2 , R^3 , and R^4 = H) in which the final cyclisation occurred in a 90% yield and 97% enantiomeric excess.⁵² Trimethylsilyl chloride (TMSCl) was used to generate the *N*-acyliminium ion; this avoided the formation of water, which was shown to be detrimental to the enantioselectivity. The reaction is believed to proceed via an S_N1 -type process (Scheme 47) in which the hydroxylactam **125** initially reacts with the TMSCl to afford the corresponding chlorolactam **127**. This can equilibrate and form an *N*-acyliminium chloride ion pair. The thiourea catalyst **121** is then believed to form a chiral complex with the *N*-acyliminium chloride, which promotes asymmetric attack from the indole nucleophile to yield the cyclised product **126**. This notion is supported by pronounced counterion and solvent effects, and the higher conversions for more highly substituted reacting centres compared to their less substituted counterparts.



Scheme 46: Enantioselective synthesis of β -indolyl ethyl hydroxylactams by Jacobsen et al.⁵²



Scheme 47: Reaction mechanism proposed by Jacobsen et al.⁵²

The scope of this reaction was also expanded to include other π nucleophiles, successfully cyclising pyrrole-based species tethered at the 3-position in enantiomeric excesses of up to 96%.⁶⁶ Once again, higher levels of conversion and enantioselectivity were seen with increased substitution at the

reactive electrophilic centre, consistent with a more stabilised S_N1 -type intermediate. Additionally, selective cyclisation at the less reactive 4-position of the pyrrole ring was achieved by blocking the more reactive 2-position with an *N*-triisopropyl silyl (TIPS) group. Higher regioselectivity was demonstrated in the presence of the thiourea catalyst, demonstrating its dual role in conferring enantioselectivity and regiocontrol. Interestingly, the corresponding thiophene and aryl-derived nucleophiles performed poorly by comparison, resulting in enantiomeric excesses of only 30% and 0%, respectively.

BINOL-derived catalysts

The 1,1'-bi-2-naphthol (BINOL) framework represents one of the most prominent chiral ligands in asymmetric synthesis, owing to its low cost and high versatility (as well as the availability of both enantiomeric forms). Its derivatives have been demonstrated to yield high enantioselectivity in both intermolecular and intramolecular reactions of *N*-acyliminium species and have provided a convenient route to several enantioenriched alkaloids and natural products.^{77–80} The BINOL scaffold can be easily functionalised to produce reaction-tailored catalysts; in the context of *N*-acyliminium ion generation, this usually entails a Brønsted or Lewis acid moiety. Many examples employ a hydrogen phosphate group linked by the two axial chiral oxygens of the parent BINOL compound (

Figure 15). It is thought that the resulting chiral phosphoric acids act as bifunctional catalysts, possessing both Brønsted-acidic and Lewis-basic sites that activate and stabilise the electrophile in a synergistic manner.⁷⁵

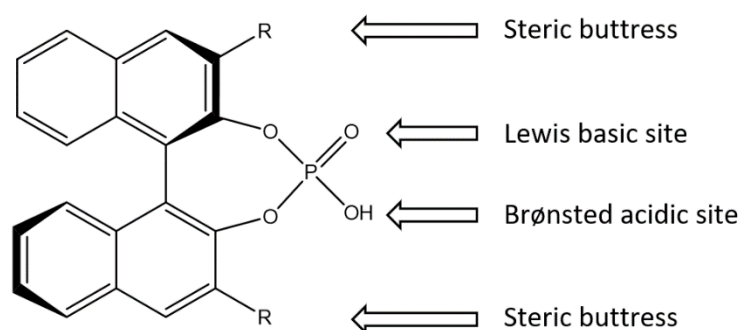
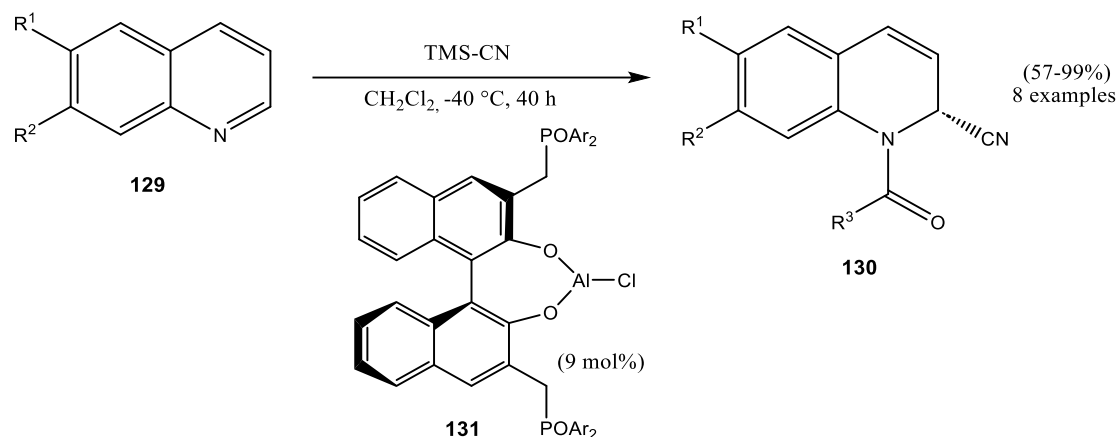


Figure 15: General structure of BINOL-derived phosphoric acid catalysts.⁷⁵

One of the first examples of BINOL derived catalysts as used in *N*-acyliminium reactions was presented by Shibasaki *et al.* in 2000. The Reissert reaction involves the addition of a cyanide ion to an *N*-acylquinolinium and is a valuable tool in synthesising biologically important alkaloids.⁸¹ By employing catalyst **131**, Shibasaki and co-workers successfully demonstrated an asymmetric variation of this reaction, resulting in enantiomeric excesses of 67–91% under optimised reaction conditions (Scheme 48).⁶⁸ The process is thought to proceed through intermediate **132** (Figure 16), wherein a complex with the Lewis acid portion of the BINOL catalyst is formed. At the same time, substituents at the 3

and 3' positions instigate steric constraints around the reacting centre, while acting as a Lewis base to activate the TMS-CN nucleophile.



Scheme 48: Asymmetric Reissert-type reaction presented by Shibasaki *et al.*⁶⁸

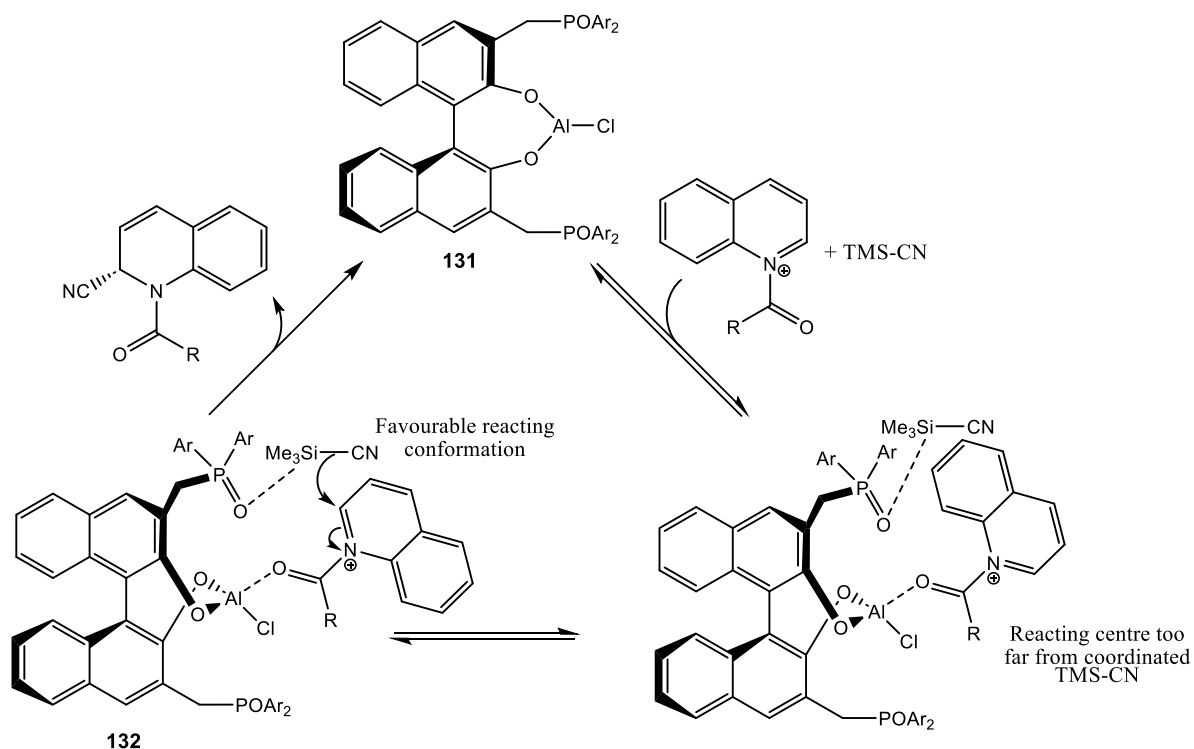
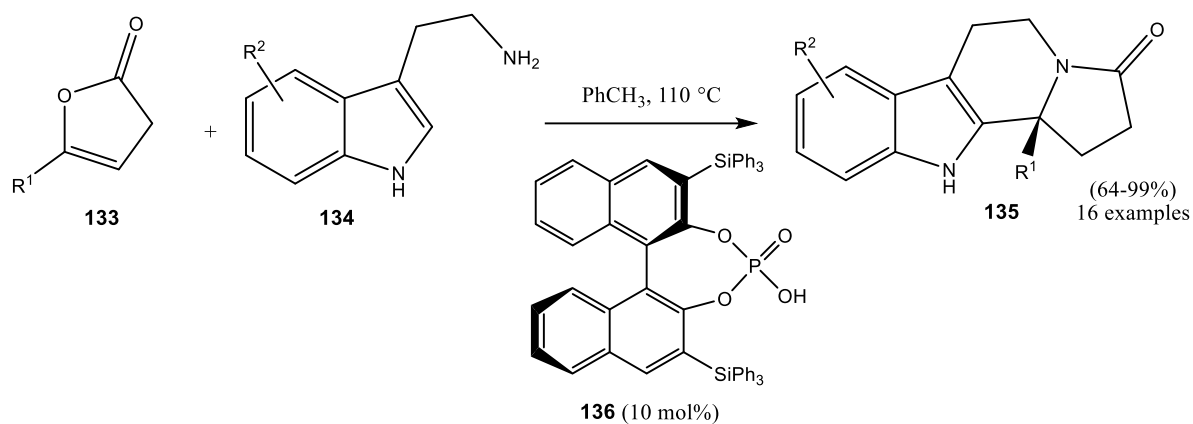


Figure 16: Mechanistic considerations of the Reissert-type reaction demonstrated by Shibasaki *et al.*⁶⁸

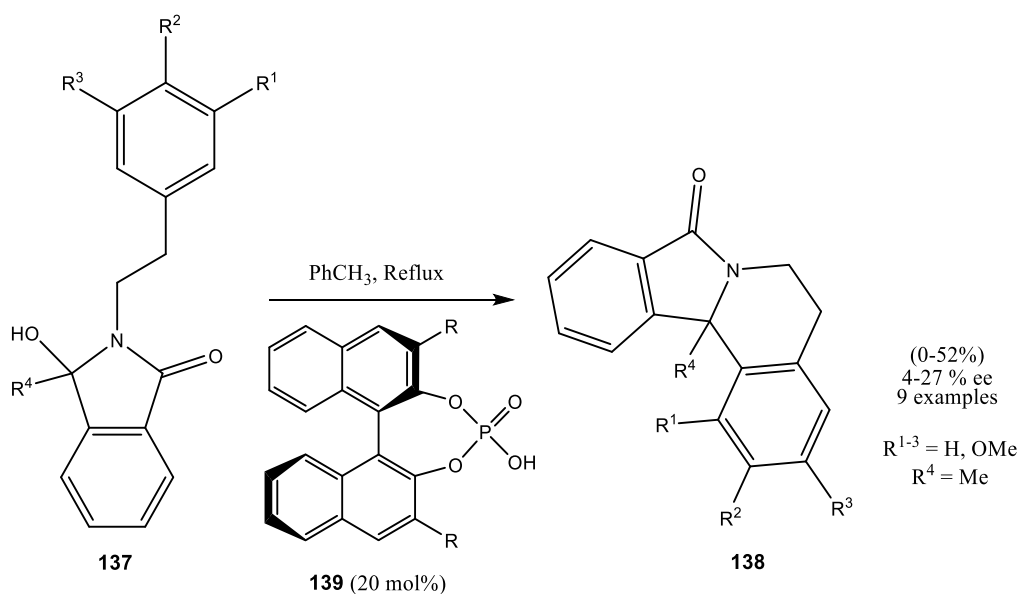
The use of such catalysts in cyclisation reactions was subsequently demonstrated by Dixon *et al.*, who successfully synthesised chiral cyclised indole species (Scheme 49).⁸² Compounds **133** and **134** were heated at reflux in toluene in the presence of 10 mol% catalyst **136**, which afforded the desired heterocycles **135** in yields of 64-99% and ee's of 72-99%. These results broadly correlated to the reaction performance afforded by the thiourea catalyst employed by Jacobsen *et al.*⁵² Additionally, the pronounced solvent effects observed also suggest an S_N1 type process as previously mentioned. It

appears that the natures of the substituents at the 3 and 3' positions impart a major influence on the efficacy of the catalyst; a triphenylsilyl group was found to be optimal in inducing high enantioselectivity.



Scheme 49: Cyclisation of tethered indole nucleophiles documented by Dixon et al.⁸²

Beyond indole-based reactions, the successful enantioselective cyclisations of weaker nucleophilic components has also been observed employing BINOL derived catalysts. Work performed by Lete *et al.* concerned the synthesis of compounds **138**, albeit in low yields and enantioselectivities (Scheme 50).⁶⁷ This nonetheless marks an improvement upon thiourea-based catalyst, for which, no reaction was observed in the case of aryl nucleophiles. One explanation could be the more acidic nature of the phosphoric acid component, which imparts slightly more forcing conditions than the hydrogen-bond catalysis afforded by the thiourea. These findings indicate that the nature of the nucleophilic component also plays an important role in the feasibility of an asymmetric synthesis.



*Scheme 50: Enantioselective synthesis of **135** documented by Lete et al.⁶⁷*

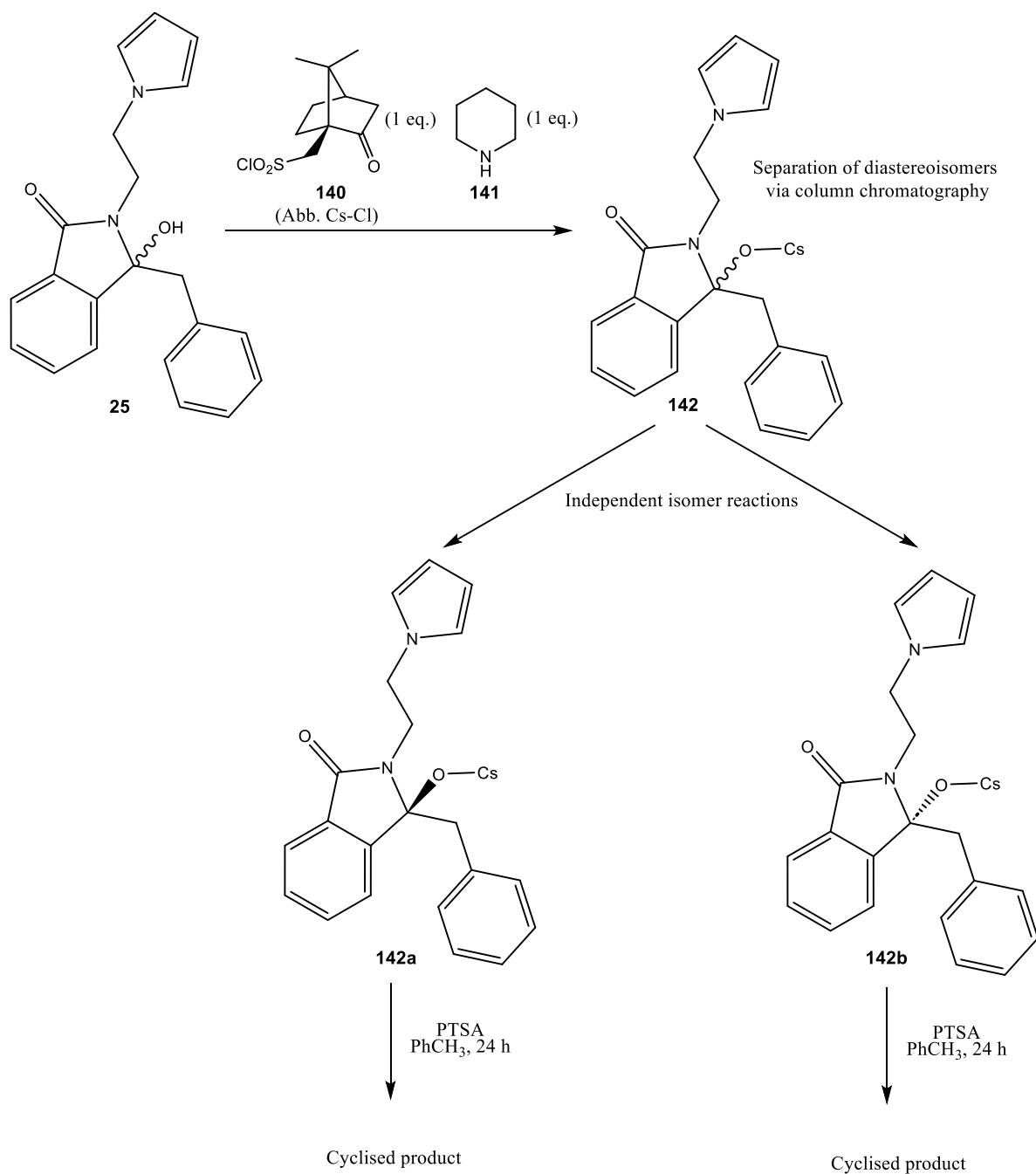
4.2 Results and discussion

4.2.1 Determining the reaction pathway

Our preliminary objective was to probe the reaction mechanism of our *N*-acyliminium ion cyclisation to determine whether the reaction proceeded via a dissociative or concerted process, as discussed in chapter 2. While most of the literature previously highlighted was indicative of the former, we were inclined to examine this theory for ourselves as it would determine the strategy employed for accessing the two enantiomers.

We initially attempted to examine the reaction pathway by isolating the enantiomers of the hydroxy intermediate **25** through a chiral resolution. We theorised that the enantiomers could then be independently evaluated in cyclisation reactions to furnish the desired isoindolone compound (Scheme 51). If the final product were obtained as a racemate in both cases, this would suggest an S_N1 type process, due to the loss of chirality through the achiral *N*-acyliminium intermediate. However, if the reaction proceeded exclusively via a concerted pathway (or associated tight ion pairing), the stereochemistry of the hydroxy intermediate would determine that of the final product and only one enantiomer (or a non-racemic product) would be obtained in each case.

To achieve the desired enantiomeric separation, we initially opted to use (1*S*)-(+)-10-camphorsulfonyl chloride (Abb. CS-Cl) as a chiral derivatising agent. This would react with the hydroxyl group of the intermediate **25** to yield a pair of diastereomers, which we hoped could then be resolved using column chromatography (Scheme 51). As such, compound **1** (synthesised as described in chapter one) was reacted with camphorsulfonyl chloride. The reaction was monitored through TLC and was indicated by the gradual disappearance of the starting materials. Post reaction ^1H NMR analysis and subsequent chiral chromatography indicated only the presence of the racemic, fully cyclised product **1** in a 67% yield. We reasoned that this could be due to the instability of the tertiary-substituted sulfonyl ester; as a good leaving group, it is feasible that cyclisation occurred even in the absence of an additional acid catalyst or heating. This had interesting connotations as an alternative activation strategy, and offers scope for potentially less reactive substrates, but did not achieve our outlined goal of an enantiomeric excess of hydroxyisoindolone derivative **142**.



Scheme 51: Proposed method for the chiral resolution of the hydroxyisoindolone intermediate **25**, with (1*S*)-(+)-10-camphorsulfonyl chloride (**137**) shown as the chiral derivatising agent

With this in mind, we attempted the same resolution but using menthyl chloroformate as the chiral derivatising agent. It was thought that the resulting organic carbonate should have a greater degree of stability compared to the sulfonate ester. Following the same procedure as described above, the reaction mixture gradually darkened to a yellow/orange colour. Removal of the solvent *in vacuo*, and analysis of the crude material by ¹H NMR proved inconclusive; however, TLC indicated the presence of two products, and so separation via column chromatography was attempted (eluent-dichloromethane: hexane: acetone 40:10:1). Unfortunately, analysis of the two products isolated

indicated they were the racemic hydroxy intermediate **25** and enamide species **43**. We were unable to clarify if these were the reaction products or if the acidic nature of the silica instigated hydrolysis of the diastereomers as they travelled down the column.

4.2.2 Diastereomeric reactions

Having been unable to conveniently resolve the hydroxyisoindolone species **25** through chiral resolution (Scheme 51), we instead decided to try and gain a better understanding of the reaction mechanism through investigation of related diastereoselective reactions. By employing chiral nucleophilic components, we thought we may observe an effect on stereoselectivity. We subsequently identified (*R*)-1-phenylethylamine (**143a**) and (*R*)-2-phenylpropan-1-amine (**143b**) (Figure 17) as two commercially available and relatively inexpensive species that could participate in the *N*-acyliminium cyclisation step.

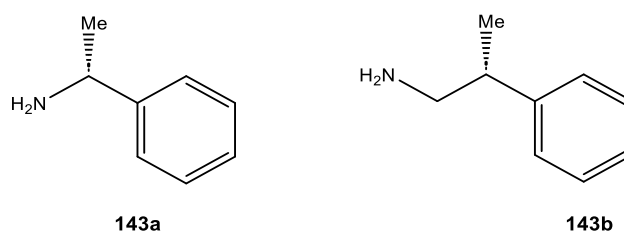
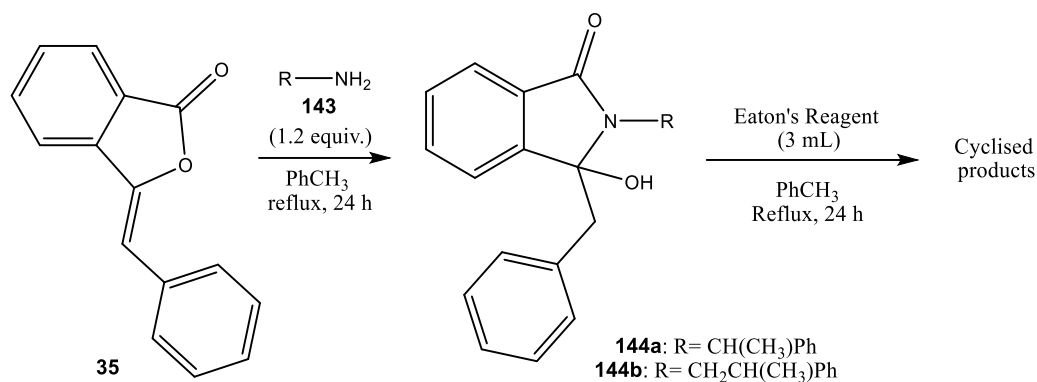


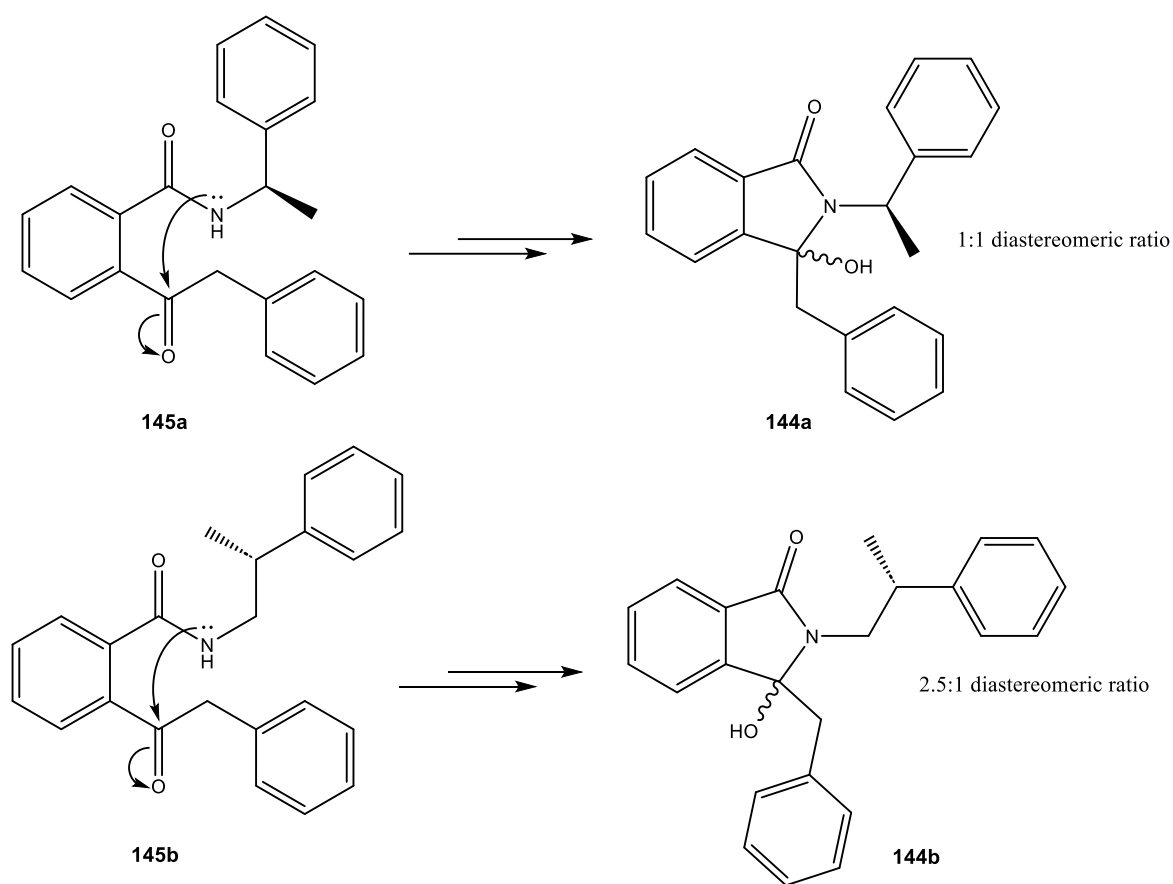
Figure 17: (*R*)-1-phenylethylamine (left) and (*R*)-2-phenylpropan-1-amine (right).

Based upon previous literature reports, we anticipated that greater diastereoselectivity would be observed in the cyclisation of **143a**, due to the position of the methyl substituent relative to the reacting centre. As mentioned above, substituents on the carbon directly adjacent to the *N*-acyliminium centre tend to hinder the formation of one diastereomer due to A^(1,3) strain arising in the transition state.⁶¹ From the literature and our experiments in chapter 2, we had deduced that more forcing conditions were required for the successful reaction of unsubstituted aryl nucleophiles¹⁸, and so Eaton's reagent was employed in both cases to catalyse the secondary cyclisation process. The reaction procedure was the same as previously adopted; benzaldehyde (**35**) with 1.2 equivalents of the amine component **143** were initially refluxed in toluene for 24 hours (Scheme 52).



Scheme 52: attempted diastereoselective reaction of benzaldehyde (**35**) with a.) (*R*)-1-phenylethylamine (**143a**) and b.) (*R*)-2-phenylpropan-1-amine (**143b**).

In both cases, effectively quantitative conversions to the corresponding hydroxyisoindolone intermediates **144a** and **144b** were observed. In the case of (*R*)-1-phenylethylamine (**140a**), the intermediate alcohol **144a** was produced as a 1:1 mixture of diastereomers, as confirmed by ¹H NMR and LC-MS. Interestingly, the product from (*R*)-2-phenylpropan-1-amine (**143b**) was produced in a diastereomeric ratio of approximately 2.5:1. This was a surprising result; as the hydroxyisoindolone intermediate **144** is presumably formed through attack of the carbonyl in species **145** (Scheme 53), one would assume that greater selectivity would be observed with the methyl substituent positioned closer to the nucleophilic amine group.



*Scheme 53: Formation of the hydroxyisoindolone intermediate **144** from species **145**.*

Following formation of the intermediates **144a** and **144b** (Scheme 52), we reasoned that if the ratio of diastereomers drastically changed following cyclisation, the reaction could be viewed as proceeding through an S_N1 type process, as this could only occur via the planar *N*-acyliminium ion intermediate. Conversely, an S_N2 process would be more likely if the diastereomeric ratio remained constant, as the configuration of the diastereomeric intermediate would determine the final product. Following the addition of the Eaton's reagent acid catalyst, the solutions were refluxed for a further 24 hours, during which a yellowing of the solution was observed. Disappointingly, species **144a** was found to be incapable of cyclising; instead, ^1H NMR analysis indicated the alternative enamide **147** as the sole product (Figure 18). This result was somewhat unsurprising; the lower reactivity of the unsubstituted aryl nucleophile was presumably insufficient to overcome the unfavourable 5-*endo-trig* cyclisation required to yield the desired product. By contrast, species **144b** appeared to cyclise successfully to **148** (Figure 18) as a 1:2 mixture of diastereomers. While the diastereomeric ratio changed slightly from intermediates to products, the difference is too small to say with certainty whether the reaction proceeds exclusively via an S_N1 or S_N2 type mechanism.

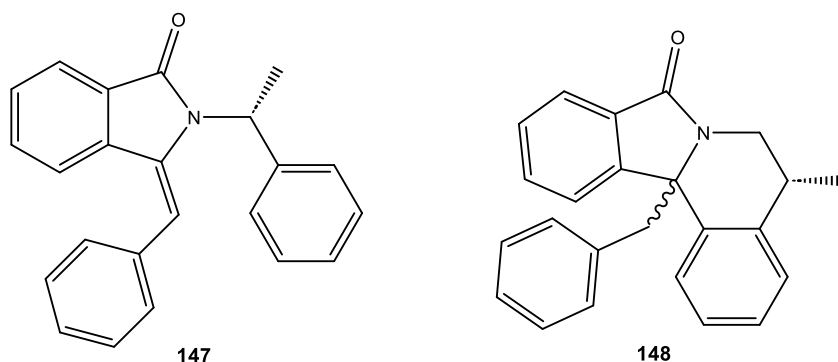


Figure 18: enamide product obtained from **144a** (left) and fully cyclised product of **144b** (right).

4.2.3 Asymmetric synthesis via chiral catalysis

Although we had been unable to conclusively determine the reaction pathway, due to time constraints on the project we opted, based upon literature precedent, to assume an S_N1 -type pathway and pursue an asymmetric synthesis using a chiral acid catalyst. The examples of asymmetric *N*-acyliminium cyclisations in the literature gave us confidence that we would be able to perform a similar enantioselective reaction. However, we wished to try employing alternative chiral acidic reagents to those previously disclosed. This was primarily due to their nontrivial preparation; in particular, the asymmetric thioureas documented by Jacobsen *et al.* represent a formidable and time-consuming synthesis, involving the use of highly toxic thiophosgene in a 5-step process. We therefore wanted to explore the possibility of using more readily accessible catalysts while still achieving an enantiomeric excess. As such, (1*S*)-(+)-10-camphorsulfonic acid **149** and *L*-(+)-tartaric acid **151** were initially identified as feasible candidates for inducing enantioselectivity. Additionally, while the synthesis of the substituted BINOL derivatives mentioned above is challenging, we were able to easily synthesise the unsubstituted BINOL phosphoric acid **150** from (*R*)-BINOL following a procedure detailed by Jacques *et al.*⁸³ As such, its enantioselective potential was also examined.

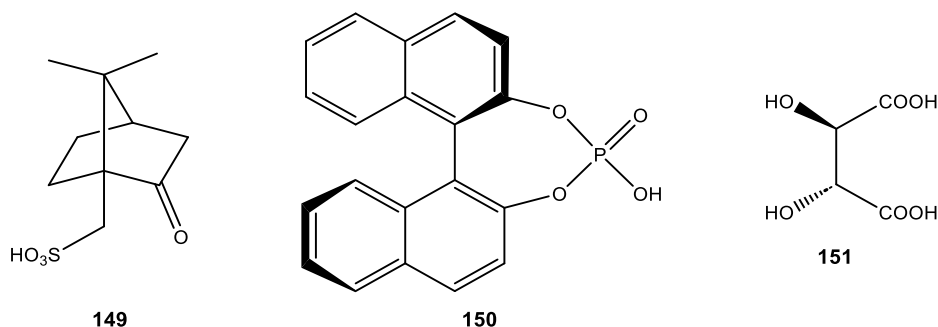
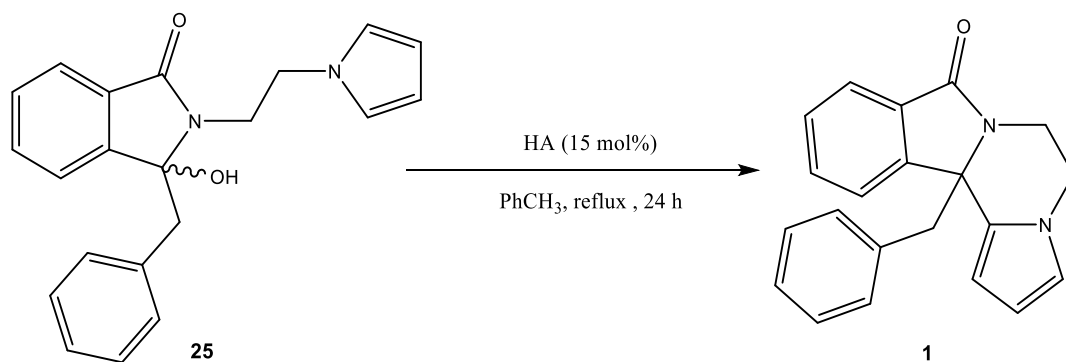


Figure 19: (1*S*)-(+)-10-camphorsulfonic acid (**149**), (*R*)-(-)-1,1'-binaphthyl-2,2'-diyl hydrogenphosphate (**150**) and *L*-(+)-tartaric acid (**151**).

In each case, the hydroxy intermediate **25** was dissolved in toluene, and 15 mol% of the chiral catalyst (HA) was added (Scheme 54). The solution was then heated at reflux for 24 hours, followed by work-up. Recrystallisation was not performed to avoid the potential for spontaneous resolution of both enantiomers. Enantiomeric excess was determined through the use of a chiral HPLC, with the racemic product **1** prepared in chapter one being used for comparison.



Scheme 54: chiral acid catalysed cyclisation of hydroxyisoindolone 25.

Analysis of the ¹H NMR spectra indicated that *L*-(+)-tartaric acid failed to induce the cyclisation of the hydroxyisoindolone intermediate **25**, instead yielding a mixture of the starting material and alternative enamide product **43**. This is likely due to the weaker acidity of the carboxylic acid moiety (*L*-(+)-tartaric acid at 25 °C (Aq. p*K*_{a1} = 2.9, p*K*_{a2} = 4.4⁸⁴). By contrast, both camphorsulfonic acid (p*K*_a = 1.2¹) and (*R*)-(-)-1,1'-binaphthyl-2,2'-diyl hydrogen phosphate (p*K*_a = 1.1ⁱ) were able to facilitate complete conversion of the hydroxy intermediate **25** to the cyclised product **1**. Unfortunately, no enantiomeric excess was determined for either transformation. We reasoned that this could be a result of the high temperatures employed to induce cyclisation; as the energy difference between the transition states of the two enantiomers is presumably low, a reduced temperature would therefore help to increase any selectivity. We therefore opted to retry the BINOL catalyst, this time in dichloromethane at room temperature.

Analysis of the ¹H NMR spectrum indicated 84% conversion to the fully cyclised product, with the remaining material being assigned as the enamide intermediate **43**. This time, a small enantiomeric excess of 4% was observed (chiral HPLC). The low performance compared to literature examples is most likely due to the lack of substitution at the 3 and 3' positions of the BINOL skeleton; these groups surround the reacting *N*-acyliminium centre, and thus contribute to greater selectivity by acting as steric blocks. Thus, despite the minimal enantioselectivity, this result indicates that an asymmetric

¹ p*K*_a values calculated using Advanced Chemistry Development (ACD/Labs) Software V11.02 (© 1994-2022 ACD/Labs)

synthesis could be feasible with a more functionalised BINOL-phosphoric acid catalyst, with substitutions at the 3 and 3' positions tailored to this specific reaction.

Table 5: conversion and enantiomeric excess observed employing each acid catalyst

Acid catalyst	Solvent	Temperature/ °C	% Conversion	% Enantiomeric excess
<i>L</i> -(+)-tartaric acid	Toluene	110	0	Racemic
(1 <i>S</i>)-(+)-10-camphorsulfonic acid	Toluene	110	100	Racemic
(<i>R</i>)-(-)-1,1'-binaphthyl-2,2'-diyl hydrogenphosphate	Toluene	110	100	Racemic
(<i>R</i>)-(-)-1,1'-binaphthyl-2,2'-diyl hydrogenphosphate	Dichloromethane	25	84	4

5: Conclusion and future work

N-Acyliminium ions are powerful reactive species for the formation of carbon-carbon and carbon-heteroatom bonds. Strategies relying on *N*-acyliminium ion cyclisation reactions have been employed for the construction of structurally diverse scaffolds, ranging from simple bicyclic skeletons to complex polycyclic systems and natural-product-like compounds. The continued and rapid development of this chemistry since its origins in the 1950's illustrates the importance and applicability of such amidoalkylation reactions.

This project sought to explore the value of *N*-acyliminium chemistry in the synthesis of biologically active compounds, through the preparation of a set of isoindolone compounds based on the scaffold **1** for structure-activity testing (chemistry performed in Chapter 2). To this end, we were able to establish a simple and effective synthetic route to our target molecule, using readily available starting materials in an overall yield of 58% (for the parent compound, 4 steps). The synthesis of functionalised derivatives **1b-1k** was also achieved, albeit in reduced conversion and isolated yields in some cases. The preparation will allow their biological activities to be examined *in vitro* which, if successful, provides a structural framework that can be used to further optimise structures as lead compounds for the treatment for colon cancer and leishmania. Additionally, confirmation of the compounds' activity *in vitro* would provide further credence to DRUIDom as a computational method for predicting drug-protein interactions.

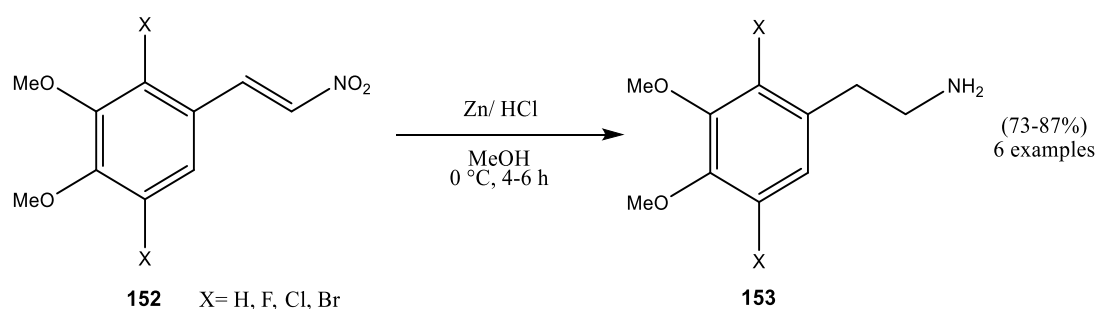
Furthermore, we were able to demonstrate the scope of the cyclisation, through the implementation of various tethered nucleophiles (work detailed in Chapter 3). The tolerance of the reaction toward nucleophiles of differing reactivities and the ability to form hindered quaternary carbon centres has helped to illustrate the value of *N*-acyliminium reactions as a tool in diversity-oriented synthesis. This reactive species could prove invaluable in addressing the traditional, sp^2 -oriented combinatorial chemistry associated with pharmaceutical libraries, allowing easy access to more architecturally complex molecules that occupy a greater region of chemical space.

Finally, we sought to examine the mechanistic implications of the reaction, first through the attempted separation of the enantiomers of hydroxyisoindolone **25**, and subsequently through related diastereoselective reactions (work reported in Chapter 4). While we were unable to prepare the separate enantiomeric forms of **1** in the given time, we believe that these preliminary experiments have given us a mechanistic insight that would be invaluable in constructing an asymmetric synthesis.

With regards to future work, optimisation of the reaction conditions would be beneficial, particularly with regards to the initial formation of the substituted hydroxyisoindolone intermediates **25b-k**. It

may be the case that the formation of the hydroxyisoindolone intermediates and the subsequent cyclisations proceed most efficiently under differing reaction conditions. Employing a different solvent and experimenting with temperature may provide an increased conversion to the hydroxyisoindolone intermediate (most notably in the case of the reactions of **1d** and **1f**) leading to an increased overall yield. Alternatively, the camphorsulfonyl chloride used in chapter 4 has shown that the tertiary alcohol group of the intermediate **25** could be activated using an equivalent to potentially increase the final product yield, particularly for the former cases where conversion was lower.

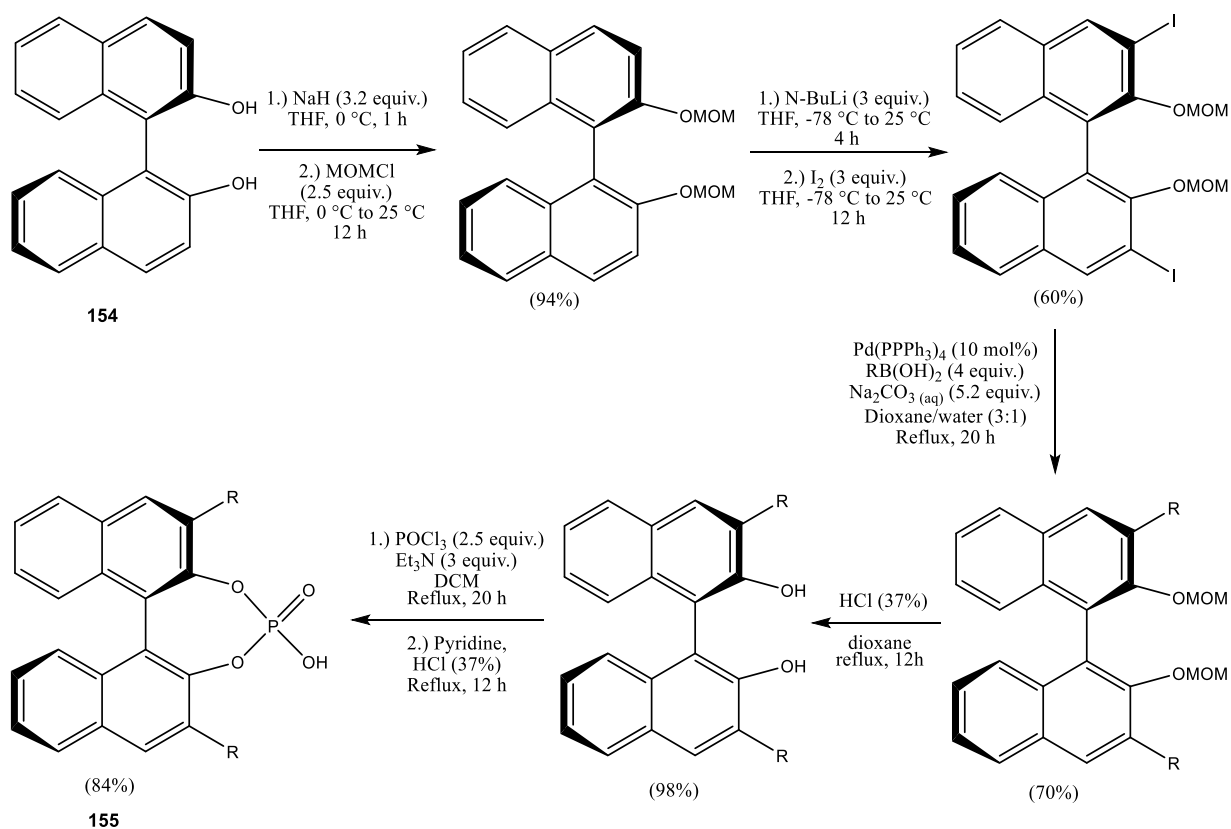
Additionally, further exploring the reactivity of aryl-based nucleophiles would provide a more thorough and quantitative insight into the stereoelectronic factors affecting the cyclisation reaction. As mentioned in chapter 2, we attempted the preparation of methoxy-substituted phenylethylamines with different degrees and locations of substitution; while the syntheses of the corresponding β -nitrostyrenes were successful, we were unable to perform the subsequent hydrogenation step using a Pd-C catalyst. Fortunately, there are other procedures that could be followed in this respect that have been documented in the literature. One of the most straightforward is documented by Maresh *et al.*, which employs zinc and hydrochloric acid as the reducing agent and affords substituted phenylethylamines in yields of 73-87% (Scheme 55).⁸⁵



*Scheme 55: Zn/HCl reduction of substituted B-nitrostyrenes by Maresh et al.*⁸⁵

Finally, we are yet to establish a means of preparing the separated enantiomers of compound **1**. The racemic products obtained from the chiral acid-catalysed reactions of **25** suggests that a more specialised catalyst would be required to impart greater selectivity. However, the existing literature, combined with the small enantiomeric excess obtained from (*R*)-(-)-1,1'-Binaphthyl-2,2'-diyl hydrogenphosphate indicate that a more specialised BINOL-derived phosphoric acid would likely be successful in this regard. In particular, installing bulky substitutions at the 3 and 3' prime positions would help to impart greater selectivity upon the reacting centre. The preparation of such catalysts represents a more complex synthesis that was outside the scope of this project. One potential route is provided by Yeung *et al.*, who described the 5-step synthesis of aryl and silyl-substituted BINOL phosphoric acids **155** from (*R*)-BINOL (**154**) (Scheme 56).⁸⁶ The catalyst was synthesised in a 32%

overall yield, with the attachment of the R groups achieved via a Suzuki coupling. As mentioned previously, acquisition of the separated enantiomers of **1** would be invaluable from a pharmaceutical standpoint, as it would permit the biological activities of both enantiomers to be independently assessed.



Scheme 56: Preparation of 3,3'-substituted BINOL phosphoric acids presented by Yeung et al.⁸⁶

6: Experimental procedures

6.1: General Information

The chemicals used were obtained from the companies Sigma-Aldrich™, Alfa Aesar™, TCI™ or Fluorochem™ and were used without further purification.

Chromatography: For TLC chromatography Merck™ TLC silicon dioxide 60 F254 with glass backing were used. Detection was carried out either by UV absorption or by treatment of the plate with an acidic solution of potassium permanganate and drying using a handheld hot-air dryer. Solvents were obtained from Fisher Scientific™.

The NMR spectra were recorded on a Bruker 400 Ultrashield (¹H NMR at 400MHz; ¹³C NMR at 101MHz; ¹⁹F NMR at 376MHz) spectrometer in the indicated solvent at a temperature of 297 K. Commercially available deuterated chloroform (CDCl₃) or deuterated dimethylsulfoxide (*d*₆-DMSO) was used as a solvent. The multiplicity of the signal is indicated as: s – singlet, d – doublet, t – triplet, q – quartet and m – multiplet, dd – doublet of doublets, dt – doublet of triplets, etc. Coupling constants (*J*) were measured to the nearest 0.1 Hz.

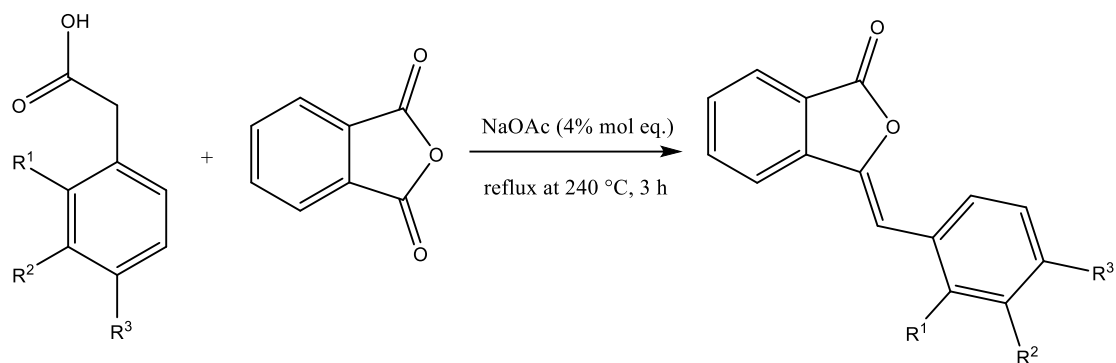
Liquid chromatography-mass spectrometry (LCMS) was performed on an SQD mass spectrometer and an Acquity UPLC system. Column: Acquity UPLC BEH C₁₈ 1.7μm (2.1mm × 50mm). Mobile phase: water containing formic acid (0.1% v/v): acetonitrile.

High resolution mass spectra (HRMS) were recorded on a QToF Premier mass spectrometer and an Acquity UPLC system. Column: Acquity UPLC BEH C₁₈ 1.7μm (2.1mm × 100mm). Mobile phase: water containing formic acid (0.1% v/v): acetonitrile.

IR spectra were recorded neat on a Perkin-Elmer Paragon 1000 FT-IR spectrometer fitted with a Diamond attenuated total reflection (ATR) accessory (Golden Gate). Assigned peaks are reported in wavenumbers (cm⁻¹), with the following abbreviations used to describe the appearance: s (strong, signal >70% of strongest signal), m (moderate, signal between 40-70% of the strongest signal), w (weak, signal <40% of strongest signal), br (broad).

X-Ray crystal structure determination was performed by Dr Dmitry Yufit at the Department of Chemistry, University of Durham using a Bruker D8 Venture detector. Crystallographic data can be found in the supplementary information booklet.

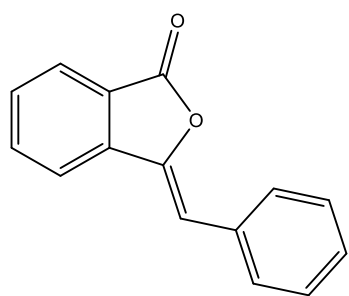
6.2: Synthesis of benzalphthalide derivatives 35-35k



General procedure:

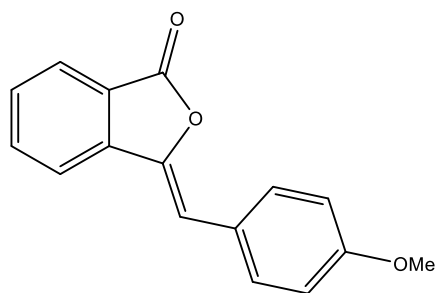
Phthalic anhydride (2.61 g, 17.6 mmol) and the correspondingly substituted phenylacetic acid derivative (17.0 mmol) were added to a 50 mL round bottomed flask. A catalytic amount of sodium acetate (0.06 g, 0.73 mmol) was added, and the mixture was melted together by heating to 240 °C for 3 h with stirring. A colour change from white to off white/yellow was observed. The mixture was subsequently allowed to cool to room temperature, at which point the mixture solidified. The solid was dissolved in boiling ethanol (10.0 mL), before being filtered and cooled, resulting in the growth of crystals of the corresponding benzalphthalide derivative.

(*Z*)-3-(benzylidene)isobenzofuran-1(*H*)-one 35



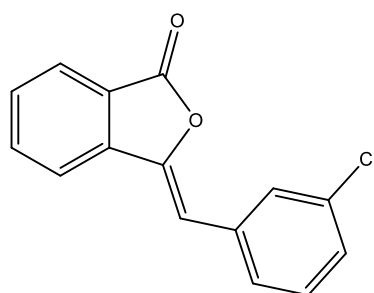
¹H NMR (400 MHz, DMSO-*d*₆) δ 8.11 – 8.02 (m, 1H), 7.91 (dt, *J* = 7.7, 1.0 Hz, 1H), 7.87 – 7.74 (m, 3H), 7.62 (td, *J* = 7.5, 0.9 Hz, 1H), 7.44 (dd, *J* = 8.4, 7.0 Hz, 2H), 7.37 – 7.27 (m, 1H), 6.88 (s, 1H). ¹³C NMR (101 MHz, DMSO-*d*₆) δ 166.8 (C), 144.7 (C), 140.6 (C), 135.5 (CH), 133.7 (C), 130.7 (CH), 130.2 (CH), 129.3 (CH), 128.7 (CH), 125.6 (CH), 122.9 (C), 121.2 (CH), 107.3 (CH). IR ν = 1773 (s), 1665 (w), 1607 (w), 1492 (w), 1472 (w), 1448 (w), 1353 (w), 1297 (w), 1203 (w), 1165 (w), 1083 (m), 878 (s), 962 (s), 864 (m), 851 (m), 765 (s), 758 (s), 704 (m), 685 (s), 636 (m), 521 (s), 411 (w) cm⁻¹. LC-MS: Rt = 2.75 min peak found for 223.2 (M+H) and 445.2 [2M+H]. HR-MS (ES⁺) calculated for C₁₅H₁₁O₂ 223.0759, found 239.0919 Δ = 10.5 ppm (mDa 2.5). Melting point: 97.7–98.9 °C (EtOH), literature 96–98 °C (MeOH).⁸⁷

(Z)-3-(4-methoxybenzylidene)isobenzofuran-1(H)-one **35b**



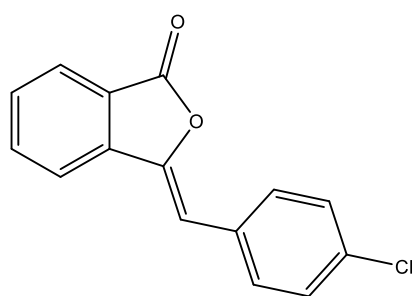
$^1\text{H NMR}$ (400 MHz, CDCl_3) δ 7.94 (dt, $J = 7.7, 1.0$ Hz, 1H), 7.84 – 7.79 (m, 2H), 7.77 – 7.66 (m, 2H), 7.53 (ddd, $J = 7.9, 6.8, 1.3$ Hz, 1H), 6.99 – 6.90 (m, 2H), 6.40 (s, 1H), 3.87 (s, 3H). $^{13}\text{C NMR}$ (101 MHz, CDCl_3) δ 167.3 (C), 159.8 (C), 143.1 (C), 140.8 (C), 134.4 (CH), 131.7, 129.3, 125.9 (C), 125.5 (CH), 123.1 (C), 119.5 (CH), 114.3 (CH), 107.0 (CH), 55.3 (CH_3). IR $\nu = 1780$ (m), 1761 (m), 1512 (m), 1259 (m), 1172 (m), 1081 (m), 1027 (m), 938 (s), 857 (s), 819 (s), 758 (s), 685 (s), 609 (w), 576 (w), 528 (s), 511 (w) cm^{-1} . LC-MS: $R_t = 2.73$ min peak found for 253.1 (M+H) and 506.3 [2M+H]. HR-MS (ES+) calculated for $\text{C}_{16}\text{H}_{13}\text{O}_3$ 253.0865, found 253.0890 $\Delta = 9.9$ ppm (mDa 2.5). Melting point: 147.3–148.7 $^\circ\text{C}$ (EtOH), literature 147–149 $^\circ\text{C}$.⁸⁸

(Z)-3-(3-chlorobenzylidene)isobenzofuran-1(H)-one **35c**



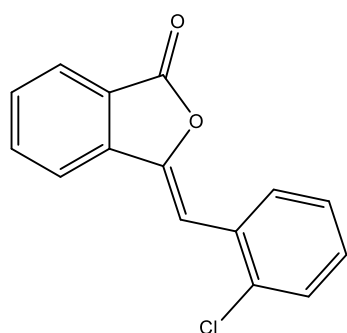
$^1\text{H NMR}$ (400 MHz, CDCl_3) δ 7.99 (dt, $J = 7.7, 1.0$ Hz, 1H), 7.86 (t, $J = 1.8$ Hz, 1H), 7.83 – 7.74 (m, 3H), 7.61 (ddd, $J = 7.7, 6.8, 1.4$ Hz, 1H), 7.41 – 7.29 (m, 2H), 6.39 (s, 1H). $^1\text{H NMR}$ (400 MHz, $\text{DMSO}-d_6$) δ 8.08 (dd, $J = 7.8, 1.0$ Hz, 1H), 7.96 (dd, $J = 7.8, 1.0$ Hz, 1H), 7.89 (td, $J = 7.6, 1.1$ Hz, 1H), 7.83 (t, $J = 1.9$ Hz, 1H), 7.75 – 7.64 (m, 2H), 7.47 (d, $J = 7.8$ Hz, 1H), 7.40 (ddd, $J = 8.0, 2.2, 1.1$ Hz, 1H), 6.93 (s, 1H). $^{13}\text{C NMR}$ (101 MHz, $\text{DMSO}-d_6$) δ 166.6 (C), 145.7 (C), 140.3 (C), 135.8 (C), 135.7 (CH), 133.9 (C), 131.2 (CH), 131.2 (CH), 129.3 (CH), 128.8 (CH), 128.4 (CH), 125.8 (CH), 123.1 (C), 121.4 (CH), 105.6 (CH). IR (neat) $\nu = 1783$ (s), 1665 (w), 1606 (w), 1591 (w), 1560 (w), 1479 (w), 1471 (w), 1421 (w), 1356 (m), 1270 (m), 1183 (w), 1075 (m), 980 (s), 885 (s), 877 (s), 776 (m), 720 (w), 757 (s), 750 (m), 685 (s), 673 (s), 639 (w), 430 (w), 461 (m) cm^{-1} . LC-MS: $R_t = 3.03$ min peak found for 257.1 (M(Cl^{35})+H). HR-MS (ES+) calculated for $\text{C}_{15}\text{H}_{10}\text{ClO}_2$ 257.0369, found 257.0396 $\Delta = 10.5$ ppm (mDa 2.7). Melting point: 158.7–160.0 $^\circ\text{C}$ (EtOH), literature 160–161 $^\circ\text{C}$ (EtOH).⁸⁹

(Z)-3-(4-chlorobenzylidene)isobenzofuran-1(H)-one **35d**



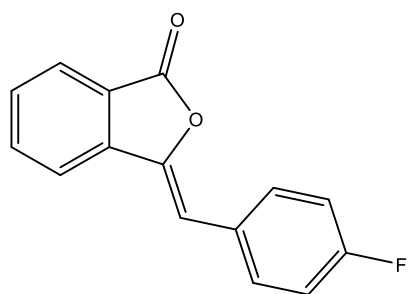
^1H NMR (400 MHz, CDCl_3) δ 7.91 (dt, $J = 7.7, 1.0$ Hz, 1H), 7.79 – 7.68 (m, 4H), 7.55 (ddd, $J = 8.0, 6.1, 2.1$ Hz, 1H), 7.38 – 7.30 (m, 2H), 6.34 (s, 1H). ^{13}C NMR (101 MHz, CDCl_3) δ 166.8 (C), 144.9 (C), 140.3 (C), 134.6 (CH), 134.2 (C), 131.6 (C), 131.2 (CH), 130.0 (CH), 128.9 (CH), 125.6 (CH), 123.3 (C), 119.9 (CH), 105.7 (CH). IR (neat) $\nu = 1792$ (m), 1655 (w), 1597 (w), 1489 (w), 1472 (w), 1406 (w), 1354 (m), 1326 (w), 1308 (w), 1268 (m), 1202 (m), 1091 (w), 1079 (m), 1012 (w), 967 (s), 868 (w), 849 (s), 823 (w), 805 (s), 758 (s), 748 (m), 685 (s), 648 (w), 597 (m), 574 (m), 524 (m), 515 (s) cm^{-1} . LC-MS: Rt = 3.05 min peak found for 257.1 (M(Cl 35)+H). HR-MS (ES+) calculated for $\text{C}_{15}\text{H}_{10}\text{ClO}_2$ 257.0369, found 257.0397 $\Delta = 10.9$ ppm (mDa 2.7). Melting point: 151.5–152.8 $^\circ\text{C}$ (EtOH), literature 151–153 $^\circ\text{C}$ (EtOH).⁸⁹

(Z)-3-(2-chlorobenzylidene)isobenzofuran-1(H)-one **35e**



^1H NMR (400 MHz, $\text{DMSO}-d_6$) δ 8.22 (dd, $J = 7.8, 1$ Hz, 1H), 8.10 (dd, $J = 7.9, 1.7$ Hz, 1H), 8.01 – 7.94 (m, 1H), 7.89 (td, $J = 7.6, 1$ Hz, 1H), 7.70 (td, $J = 7.5, 0.8$ Hz, 1H), 7.55 (dd, $J = 7.9, 1.3$ Hz, 1H), 7.46 (td, $J = 7.7, 1.4$ Hz, 1H), 7.37 (td, $J = 7.7, 1.7$ Hz, 1H), 6.99 (s, 1H). ^{13}C NMR (101 MHz, $\text{DMSO}-d_6$) δ 166.6 (C), 146.4 (C), 140.0 (C), 135.8 (CH), 133.2 (C), 131.8 (CH), 131.4 (CH), 131.3 (C), 130.3 (CH), 130.2 (CH), 128.0 (CH), 125.7 (CH), 123.3 (C), 121.8 (CH), 102.2 (CH). IR (neat) $\nu = 1774$ (m), 1468 (m), 1277 (m), 1078 (m), 943 (m), 743 (s), 681 (s), 467 (s) cm^{-1} . LC-MS: Rt = 3.05 min peak found for 257.1 (M(Cl 35)+H). HR-MS (ES+) calculated for $\text{C}_{15}\text{H}_{10}\text{ClO}_2$ 257.0369, found 257.0369 $\Delta = 8.9$ ppm (mDa 2.3). Melting point: 169.6–170.7 $^\circ\text{C}$ (EtOH), literature 163 $^\circ\text{C}$.⁹⁰

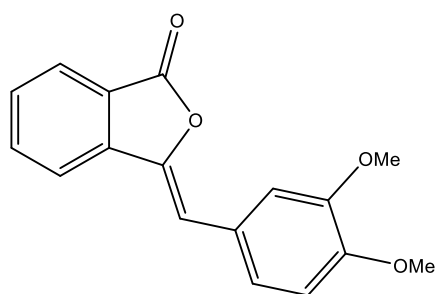
(Z)-3-(4-fluorobenzylidene)isobenzofuran-1(H)-one **35f**



^1H NMR (400 MHz, CDCl_3) δ 7.97 (dt, $J = 7.7, 1.0$ Hz, 1H), 7.91 – 7.84 (m, 2H), 7.83 – 7.72 (m, 2H), 7.59 (ddd, $J = 8.0, 6.9, 1.3$ Hz, 1H), 7.17 – 7.08 (m, 2H), 6.42 (s, 1H). ^1H NMR (400 MHz, $\text{DMSO}-d_6$) δ 8.11 (dd, $J = 8.0, 1.0$ Hz, 1H), 7.97 (dt, $J = 7.7, 1.0$ Hz, 1H), 7.93 – 7.81 (m, 3H), 7.71 – 7.63 (m, 1H), 7.33 (ddd, $J = 9.0, 7.9, 0.9$ Hz, 2H), 6.97 (s, 1H). ^{13}C NMR (101 MHz, $\text{DMSO}-d_6$) δ 166.7 (C), 162.0 (C, d, $J = 247.4$ Hz), 144.4 (C), 140.5 (C), 135.6 (CH), 132.3 (CH, d, $J = 8.3$ Hz), 130.7 (CH), 130.3

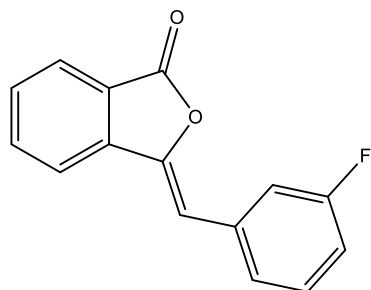
(C, $d, J = 2.8$ Hz), 125.6 (CH), 122.8 (C), 121.1 (CH), 116.3 (CH, $d, J = 21.8$ Hz), 106.1 (CH). ^{19}F NMR (376 MHz, $\text{DMSO-}d_6$) δ -112.25. IR (neat) $\nu = 1789$ (m), 1666 (w), 1598 (m), 1507 (m), 1472 (w), 1355 (w), 1271 (w), 1198 (w), 1158 (w), 1091 (w), 1077 (m), 966 (s), 859 (s), 755 (s), 684 (s), 634 (w), 650 (w), 521 (s), 441 (w), 411 (s) cm^{-1} . LC-MS: $R_t = 2.79$ min peak found for 241.1 (M+H). HR-MS (ES+) calculated for $\text{C}_{15}\text{H}_{10}\text{FO}_2$ 241.0665, found 241.0692 $\Delta = 11.2$ ppm (mDa 2.7). Melting point: 143.7–144.3 °C (EtOH), literature 135–136 °C.⁹¹

(Z)-3-(3,4-dimethoxybenzylidene)isobenzofuran-1(H)-one 35g



^1H NMR (400 MHz, CDCl_3) δ 7.96 (dt, $J = 7.7, 1.0$ Hz, 1H), 7.81 – 7.68 (m, 2H), 7.58 – 7.50 (m, 2H), 7.43 – 7.35 (m, 1H), 6.93 (d, $J = 8.4$ Hz, 1H), 6.40 (s, 1H), 4.00 (s, 3H), 3.95 (s, 3H). ^1H NMR (400 MHz, $\text{DMSO-}d_6$) δ 8.03 (dd, $J = 7.9, 1.2$ Hz, 1H), 7.92 (dd, $J = 7.7, 1.0$ Hz, 1H), 7.84 (t, $J = 7.6$ Hz, 1H), 7.61 (t, $J = 7.6$ Hz, 1H), 7.44 – 7.34 (m, 2H), 7.04 (d, $J = 8.3$ Hz, 1H), 6.84 (d, $J = 1.6$ Hz, 1H), 3.82 (s, 3H), 3.80 (s, 3H). ^{13}C NMR (101 MHz, $\text{DMSO-}d_6$) δ 166.9 (C), 149.7 (C), 149.1 (C), 143.0 (C), 140.8 (C), 135.4 (CH), 130.2 (CH), 126.4 (C), 125.6 (CH), 123.8 (CH), 122.5 (C), 120.8 (CH), 113.4 (CH), 112.4 (CH), 107.7 (CH), 55.9 (CH_3), 55.9 (CH_3). IR (neat) $\nu = 1760$ (s), 1660 (w), 1597 (m), 1581 (w), 1515 (s), 1460 (m), 1443 (w), 1312 (w), 1274 (m), 1234 (s), 1141 (s), 1078 (w), 1023 (s), 975 (s), 939 (m), 888 (m), 865, 814 (m), 801 (w), 753 (s), 684 (s), 627 (m), 605 (s), 523 (w), 477 (m) cm^{-1} . LC-MS: $R_t = 2.51$ min peak found for 282.9 (M+H) and 566.3 [2M+H]. HR-MS (ES+) calculated for $\text{C}_{17}\text{H}_{15}\text{O}_4$ 283.0970, found 283.0995 $\Delta = 8.8$ ppm (mDa 2.5). Melting point: 129.8–130.8 °C (EtOH), literature 130–131 °C (EtOH).⁸⁹

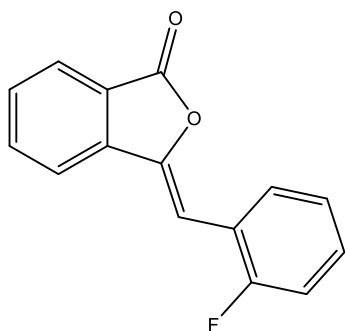
(Z)-3-(3-fluorobenzylidene)isobenzofuran-1(H)-one 35h



^1H NMR (400 MHz, CDCl_3) δ 7.98 (dt, $J = 7.7, 1.0$ Hz, 1H), 7.84 – 7.72 (m, 2H), 7.68 – 7.55 (m, 3H), 7.39 (td, $J = 8.0, 6.0$ Hz, 1H), 7.04 (tdd, $J = 8.3, 2.6, 1.0$ Hz, 1H), 6.41 (s, 1H). ^1H NMR (400 MHz, $\text{DMSO-}d_6$) δ 8.07 (dd, $J = 7.8, 2.4$ Hz, 1H), 7.94 (dd, $J = 7.8, 2.4$ Hz, 1H), 7.90 – 7.80 (m, 1H), 7.66 (td, $J = 7.6, 2.0$ Hz, 1H), 7.57 (tt, $J = 7.0, 2.0$ Hz, 2H), 7.48 (tdd, $J = 8.3, 6.3, 2.0$ Hz, 1H), 7.17 (td, $J = 8.3, 2.6$ Hz, 1H), 6.92 (d, $J = 3.2$ Hz, 1H). ^{13}C NMR (101 MHz, $\text{DMSO-}d_6$) δ 166.5 (C), 162.6 (C, $d, J = 242.5$ Hz), 145.6 (C), 140.3 (C), 136.0 (C, $d, J = 8.7$ Hz), 135.7 (CH), 131.2 (CH, $d, J = 8.4$ Hz), 131.1 (CH), 126.4 (CH, $d, J = 2.3$ Hz), 125.7 (CH), 123.0 (C), 121.3 (CH), 116.1 (CH, $d, J = 22.7$ Hz), 115.5 (CH, $d, J = 21.2$ Hz), 105.9 (CH). ^{19}F NMR (376 MHz, $\text{DMSO-}d_6$) δ -112.82. IR (neat) $\nu = 1789$ (m), 1451 (m), 1277 (m), 1078 (m), 966 (m), 845

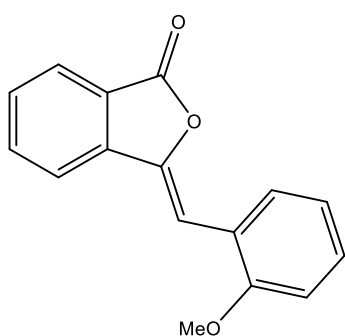
(m), 745 (s), 685 (s), 485 (s) cm^{-1} . LC-MS: $R_t = 2.81$ min peak found for 241.1 (M+H). HR-MS (ES+) calculated for $\text{C}_{15}\text{H}_{10}\text{FO}_2$ 241.0665, found 241.0688 $\Delta = 9.5$ ppm (mDa 2.3). Melting point: 128.3–129.2 $^\circ\text{C}$ (EtOH), literature 127–128 $^\circ\text{C}$ (EtOH).⁸⁸

(Z)-3-(2-fluorobenzylidene)isobenzofuran-1(H)-one 35i



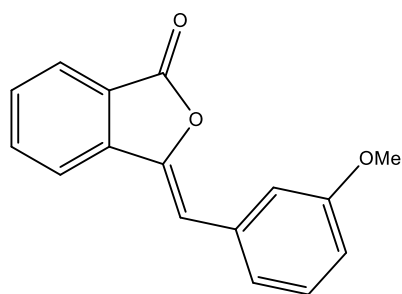
^1H NMR (400 MHz, CDCl_3) δ 8.35 (td, $J = 7.8, 1.8$ Hz, 1H), 7.98 (dt, $J = 7.8, 1.0$ Hz, 1H), 7.86 (dt, $J = 7.8, 1.0$ Hz, 1H), 7.78 (ddd, $J = 7.8, 7.2, 1.0$ Hz, 1H), 7.61 (td, $J = 7.5, 0.9$ Hz, 1H), 7.37 – 7.21 (m, 2H), 7.13 (ddd, $J = 10.7, 8.1, 1.4$ Hz, 1H), 6.76 (s, 1H). ^1H NMR (400 MHz, $\text{DMSO}-d_6$) δ 8.27 (dd, $J = 7.9, 0.9$ Hz, 1H), 8.12 (td, $J = 7.8, 1.8$ Hz, 1H), 7.98 (dd, $J = 7.7, 1.0$ Hz, 1H), 7.89 (td, $J = 7.6, 1.1$ Hz, 1H), 7.70 (td, $J = 7.5, 0.9$ Hz, 1H), 7.46 – 7.38 (m, 1H), 7.37 – 7.27 (m, 2H), 6.96 (s, 1H). ^{13}C NMR (101 MHz, $\text{DMSO}-d_6$) δ 166.6 (C), 160.1 (C, d, $J = 249.3$ Hz), 146.3 (C), 140.1 (C), 135.7 (CH), 131.3 (CH), 131.2 (CH, d, $J = 2.6$ Hz), 130.8 (CH, $J = 8.5$ Hz), 125.7 (CH), 125.4 (CH, d, $J = 3.5$ Hz), 123.2 (C), 121.8 (CH), 121.3 (C, d, $J = 12.3$ Hz), 116.0 (CH, d, $J = 21.7$ Hz), 98.1 (CH, d, $J = 6.9$ Hz). ^{19}F NMR (376 MHz, $\text{DMSO}-d_6$) δ -115.76. IR (neat) $\nu = 1788$ (s), 1435 (m), 1227 (s), 1124 (m), 968 (s), 844 (m), 752 (s), 722 (m), 685 (s), 627 (m), 585 (w), 540 (w), 484 (m) cm^{-1} . LC-MS: $R_t = 2.86$ min peak found for 241.1 (M+H) and 481.3 [2M+H]. HR-MS (ES+) calculated for $\text{C}_{15}\text{H}_{10}\text{FO}_2$ 241.0665, found 241.0692 $\Delta = 11.2$ ppm (mDa 2.7). Melting point: 149.0–150.2 $^\circ\text{C}$ (EtOH), literature 154–155 $^\circ\text{C}$ (EtOH).⁸⁸

(Z)-3-(2-methoxybenzylidene)isobenzofuran-1(3H)-one 35j



^1H NMR (400 MHz, CDCl_3) δ 8.30 (dd, $J = 7.9, 1.7$ Hz, 1H), 7.95 (d, $J = 7.7$ Hz, 1H), 7.86 (d, $J = 7.8$ Hz, 1H), 7.73 (t, $J = 7.5$ Hz, 1H), 7.55 (t, $J = 7.5$ Hz, 1H), 7.32 (t, $J = 7.6$ Hz, 1H), 7.07 (t, $J = 7.6$ Hz, 1H), 6.99 (s, 1H), 6.94 (d, $J = 8.3$ Hz, 1H), 3.94 (s, 3H). ^{13}C NMR (101 MHz, CDCl_3) δ 167.4 (C), 157.1 (C), 144.5 (C), 141.0 (C), 134.4 (CH), 131.4 (CH), 129.8 (CH), 129.5 (CH), 125.4 (CH), 123.3 (C), 122.0 (C), 121.1 (CH), 120.1 (CH), 110.5 (CH), 100.9 (CH), 55.6 (CH_3). IR (neat) $\nu = 1762$ (s), 1573 (m), 1463 (m), 1240 (s), 967 (s), 760 (s), 684 (s) cm^{-1} . LC-MS: $R_t = 3.13$ min peak found for 253.5 (M+H) and 505.5 [2M+H]. HR-MS (ES+) calculated for $\text{C}_{16}\text{H}_{13}\text{O}_3$ 253.0865, found 253.0878 $\Delta = 5.1$ ppm (mDa 1.3). Melting point: 145.8–148.5 $^\circ\text{C}$, literature 155–156 $^\circ\text{C}$ (EtOH).⁸⁸

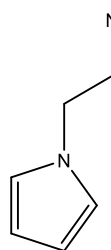
(Z)-3-(3-methoxybenzylidene)isobenzofuran-1(3H)-one **35k**



^1H NMR (400 MHz, CDCl_3) δ 7.95 (dt, $J = 7.6, 1.0$ Hz, 1H), 7.82 – 7.69 (m, 2H), 7.56 (ddd, $J = 8.0, 7.0, 1.2$ Hz, 1H), 7.48 – 7.41 (m, 2H), 7.34 (t, $J = 8.1$ Hz, 1H), 6.90 (ddd, $J = 8.2, 2.5, 1.1$ Hz, 1H), 6.41 (s, 1H), 3.89 (s, 3H). ^{13}C NMR (101 MHz, CDCl_3) δ 167.0 (C), 159.8 (C), 144.7 (C), 140.6 (C), 134.5 (CH), 134.4 (C), 129.8 (CH), 129.7 (CH), 125.6 (CH), 123.4 (C), 122.8 (CH), 119.9 (CH), 115.0 (CH), 114.5 (CH), 107.0 (CH), 55.4 (CH_3). IR (neat) $\nu = 1764$ (s), 1572 (m), 1474 (m), 1276 (s), 971 (s), 762 (s), 685 (s) cm^{-1} . LC-MS: Rt = 3.32 min peak found for 253.6 (M+H) and 505.5 [2M+H]. HR-MS (ES+) HR-MS (ES+) calculated for $\text{C}_{16}\text{H}_{13}\text{O}_3$ 253.0865, found 253.0886 $\Delta = 8.3$ ppm (mDa 2.1). Melting point: 120.3–123.8 $^\circ\text{C}$, literature 118–119 $^\circ\text{C}$.⁹²

6.3: Synthesis of amine components **38** and **42**

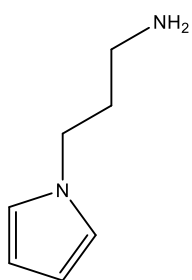
2-(1H-pyrrol-1-yl)ethan-1-amine **38**



Sodium hydroxide (28.8 g, 0.72 mol) and tetrabutylammonium hydrogen sulfate (TBAS) (2.44 g, 7.20 mmol) were added to a solution of pyrrole (10.0 mL, 144 mmol) in acetonitrile (440 mL). After stirring for 30 min at room temperature, 2-chloroethylamine hydrochloride (20.0 g, 172 mmol) was added in one portion. The reaction mixture was then heated at reflux for 24 h, during which the precipitation of sodium chloride was observed. After cooling to rt, deionised water (500 mL) was added to the reaction mixture. The product was extracted into diethyl ether (3 \times 200 mL), and the combined fractions were dried over sodium sulfate. The solvents were removed *in vacuo* to afford the crude product as a dark oil. The product was purified via Kugelrohr distillation (190 $^\circ\text{C}$, 40 mbar, 25 rpm) collected as a clear, colourless oil (10.6 g, 67%). ^1H NMR (400 MHz, CDCl_3) δ 6.70 (t, $J = 2.1$ Hz, 2H), 6.19 (t, $J = 2.1$ Hz, 2H), 3.95 (t, $J = 5.9$ Hz, 2H), 3.04 (t, $J = 5.9$ Hz, 2H), 1.62 (s, 2H). ^{13}C NMR (101 MHz, CDCl_3) δ 120.7 (CH), 108.4 (CH), 52.7 (CH_2), 43.3 (CH_2). IR (neat) $\nu = 3295$ (br), 1661 (m), 1499 (m), 1282 (m), 1089 (m), 723 (s) cm^{-1} . GC-MS: Rt = 2.89 min peak found for 110.1 [M^+] and 81.1 [$\text{M} - \text{CH}_2\text{NH}_2$] $^+$.

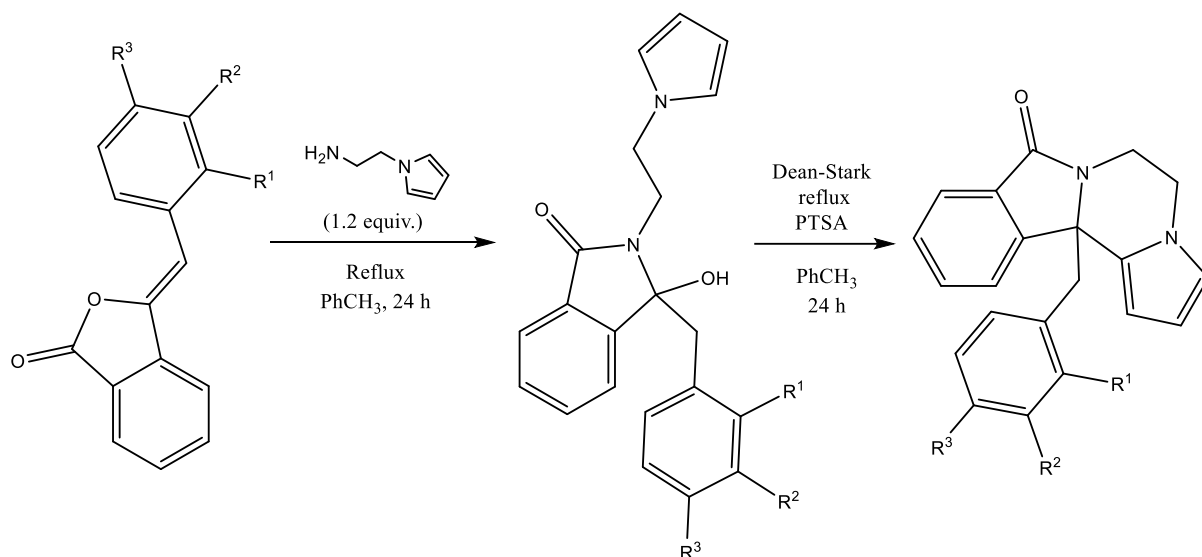
3-(1H-pyrrol-1-yl)propan-1-amine **42**

Sodium hydroxide (14.4 g, 0.36 mol) and tetrabutylammonium hydrogen sulfate (TBAS) (1.22 g, 3.60 mmol) were added to a solution of pyrrole (5.0 mL, 72.1 mmol) in acetonitrile (220 mL). After stirring for 30 min at room temperature, 3-chloropropylamine hydrochloride (11.2 g, 86 mmol) was added in one portion. The reaction mixture was then heated at reflux for 24 h, during which the precipitation



of sodium chloride was observed. After cooling to rt, deionised water (500 mL) was added to the reaction mixture. The product was extracted into diethyl ether (3 × 100 mL), and the combined fractions were dried over sodium sulfate. The solvents were removed *in vacuo* to afford the crude product as a dark oil. The product was purified via Kugelrohr distillation (240 °C, 40 mbar, 25 rpm) and collected as a clear, colourless oil (7.1 g, 79%). ¹H NMR (400 MHz, CDCl₃) δ 6.68 (t, *J* = 2.1 Hz, 2H), 6.16 (t, *J* = 2.1 Hz, 2H), 3.97 (t, *J* = 6.9 Hz, 2H), 2.70 (t, *J* = 6.9 Hz, 2H), 1.91 (p, *J* = 6.9 Hz, 2H), 1.63 (s, 2H). ¹³C NMR (101 MHz, CDCl₃) δ 120.5 (CH), 108.0 (CH), 47.2 (CH₂), 39.3 (CH₂), 35.0 (CH₂). IR (neat) ν = 3201 (br), 1501 (m), 1279 (m), 1091 (m), 720 (s) cm⁻¹. GC-MS: Rt = 3.33 min peak found for 124.1 [M⁺] and 81.2 [M – CH₂CH₂NH₂]⁺.

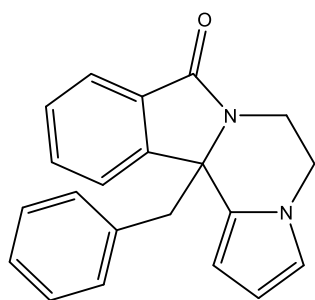
6.4: Synthesis of isoindolone product and substituted derivatives 1-1k



General procedure:

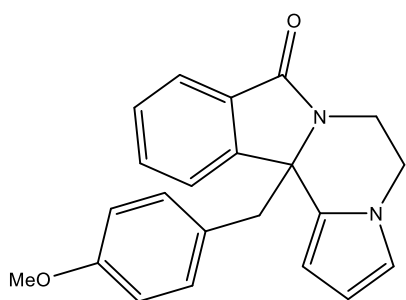
A mixture of 2-(1*H*-pyrrol-1-yl)ethanamine (1.32 g, 12 mmol) and the corresponding benzaldehyde derivative (10 mmol) were heated at reflux in toluene (50 mL) for 24 hours. The mixture was cooled and *p*-toluenesulfonic acid monohydrate (0.25 g, 1.25 mmol) was added, and the reaction mixture was again heated at reflux under Dean-Stark conditions for a further 24 hours. The reaction progress was monitored through the collection of water in the distillation trap. The toluene was removed *in vacuo*, and the resulting residue was redissolved in dichloromethane (50 mL). The solution was washed with water (30 mL) and saturated solution of sodium hydrogen carbonate (30 mL), before being dried over sodium sulfate. The solvent was subsequently removed *in vacuo* to yield the crude product, which was purified via recrystallisation using a solvent system that depended on the derivative (see individual experimental data).

12*b*-benzyl-5,6-dihydropyrrolo[2',1':3,4]pyrazino[2,1-*a*]isoindol-8(12*bH*)-one 1:



Addition of the *p*-toluenesulfonic acid monohydrate resulted in a colour change of the solution from clear to orange. The product was recrystallised from isopropyl alcohol, yielding the pure compound as orange crystals (2.26 g, 72%²). ¹H NMR (400 MHz, CDCl₃) δ 7.83 (dt, *J* = 7.7, 0.9 Hz, 1H), 7.74 – 7.57 (m, 2H), 7.41 (td, *J* = 7.5, 0.9 Hz, 1H), 7.21 – 7.02 (m, 3H), 6.89 – 6.73 (m, 2H), 6.59 (dd, *J* = 2.7, 1.6 Hz, 1H), 6.44 (dd, *J* = 3.7, 1.6 Hz, 1H), 6.26 (dd, *J* = 3.7, 2.7 Hz, 1H), 4.66 (ddd, *J* = 13.7, 4.4, 1.7 Hz, 1H), 4.02 – 3.84 (m, 2H), 3.58 (d, *J* = 13.8 Hz, 1H), 3.43 – 3.25 (m, 2H). ¹³C NMR (101 MHz, CDCl₃) δ 168.6 (C), 149.0 (C), 134.8 (C), 132.2 (CH), 130.8 (C), 129.9 (CH), 129.3 (C), 128.3 (CH), 127.9 (CH), 127.0 (CH), 123.7 (CH), 122.5 (CH), 119.8 (CH), 108.6 (CH), 104.9 (CH), 65.2 (C), 47.7 (CH₂), 44.3 (CH₂), 35.9 (CH₂). IR (neat) ν = 2917 (w), 1685 (s, C=O), 1389 (m), 700 (s) cm⁻¹. LC-MS: Rt = 2.54 min peak found for 315.8 [M+H] and 630.1 [2M+H]. HR-MS (ES⁺) calculated for C₂₁H₁₉N₂O 315.1511, found 315.1497 Δ = 4.4 ppm (mDa 1.4). Melting point: 202.1–204.2 °C (*i*-PrOH).

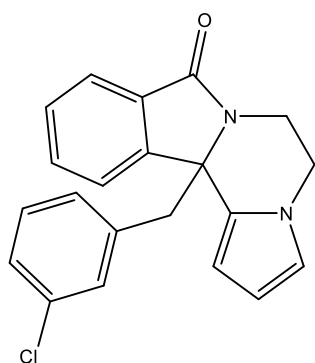
12*b*-(4-methoxybenzyl)-5,6-dihydropyrrolo[2',1':3,4]pyrazino[2,1-*a*]isoindol-8(12*bH*)-one 1*b*:



Crude product isolated as an orange residue. This was recrystallised from acetonitrile to yield the final product as off-white crystals (1.10 g, 32%). ¹H NMR (400 MHz, CDCl₃) δ 7.81 (dt, *J* = 7.8, 1.0 Hz, 1H), 7.69 (dt, *J* = 7.6, 1.0 Hz, 1H), 7.63 (td, *J* = 7.5, 1.2 Hz, 1H), 7.41 (td, *J* = 7.5, 1.0 Hz, 1H), 6.75 – 6.67 (m, 2H), 6.66 – 6.60 (m, 2H), 6.58 (dd, *J* = 2.8, 1.6 Hz, 1H), 6.41 (dd, *J* = 3.7, 1.6 Hz, 1H), 6.24 (dd, *J* = 3.7, 2.7 Hz, 1H), 4.65 (ddd, *J* = 13.6, 4.4, 1.6 Hz, 1H), 4.00 – 3.83 (m, 2H), 3.72 (s, 3H), 3.50 (d, *J* = 14.0 Hz, 1H), 3.38 – 3.28 (m, 1H), 3.25 (1 H, d, *J* = 14.0 Hz). ¹³C NMR (101 MHz, CDCl₃) δ 168.7 (C), 158.5 (C), 149.0 (C), 132.1 (CH), 130.8 (CH), 129.3 (C), 128.3 (CH), 126.9 (C), 123.7 (CH), 122.2 (C), 119.7 (CH), 116.4 (C), 113.3 (CH), 108.5 (CH), 104.8 (CH), 65.3 (C), 55.1 (CH₃), 46.9 (CH₂), 44.3 (CH₂), 35.9 (CH₂). IR (neat) ν = 2950 (w), 1695 (s, C=O), 1511 (m), 1241 (m), 1035 (m), 700 (s) cm⁻¹. LC-MS: Rt = 2.51 min peak found for 345.8 [M+H] and 690.2 [2M+H]. HR-MS (ES⁺) calculated for C₂₂H₂₁N₂O₂ 345.1603, found 345.1620 Δ = 4.9 ppm (mDa 1.7). Melting point: 142.1–144.5 °C (MeCN).

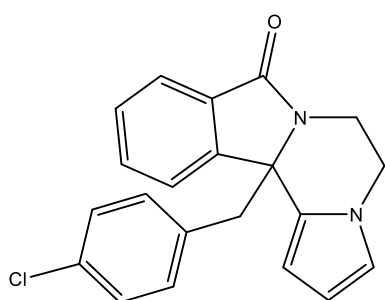
² A yield of 86% was achieved using column chromatography as a purification technique (eluent: Hexane: ethyl acetate 6:4)

12b-(3-chlorobenzyl)-5,6-dihydropyrrolo[2',1':3,4]pyrazino[2,1-a]isoindol-8(12bH)-one **1c**:



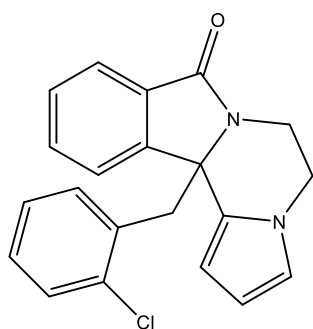
Crude product isolated as an off-white solid. The compound was recrystallised from isopropyl alcohol to yield purified product as yellow crystals (1.77 g, 51%). ^1H NMR (400 MHz, CDCl_3) δ 7.82 (dt, $J = 7.7, 0.9$ Hz, 1H), 7.75 – 7.60 (m, 2H), 7.43 (td, $J = 7.5, 0.9$ Hz, 1H), 7.11 (ddd, $J = 8.0, 2.1, 1.1$ Hz, 1H), 7.02 (t, $J = 7.8$ Hz, 1H), 6.77 (t, $J = 1.9$ Hz, 1H), 6.68 (dt, $J = 7.6, 1.4$ Hz, 1H), 6.59 (dd, $J = 2.7, 1.6$ Hz, 1H), 6.43 (dd, $J = 3.7, 1.6$ Hz, 1H), 6.26 (dd, $J = 3.7, 2.7$ Hz, 1H), 4.68 (ddd, $J = 13.7, 4.6, 1.4$ Hz, 1H), 4.02 – 3.84 (m, 2H), 3.53 (d, $J = 13.9$ Hz, 1H), 3.40 – 3.24 (m, 2H). ^{13}C NMR (101 MHz, CDCl_3) δ 168.6 (C), 148.6 (C), 136.8 (C), 133.6 (C), 132.4 (CH), 130.7 (C), 130.0 (CH), 129.1 (CH), 128.9 (C), 128.6 (CH), 128.0 (CH), 127.2 (CH), 123.9 (CH), 122.4 (CH), 120.0 (CH), 108.7 (CH), 105.0 (CH), 64.9 (C), 47.2 (CH_2), 44.3 (CH_2), 36.0 (CH_2). IR (neat) $\nu = 2929$ (w), 1688 (s, C=O), 1470 (m), 1388 (m), 706 (s) cm^{-1} . LC-MS: Rt = 2.54 min peak found for 350.3 [M+H] and 698.6 [2M+H]. HR-MS (ES+) calculated for $\text{C}_{21}\text{H}_{18}\text{N}_2\text{OCl}$ 349.1108, found 349.1124 $\Delta = 4.6$ ppm (mDa 1.6). Melting point: 175.9–177.2 °C (*i*-PrOH).

12b-(4-chlorobenzyl)-5,6-dihydropyrrolo[2',1':3,4]pyrazino[2,1-a]isoindol-8(12bH)-one **1d**:



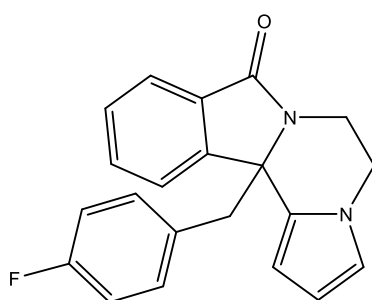
Crude product isolated as an off-white solid. The compound was recrystallised from isopropyl alcohol to yield purified product as off-white crystals (0.77 g, 22%). ^1H NMR (400 MHz, CDCl_3) δ 7.80 (dt, $J = 7.7, 0.9$ Hz, 1H), 7.70 (dt, $J = 7.6, 1.0$ Hz, 1H), 7.64 (td, $J = 7.6, 1.2$ Hz, 1H), 7.42 (td, $J = 7.5, 0.9$ Hz, 1H), 7.12 – 7.00 (m, 2H), 6.77 – 6.67 (m, 2H), 6.59 (dd, $J = 2.8, 1.6$ Hz, 1H), 6.42 (dd, $J = 3.7, 1.6$ Hz, 1H), 6.25 (dd, $J = 3.7, 2.7$ Hz, 1H), 4.68 (ddd, $J = 13.7, 4.6, 1.4$ Hz, 1H), 4.00 – 3.84 (m, 2H), 3.52 (d, $J = 13.9$ Hz, 1H), 3.42 – 3.24 (m, 2H). ^{13}C NMR (101 MHz, CDCl_3) δ 168.6 (C), 148.7 (C), 133.3 (C), 133.0 (C), 132.3 (CH), 131.1 (CH), 130.7 (C), 128.9 (C), 128.5 (CH), 128.1 (CH), 123.9 (CH), 122.4 (CH), 119.9 (CH), 108.6 (CH), 104.9 (CH), 65.0 (C), 46.9 (CH_2), 44.3 (CH_2), 36.0 (CH_2). IR (neat) $\nu = 2962$ (w), 1677 (s, C=O), 1385 (m), 831 (m), 723 (s) cm^{-1} . LC-MS: Rt = 2.75 min peak found for 350.3 [M+H] and 698.5 [2M+H]. HR-MS (ES+) calculated for $\text{C}_{21}\text{H}_{18}\text{N}_2\text{OCl}$ 349.1108, found 349.1124 $\Delta = 4.6$ ppm (mDa 1.6). Melting point: 168.4 – 171.0 °C (*i*-PrOH).

12b-(2-chlorobenzyl)-5,6-dihydropyrrolo[2',1':3,4]pyrazino[2,1-a]isoindol-8(12bH)-one **1e**:



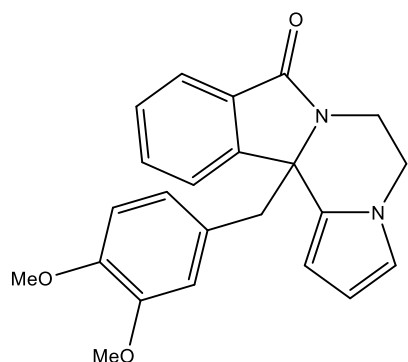
Product recrystallised from isopropyl alcohol to yield the purified compound as colourless crystals (1.62 g, 46%). Melting point: 196.3 – 198.9 °C ^1H NMR (400 MHz, CDCl_3) δ 7.87 (dt, $J = 7.7$, 0.9 Hz, 1H), 7.68 (dt, $J = 7.7$, 1.1 Hz, 1H), 7.61 (td, $J = 7.6$, 1.2 Hz, 1H), 7.40 (td, $J = 7.5$, 0.9 Hz, 1H), 7.22 (dd, $J = 8.0$, 1.3 Hz, 1H), 7.05 (ddd, $J = 8.0$, 7.4, 1.7 Hz, 1H), 6.92 (td, $J = 7.5$, 1.3 Hz, 1H), 6.73 (dd, $J = 7.8$, 1.7 Hz, 1H), 6.59 (dd, $J = 2.7$, 1.6 Hz, 1H), 6.44 (dd, $J = 3.7$, 1.6 Hz, 1H), 6.25 (dd, $J = 3.7$, 2.7 Hz, 1H), 4.70 (ddd, $J = 13.7$, 4.6, 1.4 Hz, 1H), 4.03 – 3.85 (m, 2H), 3.77 – 3.55 (m, 3H). ^{13}C NMR (101 MHz, CDCl_3) δ 168.6 (C), 148.6 (C), 135.1 (C), 132.7 (C), 132.0 (CH), 131.3 (CH), 130.8 (C), 129.5 (CH), 129.1 (C), 128.4 (CH), 128.4 (CH), 126.1 (CH), 123.6 (CH), 123.0 (CH), 119.9 (CH), 108.6 (CH), 105.1 (CH), 65.2 (C), 44.3 (CH_2), 43.1 (CH_2), 36.3 (CH_2). IR (neat) $\nu = 2980$ (w), 1684 (s, C=O), 1469 (m), 1387 (m), 756 (m), 705 (m), cm^{-1} . LC-MS: Rt = 2.54 min peak found for 350.3 [M+H] and 698.6 [2M+H]. HR-MS (ES+) calculated for $\text{C}_{21}\text{H}_{18}\text{N}_2\text{OCl}$ 349.1108, found 349.1125 $\Delta = 4.9$ ppm (mDa 1.7).

12b-(4-fluorobenzyl)-5,6-dihydropyrrolo[2',1':3,4]pyrazino[2,1-a]isoindol-8(12bH)-one **1f**:



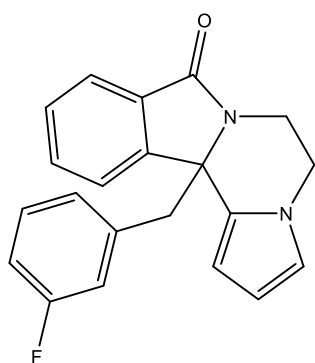
Product recrystallised from isopropyl alcohol to yield the purified product as white crystals (0.72 g, 21%). ^1H NMR (400 MHz, CDCl_3) δ 7.85 – 7.77 (m, 1H), 7.73 – 7.56 (m, 2H), 7.41 (td, $J = 7.5$, 0.9 Hz, 1H), 6.87 – 6.66 (m, 4H), 6.59 (dd, $J = 2.8$, 1.6 Hz, 1H), 6.42 (dd, $J = 3.7$, 1.6 Hz, 1H), 6.25 (dd, $J = 3.7$, 2.8 Hz, 1H), 4.68 (ddd, $J = 13.6$, 4.5, 1.5 Hz, 1H), 4.00 – 3.85 (m, 2H), 3.52 (d, $J = 14.0$ Hz, 1H), 3.41 – 3.26 (m, 2H). ^{13}C NMR (101 MHz, CDCl_3) δ 168.6 (C), 161.9 (C, d, $J = 245.7$ Hz), 148.8 (C), 132.3 (CH), 131.3 (CH, d, $J = 7.9$ Hz), 130.8 (C), 130.6 (C, d, $J = 3.3$ Hz), 129.0 (C), 128.4 (CH), 123.8 (CH), 122.4 (CH), 119.9 (CH), 114.8 (CH, d, $J = 21.2$ Hz), 108.6 (CH), 104.9 (CH), 65.0 (C), 46.8 (CH_2), 44.3 (CH_2), 35.9 (CH_2). ^{19}F NMR (376 MHz, $\text{DMSO}-d_6$) δ -116.5. IR (neat) $\nu = 2977$ (w), 1688 (s, C=O), 1509 (m), 1386 (m), 1226 (m), 720 (s) cm^{-1} . LC-MS: Rt = 2.56 min peak found for 333.8 [M+H] and 666.0 [2M+H]. HR-MS (ES+) calculated for $\text{C}_{21}\text{H}_{18}\text{N}_2\text{OF}$ 333.1403, found 349.1414 $\Delta = 3.3$ ppm (mDa 1.1). Melting point: 128.6 – 131.7 °C (*i*-PrOH).

12*b*-(3,4-dimethoxybenzyl)-5,6-dihydropyrrolo[2',1':3,4]pyrazino[2,1-*a*]isoindol-8(12*bH*)-one
1g



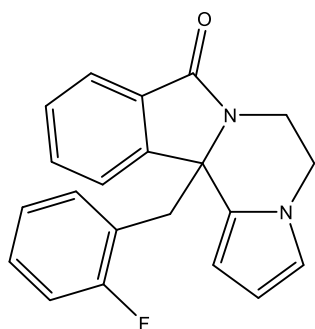
Crude product was recrystallised from toluene to yield the purified product as white crystals (2.30 g, 61%). ¹H NMR (400 MHz, CDCl₃) δ 7.84 (dt, *J* = 7.6, 0.9 Hz, 1H), 7.76 (dt, *J* = 7.6, 1.0 Hz, 1H), 7.65 (td, *J* = 7.5, 1.2 Hz, 1H), 7.45 (td, *J* = 7.5, 1.0 Hz, 1H), 6.67 (d, *J* = 8.1 Hz, 1H), 6.57 (dd, *J* = 2.7, 1.6 Hz, 1H), 6.53 – 6.43 (m, 2H), 6.27 (dd, *J* = 3.7, 2.7 Hz, 1H), 6.17 (d, *J* = 2.0 Hz, 1H), 4.64 – 4.52 (m, 1H), 3.90 – 3.84 (m, 2H), 3.83 (s, 3H), 3.59 (s, 3H), 3.54 (d, *J* = 13.9 Hz, 1H), 3.20 (d, *J* = 13.9 Hz, 1H), 3.21 – 3.09 (m, 1H). ¹³C NMR (101 MHz, CDCl₃) 168.6 (C), 149.5 (C), 148.2 (C), 148.0 (C), 132.2 (CH), 130.8 (C), 129.1 (C), 128.3 (CH), 127.6 (C), 123.9 (CH), 122.4 (CH), 122.3 (CH), 119.8 (CH), 112.4 (CH), 110.5 (CH), 108.5 (CH), 104.9 (CH), 65.2 (C), 55.7 (CH₃), 55.7 (CH₃), 47.9 (CH₂), 44.2 (CH₂), 36.0 (CH₂). IR (neat) ν = 2945 (w), 1682 (s, C=O), 1138 (s), 710 (s) cm⁻¹. LC-MS: Rt = 2.33 min peak found for 375.7 [M+H] and 750.2 [2M+H]. HR-MS (ES+) calculated for C₂₃H₂₃N₂O₃ 375.1709, found 375.1725 Δ = 4.3 ppm (mDa 1.6). Melting point: 167.4 – 169.8 °C (toluene).

12*b*-(3-fluorobenzyl)-5,6-dihydropyrrolo[2',1':3,4]pyrazino[2,1-*a*]isoindol-8(12*bH*)-one **1h**



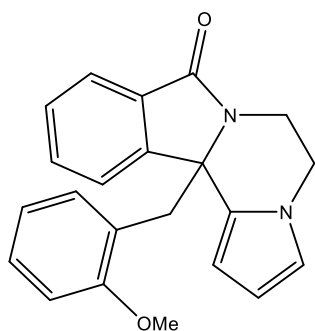
Product was recrystallised from isopropyl alcohol to yield the purified product as off-white crystals (2.20 g, 66%). ¹H NMR (400 MHz, CDCl₃) δ 7.83 (dt, *J* = 7.7, 0.9 Hz, 1H), 7.77 – 7.60 (m, 2H), 7.43 (td, *J* = 7.5, 0.9 Hz, 1H), 7.06 (td, *J* = 8.0, 6.0 Hz, 1H), 6.83 (tdd, *J* = 8.5, 2.6, 1.0 Hz, 1H), 6.64 – 6.53 (m, 2H), 6.53 – 6.39 (m, 2H), 6.26 (dd, *J* = 3.7, 2.7 Hz, 1H), 4.68 (ddd, *J* = 13.7, 4.5, 1.5 Hz, 1H), 4.01 – 3.84 (m, 2H), 3.56 (d, *J* = 13.8 Hz, 1H), 3.42 – 3.22 (m, 2H). ¹³C NMR (101 MHz, CDCl₃) δ 168.6 (C), 162.2 (C, *J* = 245.6 Hz), 148.7 (C), 137.3 (C, *J* = 7.3 Hz), 132.4 (CH), 130.7 (C), 129.3 (CH, *J* = 8.3 Hz), 129.0 (C), 128.5 (CH), 125.6 (CH, *J* = 2.8 Hz), 123.8 (CH), 122.4 (CH), 119.9 (CH), 116.7 (CH, *J* = 21.2 Hz), 114.0 (CH, *J* = 20.9 Hz), 108.7 (CH), 104.9 (CH), 64.9 (C), 47.2 (CH₂, *J* = 1.8 Hz), 44.3 (CH₂), 36.0 (CH₂). ¹⁹F NMR (376 MHz, DMSO-*d*₆) δ -114.4. IR (neat) ν = 2981 (w), 1682 (s, C=O), 1389 (m), 1138 (m), 707 (s) cm⁻¹. LC-MS: Rt = 2.56 min peak found for 333.8 [M+H] and 665.8 [2M+H]. HR-MS (ES+) calculated for C₂₁H₁₈N₂OF 333.1403, found 349.1420 Δ = 5.1 ppm (mDa 1.7). Melting point: 194.9 – 197.1 °C (*i*-PrOH).

12*b*-(2-fluorobenzyl)-5,6-dihydropyrrolo[2',1':3,4]pyrazino[2,1-*a*]isoindol-8(12*bH*)-one 1*i*



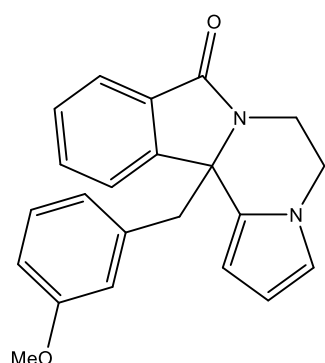
Product was recrystallised from isopropyl alcohol to yield the purified product as off-white crystals (1.91 g, 57%). ¹H NMR (400 MHz, CDCl₃) δ 7.89 (dq, *J* = 7.6, 1.0 Hz, 1H), 7.63 (ddd, *J* = 8.7, 7.5, 1.1 Hz, 2H), 7.38 (td, *J* = 7.5, 0.9 Hz, 1H), 7.06 (dddd, *J* = 8.2, 7.2, 5.3, 1.8 Hz, 1H), 6.85 (ddd, *J* = 10.2, 8.2, 1.2 Hz, 1H), 6.76 (td, *J* = 7.5, 1.2 Hz, 1H), 6.70 – 6.53 (m, 2H), 6.44 (dd, *J* = 3.7, 1.6 Hz, 1H), 6.25 (dd, *J* = 3.7, 2.7 Hz, 1H), 4.73 (ddd, *J* = 13.8, 4.6, 1.3 Hz, 1H), 4.11 – 4.01 (m, 1H), 3.96 (td, *J* = 11.8, 4.6 Hz, 1H), 3.73 (ddd, *J* = 13.7, 11.6, 4.6 Hz, 1H), 3.67 – 3.46 (m, 2H). ¹³C NMR (101 MHz, CDCl₃) δ 168.4 (C), 161.4 (C, d, *J* = 245.5 Hz), 148.1 (C), 132.0 (CH), 131.6 (CH, d, *J* = 4.1 Hz), 131.0 (C), 129.5 (C), 128.8 (CH), 128.7 (C), 128.4 (CH), 123.5 (CH), 123.3 (CH, d, *J* = 3.6 Hz), 122.7 (CH), 121.5 (C, d, *J* = 15.1 Hz), 119.8 (CH), 115.1 (CH, d, *J* = 23.1 Hz), 108.6 (CH), 104.8 (CH), 44.4 (CH₂), 39.1 (CH₂, d, *J* = 1.6 Hz), 35.7 (CH₂, d, *J* = 3.7 Hz). ¹⁹F NMR (376 MHz, DMSO-*d*₆) δ -116.5. IR (neat) ν = 2980 (w), 1684 (s, C=O), 1390 (m), 1228 (m), 763 (m), 703 (m) cm⁻¹. LC-MS: Rt = 2.56 min peak found for 333.8 [M+H] and 666.1 [2M+H]. HR-MS (ES+) calculated for C₂₁H₁₈N₂O_F 333.1403, found 349.1422 Δ = 5.7 ppm (mDa 1.9). Melting point: 199.9 – 202.2 °C (*i*-PrOH).

12*b*-(2-methoxybenzyl)-5,6-dihydropyrrolo[2',1':3,4]pyrazino[2,1-*a*]isoindol-8(12*bH*)-one 1*j*



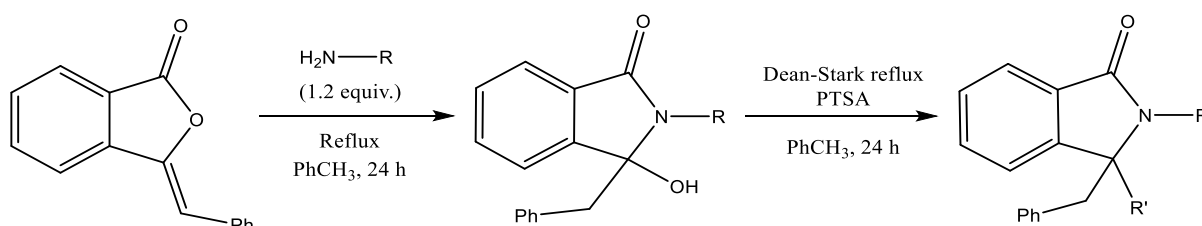
Product recrystallised from ethyl acetate/ hexane to yield the purified product as light brown crystals (2.10 g, 61%). ¹H NMR (400 MHz, CDCl₃) δ 7.87 (dd, *J* = 7.6, 1.2 Hz, 1H), 7.60 (ddd, *J* = 8.7, 7.5, 1.1 Hz, 2H), 7.36 (td, *J* = 7.5, 0.9 Hz, 1H), 7.10 – 7.01 (m, 1H), 6.68 (d, *J* = 8.2 Hz, 1H), 6.64 – 6.55 (m, 3H), 6.43 (dd, *J* = 3.8, 1.6 Hz, 1H), 6.24 (dd, *J* = 3.7, 2.8 Hz, 1H), 4.68 (ddd, *J* = 13.5, 4.5, 1.3 Hz, 1H), 4.07 – 4.00 (m, 1H), 3.95 (td, *J* = 11.7, 4.5 Hz, 1H), 3.80 (ddd, *J* = 13.6, 11.6, 4.6 Hz, 1H), 3.71 (s, 3H), 3.65 (d, *J* = 13.9 Hz, 1H), 3.52 (d, *J* = 13.8 Hz, 1H). ¹³C NMR (101 MHz, CDCl₃) δ 168.3 (C), 157.8 (C), 148.6 (C), 131.4 (CH), 131.3 (CH), 131.2 (C), 130.2 (C), 128.2 (CH), 128.1 (CH), 123.2 (CH), 123.0 (CH), 122.9 (C), 119.7 (CH), 119.6 (CH), 110.1 (CH), 108.5 (CH), 104.7 (CH), 65.5 (C), 55.0 (CH₃), 44.5 (CH₂), 39.7 (CH₂), 35.7 (CH₂). IR (neat) ν = 2983 (w), 1680 (s, C=O), 1404 (m), 1247 (m), 1022 (m), 699 (s) cm⁻¹. LC-MS: Rt = 2.59 min peak found for 345.8 [M+H] and 690.1 [2M+H]. HR-MS (ES+) calculated for C₂₂H₂₁N₂O₂ 345.1603, found 345.1630 Δ = 7.8 ppm (mDa 2.7). Melting point: 180 – 182.9 °C (EtOAc).

12*b*-(3-methoxybenzyl)-5,6-dihydropyrrolo[2',1':3,4]pyrazino[2,1-*a*]isoindol-8(12*bH*)-one **1k**



Product recrystallised from isopropyl alcohol to yield the purified compound as brown crystals (2.20 g, 64%). $^1\text{H NMR}$ (400 MHz, CDCl_3) δ 7.84 (dt, $J = 7.6, 0.9$ Hz, 1H), 7.72 (dt, $J = 7.6, 1.0$ Hz, 1H), 7.64 (td, $J = 7.5, 1.2$ Hz, 1H), 7.43 (td, $J = 7.5, 0.9$ Hz, 1H), 7.02 (dd, $J = 8.3, 7.5$ Hz, 1H), 6.68 (ddd, $J = 8.3, 2.6, 1.0$ Hz, 1H), 6.58 (dd, $J = 2.8, 1.6$ Hz, 1H), 6.48 – 6.40 (m, 2H), 6.30 – 6.22 (m, 2H), 4.62 (ddd, $J = 13.7, 4.3, 1.8$ Hz, 1H), 3.95 – 3.83 (m, 2H), 3.60 (s, 4H), 3.32 – 3.20 (m, 2H). $^{13}\text{C NMR}$ (101 MHz, CDCl_3) δ 168.6 (C), 159.0 (C), 149.2 (C), 136.4 (C), 132.2 (CH), 130.8 (C), 129.2 (C), 128.9 (CH), 128.4 (CH), 123.8 (CH), 122.4 (CH), 122.4 (CH), 119.8 (CH), 114.9 (CH), 113.0 (CH), 108.6 (CH), 104.9 (CH), 65.1 (C), 55.1 (CH₃), 47.9 (CH₂), 44.2 (CH₂), 36.0 (CH₂). IR (neat) $\nu = 2945$ (w), 1685 (s, C=O), 1391 (m), 1049 (s), 697 (s) cm^{-1} . LC-MS: $R_t = 2.51$ min peak found for 345.8 [M+H] and 690.1 [2M+H]. HR-MS (ES+) calculated for $\text{C}_{22}\text{H}_{21}\text{N}_2\text{O}_2$ 345.1603, found 345.1623 $\Delta = 5.8$ ppm (mDa 2.0). Melting point: 166.4–169.7 °C (*i*-PrOH).

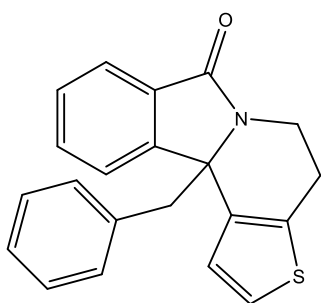
6.5: Synthesis of **80-96** through implementation of alternative amine components



General procedure:

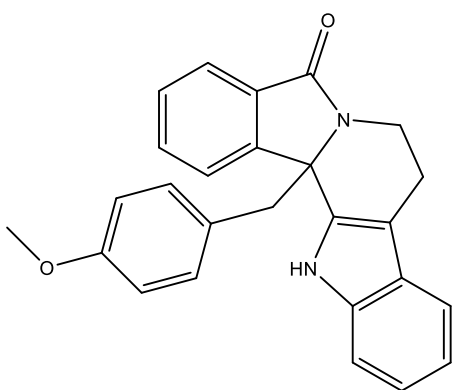
A mixture of benzaldehyde phthalide (2.22 g, 10 mmol) and the corresponding amine component (12 mmol) were heated at reflux in toluene (50 mL) for 24 hours. After cooling, *p*-toluenesulfonic acid monohydrate (0.30 g, 1.5 mmol) was added, and the reaction mixture was again heated at reflux under Dean-Stark conditions for a further 24 hours. The reaction progress was monitored through the collection of water in the distillation trap. The toluene was removed *in vacuo*, before the resulting residue was redissolved in dichloromethane (50 mL). The solution was washed with water (30 mL), saturated aqueous sodium hydrogen carbonate (30 mL), and water (30 mL), before being dried over sodium sulphate. The solvent was subsequently removed *in vacuo* to yield the crude product, which was purified via recrystallisation using a solvent system that depended on the derivative (see individual experimental data).

11*b*-benzyl-4,11*b*-dihydrothieno[3',2':3,4]pyrido[2,1-*a*]isoindol-7(5*H*)-one 80



Crude product isolated as a brown residue. The compound was recrystallised from isopropyl alcohol to yield the pure product as brown crystals (2.00 g, 60%). ¹H NMR (400 MHz, CDCl₃) δ 7.82 (dt, *J* = 7.6, 0.9 Hz, 1H), 7.72 – 7.67 (m, 1H), 7.61 (td, *J* = 7.5, 1.2 Hz, 1H), 7.44 – 7.34 (m, 2H), 7.24 (dd, *J* = 5.3, 0.9 Hz, 1H), 7.14 – 7.04 (m, 3H), 6.83 – 6.76 (m, 2H), 4.73 (ddd, *J* = 13.3, 6.2, 1.2 Hz, 1H), 3.49 (d, *J* = 13.9 Hz, 1H), 3.37 (d, *J* = 13.9 Hz, 1H), 3.21 (ddd, *J* = 13.3, 11.4, 4.8 Hz, 1H), 3.02 – 2.80 (m, 2H). ¹³C NMR (101 MHz, CDCl₃) δ 168.4 (C), 148.0 (C), 136.3 (C), 134.8 (C), 134.2 (C), 131.7 (CH), 131.5 (C), 129.9 (CH), 128.3 (CH), 127.9 (CH), 126.9 (CH), 124.4 (CH), 123.8 (CH), 123.7 (CH), 122.4 (CH), 67.1 (C), 46.1 (CH₂), 35.6 (CH₂), 25.3 (CH₂). IR (neat) ν = 3347 (w,br), 2973 (m), 1676 (s, C=O), 1391 (m), 698 (s), 645 (m) cm⁻¹. LC-MS: Rt = 2.64 min peak found for 332.8 [M+H] and 665.0 [2M+H]. HR-MS (ES+) calculated for C₂₁H₁₈NOS 332.1109, found 332.1125 Δ = 4.8 ppm (mDa 1.6). Melting point: 192.6–194.7 °C (*i*-PrOH).

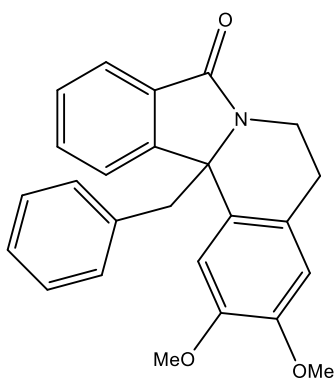
13*b*-(4-methoxybenzyl)-7,8,13,13*b*-tetrahydro-5*H*-benzo[1,2]indolizino[8,7-*b*]indol-5-one 83



Obtained as a brown powder (3.59 g, 91 % yield). ¹H NMR (400 MHz, DMSO-*d*₆) δ 11.51 (s, 1H), 8.45 (d, *J* = 7.7 Hz, 1H), 7.71 (td, *J* = 7.5, 1.3 Hz, 1H), 7.51 (dt, *J* = 7.5, 1.0 Hz, 1H), 7.48 – 7.39 (m, 3H), 7.13 (ddd, *J* = 8.2, 7.1, 1.2 Hz, 1H), 7.01 (ddd, *J* = 7.9, 7.0, 1.0 Hz, 1H), 6.76 – 6.70 (m, 2H), 6.65 – 6.58 (m, 2H), 4.58 – 4.48 (m, 1H), 3.61 (s, 3H), 3.57 (d, *J* = 3.4 Hz, 2H), 3.44 – 3.35 (m, 1H), 2.80 (dd, *J* = 15.5, 4.2 Hz, 1H), 2.67 (ddd, *J* = 15.2, 11.5, 6.0 Hz, 1H). ¹³C NMR (101 MHz, DMSO-*d*₆) δ 168.1 (C), 158.3 (C), 147.5 (C), 136.7 (C), 135.1 (C), 132.2 (CH), 131.6 (C), 131.2 (CH), 128.9 (CH), 127.3 (C), 126.5 (C), 123.8 (CH), 123.3 (CH), 122.1 (CH), 119.4 (CH), 118.8 (CH), 113.4 (CH), 111.8 (CH), 107.4 (C), 66.1 (C), 55.2 (CH₃), 42.7 (CH₂), 36.1 (CH₂), 22.0 (CH₂). IR (neat) ν = 3295 (m), 2935 (m), 1659 (s), 1512 (m), 1397 (m), 1246 (m), 1180 (m), 1038 (m), 821 (m), 739 (s) cm⁻¹. LC-MS: Rt = 2.96 min peak found for 395.3 [M+H] and 789.5 [2M+H]. HR-MS (ES+) calculated for C₂₆H₂₃N₂O₂ 395.1760 found 395.1742 Δ = 4.6 ppm (mDa 1.8).

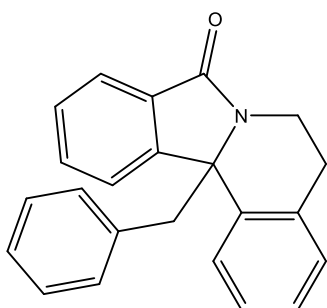
12*b*-benzyl-2,3-dimethoxy-5,12*b*-dihydroisoindolo[1,2-*a*]isoquinolin-8(6*H*)-one 86*a*

Crude product isolated as a brown powder. The product was recrystallised from ethyl acetate to yield the desired product as yellow crystals (2.20 g, 57%). ¹H NMR (400 MHz, CDCl₃) δ 7.91 (dt, *J* = 7.8, 0.9



Hz, 1H), 7.67 (dt, $J = 7.5, 1.0$ Hz, 1H), 7.61 (td, $J = 7.6, 1.2$ Hz, 1H), 7.39 (td, $J = 7.5, 0.9$ Hz, 1H), 7.30 (s, 1H), 7.14 – 7.02 (m, 3H), 6.84 – 6.75 (m, 2H), 6.63 (s, 1H), 4.64 (ddd, $J = 13.2, 6.5, 1.6$ Hz, 1H), 3.99 (s, 3H), 3.87 (s, 3H), 3.57 – 3.42 (m, 2H), 3.33 (ddd, $J = 13.2, 11.9, 4.5$ Hz, 1H), 2.96 – 3.10 (m, 1H), 2.74 (ddd, $J = 16.1, 4.5, 1.6$ Hz, 1H). ^{13}C NMR (101 MHz, CDCl_3) δ 168.0 (C), 148.4 (C), 148.3 (C), 147.6 (C), 134.9 (C), 132.0 (C), 131.4 (CH), 130.0 (CH), 129.9 (C), 128.3 (CH), 127.8 (CH), 126.8 (CH), 126.5 (C), 123.8 (CH), 122.7 (CH), 112.0 (CH), 109.7 (CH), 67.0 (C), 56.4 (CH_3), 55.9 (CH_3), 46.9 (CH_2), 35.5 (CH_2), 29.3 (CH_2). IR (neat) $\nu = 2937$ (w) 1682 (s, C=O), 1516 (m) 1257 (m), 1101 (m), 750 (m), 702 (s) cm^{-1} . LC-MS: Rt = 2.42 min peak found for 386.8 [M+H] and 772.2 [2M+H]. HR-MS (ES+) calculated for $\text{C}_{25}\text{H}_{24}\text{NO}_3$ 386.1756, found 386.1774 $\Delta = 4.7$ ppm (mDa 1.8). Melting point: 178.8–181.6 °C (EtOAc).

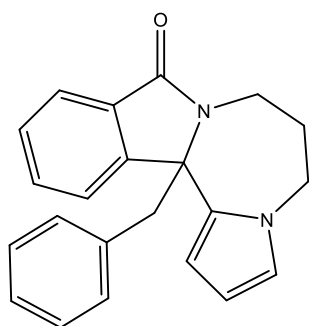
12b-benzyl-5,12b-dihydroisoindolo[1,2-a]isoquinolin-8(6H)-one 86b



Recrystallised from isopropyl alcohol (1.69 g, 52%). Melting point: 187.4–189.7 °C. ^1H NMR (400 MHz, CDCl_3) δ 8.00 (dt, $J = 7.8, 0.9$ Hz, 1H), 7.91 (dd, $J = 7.9, 1.3$ Hz, 1H), 7.69 – 7.57 (m, 2H), 7.44 – 7.32 (m, 2H), 7.25 (td, $J = 7.4, 1.3$ Hz, 1H), 7.22 – 7.15 (m, 1H), 7.13 – 7.00 (m, 3H), 6.84 – 6.69 (m, 2H), 4.66 (ddd, $J = 13.2, 6.5, 1.7$ Hz, 1H), 3.61 – 3.46 (m, 2H), 3.38 (ddd, $J = 13.2, 11.8, 4.4$ Hz, 1H), 3.18 – 3.04 (m, 1H), 2.86 (ddd, $J = 16.3, 4.5, 1.8$ Hz, 1H). ^{13}C NMR (101 MHz, CDCl_3) δ 168.1 (C), 148.2 (C), 138.3 (C), 134.8 (C), 134.0 (C), 131.9 (C), 131.5 (CH), 129.9 (CH), 129.9 (CH), 128.3 (CH), 127.8 (CH), 127.3 (CH), 126.9 (CH), 126.7 (CH), 126.4 (CH), 123.7 (CH), 122.9 (CH), 67.4 (C), 47.0 (CH_2), 35.5 (CH_2), 29.8 (CH_2). IR (neat) $\nu = 1677$ (s, C=O), 1453 (m), 1395 (m), 1138 (w), 892 (w), 759 (s), 700 (s) cm^{-1} . LC-MS: Rt = 2.70 min peak found for 326.7 [M+H] and 652.1 [2M+H]. HR-MS (ES+) calculated for $\text{C}_{23}\text{H}_{20}\text{NO}$ 326.1545 found 326.1562 $\Delta = 5.2$ ppm (mDa 1.7). Melting point: 187.4–189.7 °C (*i*-PrOH).

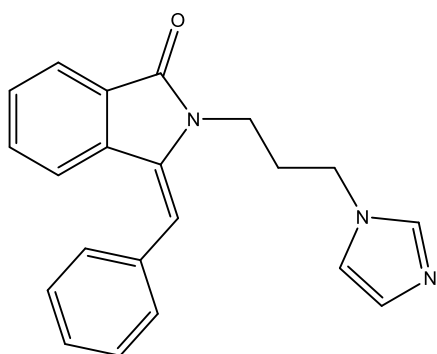
13b-benzyl-6,7-dihydro-5H-pyrrolo[2',1':3,4][1,4]diazepino[2,1-a]isoindol-9(13bH)-one 90

Crude product isolated as a brown residue. Product recrystallised from isopropyl alcohol and water to yield the purified product as fine yellow crystals (1.48 g, 45%). ^1H NMR (400 MHz, CDCl_3) δ 7.68 – 7.60 (m, 1H), 7.53 (td, $J = 7.49, 1.18$ Hz, 1H), 7.47 – 7.34 (m, 2H), 7.15 – 6.98 (m, 3H), 6.70 – 6.62 (m, 2H), 6.56 (dd, $J = 2.76, 1.76$ Hz, 1H), 6.32 (dd, $J = 3.74, 1.84$ Hz, 1H), 6.10 (dd, $J = 3.73, 2.73$ Hz, 1H), 4.53 (ddd, $J = 14.42, 7.12, 2.24$ Hz, 1H), 4.06 (ddd, $J = 14.48, 5.25, 3.90$ Hz, 1H), 3.87 (ddd, $J = 14.12, 10.04, 3.55$ Hz, 1H), 3.70 (d, $J = 13.78$ Hz, 1H), 3.51 – 3.32 (m, 2H), 2.36 – 2.18 (m, 1H), 2.15 – 2.00 (m, 1H).



^{13}C NMR (101 MHz, CDCl_3) δ 168.6 (C), 147.5 (C), 134.3 (C), 131.6 (CH), 131.1 (C), 130.2 (CH), 128.4 (CH), 127.9 (CH), 127.0 (CH), 123.6 (CH), 123.5 (CH), 123.4 (CH), 109.6 (CH), 106.9 (CH), 76.8 (C), 68.8 (C), 47.4 (CH), 44.0 (CH), 37.4 (CH), 27.2 (CH). IR (neat) ν = 2940 (w), 1681 (m, C=O), 1394 (m), 1087 (m), 703 (s) cm^{-1} . LC-MS: R_t = 2.58 min peak found for 329.8 [M+H] and 658.2 [2M+H]. HR-MS (ES+) calculated for $\text{C}_{22}\text{H}_{21}\text{N}_2\text{O}$ 329.1654 found 329.1674 Δ = 6.1 ppm (mDa 2.0). Melting point: 142.3–144.0 °C (*i*-PrOH).

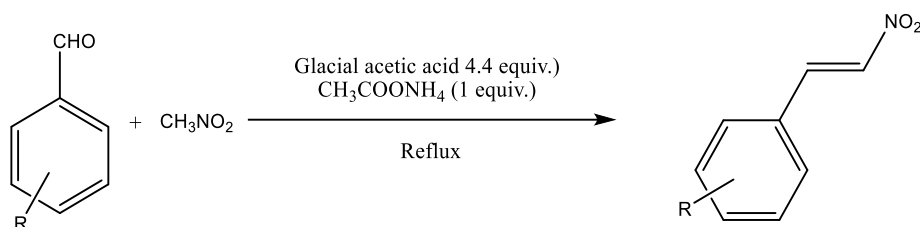
13*b*-benzyl-6,7-dihydro-5*H*-imidazo[2',1':3,4][1,4]diazepino[2,1-*a*]isoindol-9(13*bH*)-one **96**



Reflux with *p*-toluenesulfonic acid monohydrate yielded a light brown residue. Analysis determined that cyclisation was incomplete, instead yielding a compound with the structure shown on the right. Attempts to induce cyclisation via larger quantities of *p*-toluenesulfonic acid, Eaton's reagent and AcOH all proved unsuccessful. Product recrystallised from ethyl acetate to yield purified product as light brown crystals (2.07 g, 63%).

^1H NMR (400 MHz, CDCl_3) δ 7.87 (dt, J = 7.5, 1.0 Hz, 1H), 7.61 (t, J = 1.2 Hz, 1H), 7.52 – 7.39 (m, 6H), 7.38 – 7.29 (m, 2H), 7.08 (dt, J = 14.2, 1.2 Hz, 2H), 6.42 (s, 1H), 4.11 (t, J = 7.0 Hz, 2H), 3.97 (t, J = 6.7 Hz, 2H), 2.28 (p, J = 6.8 Hz, 2H). ^{13}C NMR (101 MHz, DMSO) δ 166.0 (C), 135.9 (CH), 135.4 (C), 135.3 (C), 135.0 (C), 132.5 (CH), 130.1 (CH), 130.0 (CH), 129.9 (CH), 129.2 (CH), 128.4 (CH), 123.3 (CH), 123.1 (CH), 122.4 (C), 120.2 (CH), 111.9 (CH), 46.9 (CH_2), 36.3 (CH_2), 29.0 (CH_2). IR (neat) ν = 2943 (w), 1684 (s, C=O), 1414 (s), 1086 (m), 769 (s), 697 (s) cm^{-1} . LC-MS: R_t = 1.79 min peak found for 330.9 [M+H] and 659.8 [2M+H]. HR-MS (ES+) calculated for $\text{C}_{21}\text{H}_{20}\text{N}_3\text{O}$ 330.1606, found 330.1631 Δ = 7.6 ppm (mDa 2.5). Melting point: 113.3–115.9 °C (EtOAc).

6.6: Synthesis of β -nitrostyrenes **88c-88k** via the Henry reaction

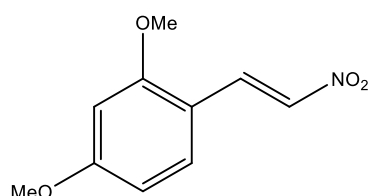


General procedure

$\text{CH}_3\text{COONH}_4$ (10 mmol, 1 eq.), glacial acetic acid (8.4 mL, 4.4 eq.) and nitromethane (30 mmol, 3 eq.) were added dropwise to a stirred solution of arylaldehyde (10 mmol, 1 eq.), in a dry round-bottomed

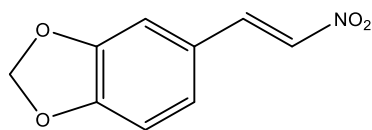
flask fitted with a condenser. The resulting mixture was refluxed until the reaction was complete as determined by TLC. The mixture was allowed to cool to room temperature and poured into ice water, and the solid was collected by filtration to afford the crude product. Purification was achieved through recrystallization from ethanol to afford corresponding β -nitrostyrenes.

(E)-2,4-dimethoxy-1-(2-nitrovinyl)benzene **88c**⁹³



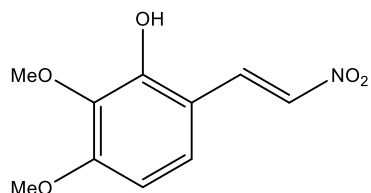
Obtained as a yellow powder (1.40 g, 67%). ¹H NMR (400 MHz, CDCl₃) δ 8.10 (d, J = 13.5 Hz, 1H), 7.85 (d, J = 13.5 Hz, 1H), 7.40 (d, J = 8.5 Hz, 1H), 6.58 (dd, J = 8.5, 2.4 Hz, 1H), 6.51 (d, J = 2.4 Hz, 1H), 3.95 (s, 3H), 3.89 (s, 3H). ¹³C NMR (101 MHz, CDCl₃) δ 164.4 (C), 161.3 (C), 136.0 (CH), 135.8 (CH), 134.5 (CH), 112.4 (C), 105.9 (CH), 98.7 (CH), 55.7 (OCH₃ and OCH₃ overlapping). IR (neat) ν = 3108 (w), 1598 (m), 1470 (m), 1244 (m), 1212 (s), 1105 (m), 1023 (s), 971 (s), 826 (s), 798 (s) cm⁻¹. LC-MS: Rt = 2.78 min peak found for 210.4 [M+H]. HR-MS (ES+) calculated for C₁₀H₁₂NO₄ 210.0766 found 210.0775 Δ = 4.3 ppm (mDa 0.9).

(E)-5-(2-nitrovinyl)benzo[d][1,3]dioxole **88d**⁹⁴



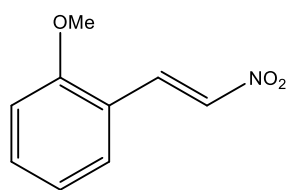
Obtained as a yellow powder (1.25 g, 65%). ¹H NMR (400 MHz, CDCl₃) δ 7.94 (d, J = 13.5 Hz, 1H), 7.49 (d, J = 13.5 Hz, 1H), 7.10 (ddd, J = 8.0, 1.8, 0.5 Hz, 1H), 7.02 (d, J = 1.8 Hz, 1H), 6.89 (d, J = 8.0 Hz, 1H), 6.08 (s, 2H). ¹³C NMR (101 MHz, CDCl₃) δ 151.4 (C), 148.8 (C), 139.2 (CH), 135.4 (CH), 126.7 (CH), 124.2 (C), 109.1 (CH), 107.0 (CH), 102.1 (CH₂). IR (neat) ν = 2920 (w), 1627 (m), 1603 (m), 1488 (m), 1328 (s), 965 (s), 811 (s) cm⁻¹. LC-MS: Rt = 2.18 min peak found for 194.0 [M+H]. HR-MS (ES+) calculated for C₉H₈NO₄ 194.0453 found 194.0451 Δ = 1 ppm (mDa 0.2).

(E)-2,3-dimethoxy-6-(2-nitrovinyl)phenol **88e**⁹⁵



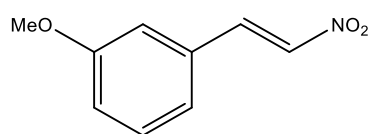
Obtained as a yellow powder (1.64 g, 73%). ¹H NMR (400 MHz, CDCl₃) δ 8.03 (d, J = 13.7 Hz, 1H), 7.56 (d, J = 13.7 Hz, 1H), 6.97 (s, 1H), 6.73 (s, 1H), 3.96 (d, J = 4.6 Hz, 1H), 3.94 (app. s, 6H). ¹³C NMR (101 MHz, CDCl₃) δ 153.2 (C), 147.4 (C), 145.5 (C), 136.4 (CH), 133.0 (CH), 114.4 (C), 109.0 (CH), 106.7 (CH), 56.4 (CH₃), 56.3 (CH₃). IR (neat) ν = 2938 (w), 1745 (m), 1514 (m), 1328 (s), 1174 (s), 966 (s), 839 (s), 551 (m) cm⁻¹. LC-MS: Rt = 2.11 min peak found for 226.0 [M+H]. HR-MS (ES+) calculated for C₁₀H₁₂NO₅ 226.0715 found 226.0717 Δ = 0.9 ppm (mDa 0.2).

(E)-1-methoxy-2-(2-nitrovinyl)benzene **88f**⁹³



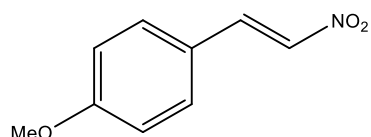
Obtained as an off-yellow powder (1.40 g, 78%). ¹H NMR (400 MHz, CDCl₃) δ 8.15 (d, *J* = 13.6 Hz, 1H), 7.90 (d, *J* = 13.6 Hz, 1H), 7.53 – 7.43 (m, 2H), 7.08 – 6.97 (m, 2H), 3.97 (s, 3H). ¹³C NMR (101 MHz, CDCl₃) δ 159.5 (C), 138.3 (CH), 135.6 (CH), 133.5 (CH), 132.5 (CH), 121.1 (CH), 119.1 (C), 111.4 (CH), 55.7 (CH₃). IR (neat) ν = 2982 (w), 1624 (m), 1596(m), 1485 (s), 1240 (s), 1163 (m), 1017 (m), 844 (m), 749 (s) cm⁻¹. LC-MS: Rt = 2.40 min peak found for 179.9 [M+H]. HR-MS (ES+) calculated for C₉H₁₀NO₃ 180.0661 found 180.0667 Δ = 3.3 ppm (mDa 0.6).

(E)-1-methoxy-3-(2-nitrovinyl)benzene **88g**⁹⁶



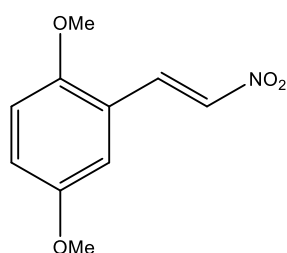
Obtained as an off-yellow powder (1.22 g, 68%). ¹H NMR (400 MHz, CDCl₃) δ 7.99 (d, *J* = 13.7 Hz, 1H), 7.59 (d, *J* = 13.7 Hz, 1H), 7.43 – 7.35 (m, 1H), 7.20 – 7.13 (m, 1H), 7.10 – 7.03 (m, 2H), 3.87 (s, 3H). ¹³C NMR (101 MHz, CDCl₃) δ 160.1 (C), 139.1 (CH), 137.3 (CH), 131.3 (C), 130.5 (CH), 121.8 (CH), 118.0 (CH), 114.0 (CH), 55.4 (CH₃). IR (neat) ν = 2978 (w), 1637 (m), 1576 (m), 1495 (s), 1345 (m), 1272 (s), 962 (s), 839 (s), 781 (s) cm⁻¹. LC-MS: Rt = 2.31 min peak found for 179.4 [M+H]. HR-MS (ES+) calculated for C₉H₁₀NO₃ 180.0661 found 180.0663 Δ = 1.1 ppm (mDa 0.2).

(E)-1-methoxy-4-(2-nitrovinyl)benzene **88h**⁹³



Obtained as a yellow powder (1.47 g, 82%). ¹H NMR (400 MHz, CDCl₃) δ 7.99 (d, *J* = 13.6 Hz, 1H), 7.58 – 7.48 (m, 3H), 7.02 – 6.94 (m, 2H), 3.89 (s, 3H). ¹³C NMR (101 MHz, CDCl₃) δ 163.0 (C), 139.1 (CH), 135.0 (CH), 131.2 (CH), 122.6 (C), 115.0 (CH), 55.6 (CH₃). IR (neat) ν = 2967 (w), 1601 (m), 1493 (s), 1246 (s), 965 (s), 805 (s), 517 (s) cm⁻¹. LC-MS: Rt = 2.26 min peak found for 179.7 [M+H]. HR-MS (ES+) calculated for C₉H₁₀NO₃ 180.0661 found 180.0666 Δ = 2.8 ppm (mDa 0.5).

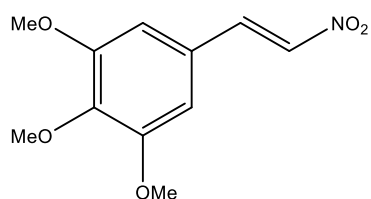
(E)-1,4-dimethoxy-2-(2-nitrovinyl)benzene **88i**⁹⁷



Obtained as a yellow powder (1.61 g, 77%). ¹H NMR (400 MHz, CDCl₃) δ 8.12 (d, *J* = 13.6 Hz, 1H), 7.87 (d, *J* = 13.6 Hz, 1H), 7.03 (dd, *J* = 9.0, 3.1 Hz, 1H), 6.97 (d, *J* = 3.1 Hz, 1H), 6.92 (d, *J* = 9.0 Hz, 1H), 3.92 (s, 3H), 3.82 (s, 3H). ¹³C NMR (101 MHz, CDCl₃) δ 154.0 (C), 153.5 (C), 138.5 (CH), 135.3 (CH), 119.5 (C), 119.2 (CH), 116.3 (CH), 112.4 (CH), 56.0 (CH₃), 55.9 (CH₃). IR (neat) ν = 2956 (w), 1619 (m), 1485 (s), 1346 (m), 1218 (s), 1035 (s), 973 (s), 835 (s), 707 (m) cm⁻¹. LC-MS: Rt =

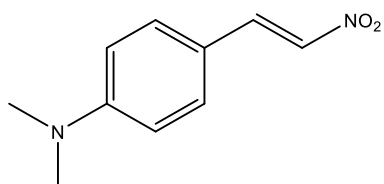
2.45 min peak found for 209.9 [M+H]. HR-MS (ES+) calculated for C₁₀H₁₂NO₄ 210.0766 found 210.0762 $\Delta = 1.9$ ppm (mDa 0.4).

(E)-1,2,3-trimethoxy-5-(2-nitrovinyl)benzene **88j**⁹³



Obtained as a yellow powder (1.74 g, 73%). ¹H NMR (400 MHz, CDCl₃) δ 7.95 (d, *J* = 13.5 Hz, 1H), 7.56 (d, *J* = 13.5 Hz, 1H), 6.78 (s, 2H), 3.94 – 3.93 (m, 3H), 3.92 (app. s, 6H). ¹³C NMR (101 MHz, CDCl₃) δ 153.7 (C), 141.7 (C), 139.4 (CH), 136.4 (CH), 125.3 (C), 106.4 (CH), 61.1 (CH₃), 56.3 (CH₃). IR (neat) ν = 2967 (w), 1628 (m), 1579 (m), 1493 (m), 1420 (m), 1313 (m), 1119 (s), 972 (s), 836 (s), 642 (s) cm⁻¹. LC-MS: Rt = 2.21 min peak found for 240.4 [M+H]. HR-MS (ES+) calculated for C₁₁H₁₄NO₅ 240.0872 found 240.0867 $\Delta = 2.1$ ppm (mDa 0.5).

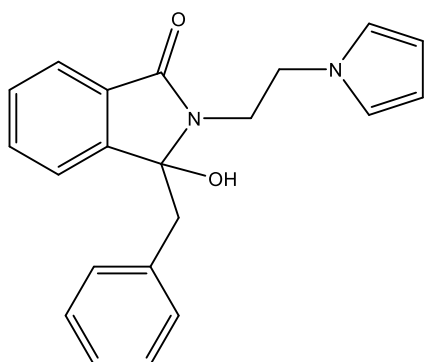
(E)-*N,N*-dimethyl-4-(2-nitrovinyl)aniline **88k**⁹⁸



Obtained as red crystals (1.32 g, 69%). ¹H NMR (400 MHz, CDCl₃) δ 7.97 (d, *J* = 13.4 Hz, 1H), 7.51 (d, *J* = 13.4 Hz, 1H), 7.47 – 7.39 (m, 2H), 6.74 – 6.66 (m, 2H), 3.09 (s, 6H). ¹³C NMR (101 MHz, CDCl₃) δ 153.0 (C), 140.4 (CH), 132.0 (CH), 131.5 (CH), 117.2 (C), 112.0 (CH), 40.1 (CH₃). IR (neat) ν = 2915 (w), 1592 (m), 1478 (s), 1233 (m), 1068 (m), 967 (s), 799 (s), 512 (m) cm⁻¹. LC-MS: Rt = 2.44 min peak found for 193.4 [M+H]. HR-MS (ES+) calculated for C₁₀H₁₃N₂O₂ 193.0977 found 193.0987 $\Delta = 5.2$ ppm (mDa 1.0).

6.7: Miscellaneous

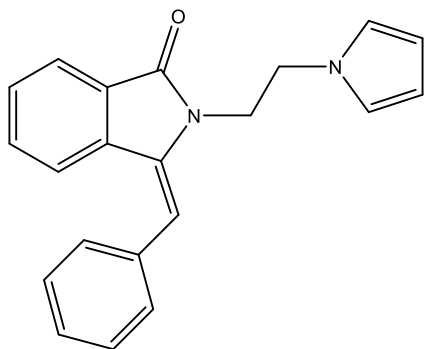
2-(2-(1*H*-pyrrol-1-yl)ethyl)-3-benzyl-3-hydroxyisoindolin-1-one **25**



Produced as a cyclisation intermediate. ¹H NMR (400 MHz, CDCl₃) δ 7.64 (dt, *J* = 7.4, 1.0 Hz, 1H), 7.53 (td, *J* = 7.5, 1.2 Hz, 1H), 7.44 (td, *J* = 7.5, 1.1 Hz, 1H), 7.30 (d, *J* = 7.0 Hz, 1H), 7.17 – 7.03 (m, 3H), 6.80 – 6.71 (m, 2H), 6.62 (t, *J* = 2.1 Hz, 2H), 6.09 (t, *J* = 2.1 Hz, 2H), 4.64 (ddd, *J* = 14.2, 10.9, 4.5 Hz, 1H), 4.16 (ddd, *J* = 14.2, 4.8, 2.4 Hz, 1H), 3.96 (ddd, *J* = 13.9, 4.6, 2.4 Hz, 1H), 3.61 (ddd, *J* = 13.8, 10.9, 4.8 Hz, 1H), 3.26 (d, *J* = 13.8 Hz, 1H), 3.03 (d, *J* = 13.8 Hz, 1H). ¹³C NMR (101 MHz, CDCl₃) δ 167.1 (C), 146.3 (C), 134.1 (C), 132.0 (CH), 131.0 (C), 129.9 (CH), 129.6 (CH), 128.0 (CH), 127.0 (CH), 122.9 (CH), 122.5 (CH), 121.4 (CH), 108.8 (CH), 91.2 (C), 46.4 (CH₂), 43.2 (CH₂), 41.8 (CH₂). IR (neat) ν = 3429 (br) 1672 (s, C=O) 1420 (m), 1280 (s), 1077 (s), 695 (s),

608 (s) cm^{-1} . LC-MS: Rt = 2.42 min peak found for 315.8 [M+H] and 629.9 [2M+H]. HR-MS (ES+) calculated for $\text{C}_{21}\text{H}_{21}\text{N}_2\text{O}_2$ 333.1603 found 333.1632 $\Delta = 8.7$ ppm (mDa 2.9). Melting point: 158.6–161.2 $^{\circ}\text{C}$ (*i*-PrOH).

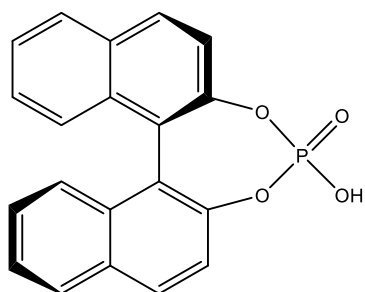
(*E*)-2-(2-(1*H*-pyrrol-1-yl)ethyl)-3-benzylideneisoindolin-1-one 43



Produced as a cyclisation intermediate. ^1H NMR (400 MHz, CDCl_3) δ 7.88 (dt, $J = 7.6, 1.1$ Hz, 1H), 7.47 – 7.29 (m, 7H), 7.22 (dt, $J = 8.0, 0.9$ Hz, 1H), 6.67 (t, $J = 2.1$ Hz, 2H), 6.20 (t, $J = 2.1$ Hz, 2H), 5.98 (s, 1H), 4.32 – 4.13 (m, 4H). ^{13}C NMR (101 MHz, CDCl_3) δ 166.7 (C), 135.9 (C), 135.1 (C), 135.0 (C), 131.7 (CH), 129.8 (C), 129.6 (CH), 129.2 (CH), 128.6 (CH), 127.8 (CH), 123.2 (CH), 123.2 (CH), 120.9 (CH), 110.1 (CH), 109.2 (CH), 48.3 (CH_2), 41.7 (CH_2).

IR (neat) $\nu = 1692$ (s, C=O) 1403 (m), 1324 (m), 1031 (m), 823 (m), 728 (s), 693 (m), 603 (m) cm^{-1} . LC-MS: Rt = 3.20 min peak found for 315.8 [M- H_2O] 333.7 [M+H] and 630.0 [2M-2 H_2O]. HR-MS (ES+) calculated for $\text{C}_{21}\text{H}_{19}\text{N}_2\text{O}$ 315.1497 found 315.1511 $\Delta = 4.4$ ppm (mDa 1.4). Melting point: 128.6–130.7 $^{\circ}\text{C}$ (*i*-PrOH).

(*R*)-(-)-1,1'-Binaphthyl-2,2'-diyl hydrogen phosphate 150



The synthesis procedure followed was by Jacques *et al.*⁸³ A 50 mL, three-necked flask, fitted with a pressure-equalizing dropping funnel, a reflux condenser and a thermometer, was charged with pyridine (23 mL) and, while stirring, (*R*)-(-)-1,1'-bi-2-naphthol (5.00 g, 0.35 mol). To this stirred suspension was added dropwise freshly distilled phosphorus oxychloride (3.68 g, 0.48 mol), resulting in a temperature rise to about 80 $^{\circ}\text{C}$, the dissolution of most of the binaphthol, and the formation of pyridine hydrochloride crystals. Complete dissolution was achieved by heating to 90 $^{\circ}\text{C}$. The stirred solution was allowed to cool to 60 $^{\circ}\text{C}$ and to the stirred suspension, water (40 mL) was added dropwise, which raised the temperature to the boiling point (ca. 118 $^{\circ}\text{C}$). The resulting solution, cooled to about 60 $^{\circ}\text{C}$, was transferred to a dropping funnel, using pyridine (2 \times 2 mL) to wash out the reaction flask. The combined solution was added dropwise with vigorous stirring to 6 N hydrochloric acid (45 mL), which gave a precipitate of pyridine-solvated binaphthylphosphoric (BNP) acid (Note 3). This crude product was collected by suction filtration. The wet cake was transferred to a 100 mL flask and stirred with 6 N hydrochloric acid (15 mL). The suspension was heated to boiling and immediately cooled. The solid was filtered by suction, washed with water (2 \times 2 mL), and air-dried to afford of (*R*)-(-)-1,1'-

binaphthyl-2,2'-diyl hydrogenphosphate (4.84 g, 80%). ^1H NMR (400 MHz, d_6 -DMSO) δ 8.17 (d, J = 8.8 Hz, 2H), 8.08 (dd, J = 8.4, 1.2 Hz, 2H), 7.62 – 7.47 (m, 4H), 7.35 (ddd, J = 8.2, 6.8, 1.3 Hz, 2H), 7.23 (dd, J = 8.5, 1.2 Hz, 2H). ^{13}C NMR (101 MHz, d_6 -DMSO) δ 148.2 (C), 148.1 (C), 132.1 (C), 131.4 (CH), 129.1 (CH), 127.3 (CH), 126.5 (CH), 125.9 (CH), 121.8 (CH, d, J = 2.7 Hz), 121.5 (C, d, J = 2.3 Hz). ^{31}P NMR (162 MHz, d_6 -DMSO) δ 2.73. IR (neat) ν = 1227 (s), 1047 (s), 950 (s), 890 (s), 811 (s), 749 (s), 561 (s), 482 (s) cm^{-1} . LC-MS: R_t = 1.76 min peak found for 349.3 [M+H] and 697.3 [2M+H]. HR-MS (ES+) calculated for $\text{C}_{20}\text{H}_{14}\text{O}_4\text{P}$ 349.0630 found 349.0644 Δ = 4.0 ppm (mDa 1.4).

7: References

- 1 S. Kraljevic, P. J. Stambrook and K. Pavelic, *European Molecular Biology Organization (EMBO) Reports*, 2004, **5**, 837–842.
- 2 O. J. Wouters, M. McKee and J. Luyten, *Journal of the American Medical Association*, 2020, **323**, 844–853.
- 3 C. A. Lipinski, F. Lombardo, B. W. Dominy and P. J. Feeney, *Advanced Drug Delivery Reviews*, 2001, **46**, 3–26.
- 4 D. F. Veber, S. R. Johnson, H.-Y. Cheng, B. R. Smith, K. W. Ward and K. D. Kopple, *Journal of Medicinal Chemistry*, 2002, **45**, 2615–2623.
- 5 W. Galloway, A. Isidro-Llobet and D. R. Spring, *Nature Communications*, 2010, **1**, 80.
- 6 F. Lovering, J. Bikker and C. Humblet, *Journal of Medicinal Chemistry*, 2009, **52**, 6752–6756.
- 7 T. Doğan, E. Akhan Güzelcan, M. Baumann, A. Koyas, H. Atas, I. R. Baxendale, M. Martin and R. Cetin-Atalay, *PLOS Computational Biology*, 2021, **17**, 10.1371/journal.pcbi.1009171.
- 8 V. Fajardo, V. Elango, B. K. Cassels and M. Shamma, *Tetrahedron Letters*, 1982, **23**, 39–42.
- 9 D.-H. Kim and G. Kim, *Bulletin of the Korean Chemical Society*, 2017, **38**, 593–594.
- 10 M. H. Abu Zarga, S. S. Sabri, S. Firdous and M. Shamma, *Phytochemistry*, 1987, **26**, 1233–1234.
- 11 X. Armoiry, G. Aulagner and T. Facon, *Journal of Clinical Pharmacy and Therapeutics*, 2008, **33**, 219–226.
- 12 M. E. Ernst and M. A. Fravel, *American Journal of Hypertension*, 2022, **35**, 573–586.
- 13 C. Mannich and W. Krösche, *Archiv der Pharmazie*, 1912, **250**, 647–667.
- 14 A. Pictet and Theod. Spengler, *Berichte der deutschen chemischen Gesellschaft*, 1911, **44**, 2030–2036.
- 15 B. Belleau, *Journal of the American Chemical Society*, 1953, **75**, 5765–5766.
- 16 B. Belleau, *Canadian Journal of Chemistry*, 1957, **35**, 651–662.
- 17 B. Belleau, *Canadian Journal of Chemistry*, 1957, **35**, 663–672.
- 18 B. E. Maryanoff, D. F. McComsey and B. A. Duhl-Emswiler, *The Journal of Organic Chemistry*, 1983, **48**, 5062–5074.
- 19 C. Grob and R. Wohl, *Helvetica Chimica Acta*, 1966, **49**, 2175–2188.
- 20 C. A. Grob and W. Baumann, *Helvetica Chimica Acta*, 1955, **38**, 594–610.
- 21 W. N. Speckamp and H. Hiemstra, *Tetrahedron*, 1985, **41**, 4367–4416.
- 22 A. J. Basson and M. G. McLaughlin, *Tetrahedron*, 2022, **114**, 132764.
- 23 A. M. Jones and C. E. Banks, *Beilstein Journal of Organic Chemistry*, 2014, **10**, 3056–3072.

- 24 J. E. Baldwin, *Journal of the Chemical Society, Chemical Communications*, 1976, 734–736.
- 25 H. E. Schoemaker, T. Boer-Terpstra, J. Dukink and W. N. Speckamp, *Tetrahedron*, 1980, **36**, 143–148.
- 26 J. B. P. A. Wijnberg, J. J. J. de Boer and W. N. Speckamp, *Recueil des Travaux Chimiques des Pays-Bas*, 2010, **97**, 227–231.
- 27 H. Neumann, D. Strübing, M. Lalk, S. Klaus, S. Hübner, A. Spannenberg, U. Lindequist and M. Beller, *Organic & Biomolecular Chemistry*, 2006, **4**, 1365–1375.
- 28 J. Dennis, C. Calyore, J. Sjöholm, J. Lutz, J. Gair and J. Johnson, *Synlett*, 2013, **24**, 2567–2570.
- 29 S. Sharma, E. Park, J. Park and I. S. Kim, *Organic Letters*, 2012, **14**, 906–909.
- 30 Q. Yu, N. Zhang, J. Huang, S. Lu, Y. Zhu, X. Yu and K. Zhao, *Chemistry - A European Journal*, 2013, **19**, 11184–11188.
- 31 R. Weiss, *Organic Syntheses*, 1933, **13**, 10.
- 32 Y. He, M. Lin, Z. Li, X. Liang, G. Li and J. C. Antilla, *Organic Letters*, 2011, **13**, 4490–4493.
- 33 J. Clayden, N. Greeves and S. Warren, *Organic Chemistry*, Oxford University Press, 2nd edition., 2012.
- 34 A. R. Katritzky, H.-Y. He and R. Jiang, *Tetrahedron Letters*, 2002, **43**, 2831–2833.
- 35 S. Kano, Y. Yuasa, T. Yokomatsu and S. Shibuya, *Synthesis*, 1983, **7**, 585–587.
- 36 B. E. Maryanoff, H. C. Zhang, J. H. Cohen, I. J. Turchi and C. A. Maryanoff, *Chemical Reviews*, 2004, **104**, 1431–1628.
- 37 S. Kano, Y. Yuasa, T. Yokomatsu and S. Shibuya, *Heterocycles*, 1983, **20**, 2411–2416.
- 38 S. P. Tanis, M. v. Deaton, L. A. Dixon, M. C. McMills, J. W. Raggon and M. A. Collins, *The Journal of Organic Chemistry*, 1998, **63**, 6914–6928.
- 39 S. P. Tanis and L. A. Dixon, *Tetrahedron Letters*, 1987, **28**, 2495–2498.
- 40 Nicolas Goudard, Yannick Carissan, Denis Hagebaum-Reignier and Stéphane Humbel, Delocalization, Mesomerism and Simple Hückel Theory: bases of a free Java Applet, <http://www.hulis.free.fr/>, (accessed 13 August 2022).
- 41 Z. Huang, Y. Meng, Y. Wu, C. Song and J. Chang, *Tetrahedron*, 2021, **93**, 132280.
- 42 W. Li, Y. Wang, H. Qi, R. Shi, J. Li, S. Chen, X.-M. Xu and W.-L. Wang, *Organic & Biomolecular Chemistry*, 2021, **19**, 8086–8095.
- 43 M. Winn and H. E. Zaugg, *The Journal of Organic Chemistry*, 1968, **33**, 3779–3783.
- 44 G. J. Hitchings and J. M. Vernon, *Journal of the Chemical Society, Perkin Transactions 1*, 1990, 1757–1763.
- 45 P. D. Bailey, K. M. Morgan, D. I. Smith and J. M. Vernon, *Tetrahedron Letters*, 1994, **35**, 7115–7118.
- 46 A. A. Bahajaj, P. D. Bailey, M. H. Moore, K. M. Morgan and J. M. Vernon, *Journal of the Chemical Society, Chemical Communications*, 1994, 2511–2512.

- 47 A. Korenova, P. Netchitailo and B. Decroix, *Journal of Heterocyclic Chemistry*, 1998, **35**, 9–12.
- 48 M. Othman, P. Pigeon and B. Decroix, *Tetrahedron*, 1997, **53**, 2495–2504.
- 49 G. A. Flynn, E. L. Giroux and R. C. Dage, *Journal of the American Chemical Society*, 1987, **109**, 7914–7915.
- 50 A. Mamouni, P. Pigeon, A. Daïch and B. Decroix, *Journal of Heterocyclic Chemistry*, 1997, **34**, 1495–1499.
- 51 B. Decroix, M. Othman, P. Pigeon, P. Netchitailo and A. Daïch, *Heterocycles*, 2000, **52**, 273–281.
- 52 I. T. Raheem, P. S. Thiara, E. A. Peterson and E. N. Jacobsen, *Journal of the American Chemical Society*, 2007, **129**, 13404–13405.
- 53 D. Rani, V. Gulati, M. Guleria, S. P. Singh and J. Agarwal, *Journal of Molecular Structure*, 2022, **1265**, 133341.
- 54 M. Kohno, S. Sasao and S.-I. Murahashi, *Bulletin of the Chemical Society of Japan*, 1990, **63**, 1252–1254.
- 55 C. J. Crawford, Y. Qiao, Y. Liu, D. Huang, W. Yan, P. H. Seeberger, S. Oscarson and S. Chen, *Organic Process Research & Development*, 2021, **25**, 1573–1578.
- 56 S. R. Johns and J. A. Lambertson, *Chemical Communications (London)*, 1966, 312–313.
- 57 S. M. Allin, C. J. Northfield, M. I. Page and A. M. Z. Slawin, *Tetrahedron Letters*, 1997, **38**, 3627–3630.
- 58 G. C. Cotzias, P. S. Papavasiliou and R. Gellene, *New England Journal of Medicine*, 1969, **280**, 337–345.
- 59 A. Jamaa, M. Latrache, E. Riguet and F. Grellepois, *The Journal of Organic Chemistry*, 2020, **85**, 9585–9598.
- 60 J. Aube, S. Ghosh and M. Tanol, *Journal of the American Chemical Society*, 1994, **116**, 9009–9018.
- 61 A. A. Bahajaj, J. M. Vernon and G. D. Wilson, *Journal of the Chemical Society, Perkin Transactions 1*, 2001, 1446–1451.
- 62 M. S. Ledovskaya, A. P. Molchanov, V. M. Boitsov, R. R. Kostikov and A. v. Stepakov, *Tetrahedron*, 2015, **71**, 1952–1958.
- 63 S. R. Shengule, G. Ryder, A. C. Willis and S. G. Pyne, *Tetrahedron*, 2012, **68**, 10280–10285.
- 64 D. J. Hart, *The Journal of Organic Chemistry*, 1981, **46**, 367–373.
- 65 W. N. Speckamp and H. Hiemstra, *Tetrahedron*, 1985, **41**, 4367–4416.
- 66 I. T. Raheem, P. S. Thiara and E. N. Jacobsen, *Organic Letters*, 2008, **10**, 1577–1580.
- 67 E. Aranzamendi, N. Sotomayor and E. Lete, *ACS Omega*, 2017, **2**, 2706–2718.
- 68 M. Takamura, K. Funabashi, M. Kanai and M. Shibasaki, *Journal of the American Chemical Society*, 2000, **122**, 6327–6328.

- 69 C. A. Holloway, M. E. Muratore, R. Ian Storer and D. J. Dixon, *Organic Letters*, 2010, **12**, 4720–4723.
- 70 L. M. Overvoorde, M. N. Grayson, Y. Luo and J. M. Goodman, *Journal of Organic Chemistry*, 2015, **80**, 2634–2640.
- 71 T. R. Kelly, P. Meghani and V. S. Ekkundi, *Tetrahedron Letters*, 1990, **31**, 3381–3384.
- 72 J. F. Blake and W. L. Jorgensen, *Journal of the American Chemical Society*, 1991, **113**, 7430–7432.
- 73 D. P. Curran and L. H. Kuo, *Tetrahedron Letters*, 1995, **36**, 6647–6650.
- 74 M. S. Sigman and E. N. Jacobsen, *Journal of the American Chemical Society*, 1998, **120**, 4901–4902.
- 75 Y. S. Lee, Md. M. Alam and R. S. Keri, *Chemistry - An Asian Journal*, 2013, **8**, 2906–2919.
- 76 M. S. Taylor and E. N. Jacobsen, *Journal of the American Chemical Society*, 2004, **126**, 10558–10559.
- 77 M. Saidah, M. I. D. Mardjan, G. Masson, J. L. Parrain and L. Commeiras, *Organic Letters*, 2022, **24**, 5298–5303.
- 78 E. Aranzamendi, N. Sotomayor and E. Lete, *ACS Omega*, 2017, **2**, 2706–2718.
- 79 A. Gómez-Sanjuan, N. Sotomayor and E. Lete, *Tetrahedron Letters*, 2012, **53**, 2157–2159.
- 80 M. E. Muratore, C. A. Holloway, A. W. Pilling, R. I. Storer, G. Trevitt and D. J. Dixon, *Journal of the American Chemical Society*, 2009, **131**, 10796–10797.
- 81 A. Reissert, *Berichte der deutschen chemischen Gesellschaft*, 1905, **38**, 1603–1614.
- 82 M. E. Muratore, C. A. Holloway, A. W. Pilling, R. I. Storer, G. Trevitt and D. J. Dixon, *Journal of the American Chemical Society*, 2009, **131**, 10796–10797.
- 83 J. Jacques and C. Fouquey, *Organic Syntheses*, 1989, **67**, 1.
- 84 R. M. C. Dawson, D. C. Elliott, W. H. Elliott and K. M. Jones, *Data for Biochemical Research (3rd Edition)*, Oxford University Press, Oxford, 1986.
- 85 J. Maresh, A. Ralko, T. Speltz, J. Burke, C. Murphy, Z. Gaskell, J. Girel, E. Terranova, C. Richtscheidt and M. Krzeszowiec, *Synlett*, 2014, **25**, 2891–2894.
- 86 J. Y. See, H. Yang, Y. Zhao, M. W. Wong, Z. Ke and Y.-Y. Yeung, *ACS Catalysis*, 2018, **8**, 850–858.
- 87 T. A. Crabb, A. Patel, R. F. Newton, B. J. Price and M. J. Tucker, *Journal of the Chemical Society, Perkin Transactions 1*, 1982, 2783–2786.
- 88 P. Hrnčiar, *Chemical Papers*, 1962, **16**, 96–104.
- 89 S. Winthrop, M. A. Davis, G. S. Myers, J. G. Gavin, R. Thomas and R. Barber, *The Journal of Organic Chemistry*, 1962, **27**, 230–240.
- 90 Ernst. D. Bergmann, *The Journal of Organic Chemistry*, 1956, **21**, 461–464.

- 91 Z. Eckstein, E. Grochowski and T. Urbanski, *Bulletin de l'Academie Polonaise de Sciences, Serie des Sciences, Chimiques, Geologiques et Geographiques*, 1959, **7**, 289–294.
- 92 S. Czaplicki, V. Kostanecki and V. Lampe, *Berichte der Deutschen Chemischen Gesellschaft*, 1909, **42**, 827–838.
- 93 S. Ambala, R. Singh, M. Singh, P. S. Cham, R. Gupta, G. Munagala, K. R. Yempalla, R. A. Vishwakarma and P. P. Singh, *RSC Advances*, 2019, **9**, 30428–30431.
- 94 T. Miao and L. Wang, *Tetrahedron Letters*, 2008, **49**, 2173–2176.
- 95 S. Kubota, T. Masui, E. Fujita and S. M. Kupchan, *Tetrahedron Letters*, 1965, **6**, 3599–3602.
- 96 M. Ramírez-Osuna, D. Chávez, L. Hernández, E. Molins, R. Somanathan and G. Aguirre, *Molecules*, 2005, **10**, 295–301.
- 97 W. E. Noland and B. L. Kedrowski, *The Journal of Organic Chemistry*, 1999, **64**, 596–603.
- 98 M. J. Kamlet, *Journal of the American Chemical Society*, 1955, **77**, 4896–4898.